Mechanistic Insights into the Cancer Cell Cytotoxicity and Blood Stability of the Garlic Compound Ajoene

By

Daniel Andreas Kusza

SUBMITTED TO THE UNVERSITY OF CAPE TOWN

In fulfilment of the requirement for the degree

Masters in Chemistry

Department of Chemistry

UNIVERSITY OF CAPE TOWN

Date of Submission:

6th of May 2016

Supervisors:

Professor Roger Hunter; Department of Chemistry; University of Cape Town

Doctor Catherine H. Kaschula; Department of Chemistry; University of Cape Town

Declaration

I, **Daniel Andreas Kusza** hereby declare that the work on which this dissertation/thesis is based is my original work (except where acknowledgements indicate otherwise) and that neither the whole work nor any part of it has been, is being, or is to be submitted for another degree in this or any other university.

I empower the university to reproduce for the purpose of research either the whole or any portion of the contents in any manner whatsoever.

Signature: Signed by candidate

Date: 6th of May 2016

Abstract

Ajoene, a garlic-derived natural product and its structural analogues are strongly cytotoxic to cancer cells. These compounds are however known to exhibit low blood stability and erythrocyte toxicity. This thesis reports on the synthesis of eight ajoene analogues designed to probe structure-activity relations into cancer cell cytotoxicity and blood stability. Structural variations included introduction of different solubility enhancing terminal groups (amide and phenol) as well as variations in the sulfoxide / vinyl-disulfide core.

The phenol ajoene analogues were found to be more cytotoxic against WHCO1 oesophageal cancer cell proliferation than the corresponding amides. The structure-activity data support a thiolysis mechanism where ajoene forms a mixed disulfide with a reactive cysteine residue on a protein target which leads to both its cytotoxicity and blood instability. This in turn is mediated by the reactivity of the disulfide pharmacophore which is enhanced by the vinyl group. The sulfoxide functional group is perceived as modulating disulphide reactivity by an inductive electron-withdrawal through the aliphatic σ-framework. The dihydroajoenes emerged as attractive candidates for further cancer therapeutic development with improved blood stability with a half-life around 120 minutes and good cancer cell cytotoxicity (IC_{50} of approximately 20 μM). A spectrophotometric and proteomic binding study demonstrated *S*-thiolation between ajoene and the cysteine 93 residue in the β-subunit of haemoglobin which may explain the observed blood instability.

A biotinylated ajoene analogue was designed and synthesised to identify ajoene's protein targets within the cancer cell. This was achieved using a convergent "Click"-strategy, involving azidated ajoene and biotin-alkyne. Both the biotin-ajoene and the azide-ajoene showed strong cytotoxicity against WHCO1 cancer cells. An immunoblotting experiment showed the successful biotinylation of haemoglobin, as a model protein by both whole probe and an *in situ* "Click"-reaction. This biotinylated probe can be used in future work to identify the ajoene protein targets in cancer cells.

Acknowledgements

I would like to dedicate this thesis to my mother (Yvonne), father (Andreas) and brother (Ashley). Without their support and encouragement all of this would not have been possible.

My deepest gratitude goes to my two supervisors:
Ever since I met Professor Hunter, his knowledge of and passion for organic chemistry has invoked much respect and admiration. My time spent as his Masters student has ever more imprinted his vision and love for the field onto me and I have set myself the goal of also becoming an enthusiastic academic who inspires his students. Furthermore, I thank him for his time, advice and attention to detail.

Doctor Kaschula's patience, diligence and guidance has been pivotal for my journey into the fields of cancer biology, biochemistry and medicinal lab practises. I greatly appreciate her open-door policy which has always led me to valuable insights. I also need to thank her for her time and care to oversee my biological experiments. I trust the momentum we have now gained on this project will lead to many more exciting results and I look forward to my upcoming doctoral studies under her supervision.

I would like to thank the following associates at UCT:
Pete Roberts, Dr. Carmen de Kock and Dr. Georgia Schäfer for their technical expertise and assistance in key experiments; Nashia Stellenboom, Mandla Mabunda, Johnathan Cotton, James Biwi and Carey Pike, who were vital contributors of the UCT-Ajoene project as their work laid the foundation for my study; past and present members of the Hunter synthetic organic chemistry group for their companionship in the lab and beyond; and lastly Marwaan Rylands, who deserves a special mention, as he has become a good friend and a helpful colleague. I admire his camaraderie and strong morale in the academic pursuit.

There are some people that are not involved with chemistry but have greatly supported me especially during the time of my writing, they are:
Rolanda Londt, who has stood by me and lovingly encouraged me to continue when I was struggling, gave moral support and helped me keep my focus on the goal; Robert Schlegel and Alan Shelley, my cohabitants who always provided a good helping of humour and often lent an ear to my frustrations; And lastly, My Taekwon-Do teammates, especially Junior Hlahla, who facilitate balancing my body with the often expended mind.

The South African National Research Foundation is gratefully acknowledged for financial support towards this project.

Table of Contents

List of Figures

List of Tables

Abbreviations

^{13}C-NMR	Carbon-13 nuclear magnetic resonance
^{1}H-NMR	Hydrogen-1 nuclear magnetic resonance
2-PTS	2-Propenyl-thiosulfate
ACCN	1-1'-Azobis(cyclohexanecarbonitrile)
AIBN	Azobisisobutyronitrile
aq.	Aqueous
ATR	Attenuated total reflectance
b.p.	Boiling point
B16	Melanoma cell line
Bcl-2	B-Cell lymphoma 2
bis-PMB	*bis*-Paramethoxybenzyl-ajoene
BL6	Melanoma cancer cell line
Boc	*tert*-Butyloxycarbonyl
BtOH	Hydroxybenzotriazole
BnOH	Benzyl alcohol
C=O	Carbonyl
$CDCl_3$	Deuterated chloroform
$-CH_2-$	Methylene
CH_3CN	Acetonitrile
CH_3COSH	Thiol acetic acid
CO_2	Carbon dioxide
COSY	Correlation spectroscopy
CPGR	Centre for proteomic and genomic research
C_{quat}	Quaternary carbon
Cs_2CO_3	Caesium carbonate
CuAAC	Copper(I) catalysed alkyne-azide cycloaddition
$CuSO_4$	Copper(II) sulfate
Cys	Cysteine
DADS	Diallyl disulfide
DAS	Diallyl sulfide

DAS4	Diallyl tetrasulfide
DAS5	Diallyl pentasulfide
DAS6	Diallyl hexasulfide
DATS	Diallyl trisulfide
DCC	*N*,*N*'-Dicyclohexylcarbodiimide
DCM	Dichloromethane
DCU	Dicyclohexylurea
dd	Doublet of doublets
ddd	Doublet of doublet of doublets
ΔG	Gibbs free energy
DIPEA	*N*,*N*-Diisopropylethylamine
DMAP	4-Dimethylaminopyridine
DMEM	Dulbecco's modified eagle's medium
DMF	*N*,*N*-Dimethylformamide
DMSO	Dimethyl sulfoxide
DP	Dansylated ajoene
DTT	1,4-Dithiothreitol
EDTA	Ethylenediaminetetraacetic acid
eq	Equivalent(s)
ER	Endoplasmic reticulum
ES	Electrospray
et al.	*et alia*
EtOAc	Ethyl acetate
FBS	Fetal bovine serum
GSH	Glutathione
GSSG	Glutathione disulfide
GST	Glutathione *S*-transferase
H_2O	Dihydrogen monoxide
H_2O_2	Hydrogenperoxide
Hb	Haemoglobin
HBr	Hydrogen bromide
HCl	Hydrogen chloride

HEPES	2-[4-(2-Hydroxyethyl)piperzin-1-yl]ethanesulfonic acid
HSQC	Heteronuclear single quantum coherence spectroscopy
HRMS	High-resolution mass spectrometry
Hz	Hertz
I_2	Iodine
IC_{50}	Half maximal inhibitory concentration
IR	Infrared
JACS	Journal of the American chemical society
$KSSO_2tol$	Potassium *p*-toluenethiosulfonate
K_2CO_3	Potassium carbonate
Da	Dalton
$KMnO_4$	Potassium permanganate
KOH	Potassium hydroxide
LC-MS	Liquid chromatography mass spectrometry
LG	Leaving group
$LiAlH_4$	Lithium aluminium hydride
m/z	Mass to charge ratio
$[M]^+$	Molecular ion peak
MALDI-TOF	Matrix-assisted laser desorption/ionisation – time of flight
MBA-MB-231	Homo sapiens mammary gland/breast cancer cell
m-CPBA	3-Chloroperoxybenzoic acid
MeOH	Methanol
MetHb	Methemoglobin
$MgSO_4$	Magnesium sulfate
MTT	3-(4,5-Dimethyl-2-thiazolyl)-2,5-diphenyl-2H-tetrazolium bromide
N=N	Nitrogen-nitrogen double bond
N_2	Nitrogen
NaN_3	Sodium azide
NEt_3	Triethylamine
N-H	Nitrogen-hydrogen
NH_4Cl	Ammonium chloride
NHS	*N*-Hydroxylsuccinimide

O-H	Oxygen-hydrogen
OSC's	Organosulfur compounds
PAGE	Polyacrylamide gel electrophoresis
PBS	Phosphate-buffered saline
PEG	Polyethylene glycol
$(PH_3)PO$	Triphenylphosphine oxide
PMB	*para*-Methoxylbenzyl
PMCl	4-Methoxybenzyl chloride
$P(PH)_3$	Triphenylphosphine
p-$TolSO_2S$-	4-Methylbenzenethiosulfonate
R_f	Retardation factor
ROS	Reactive oxygen species
-S^-	Thiolate
-$S_{(X)}H$	Polysulfide
-SH	Thiol
-SSH	Persulfide
Rt	Room temperature
SAC	*S*-Allyl cysteine
SAM	*S*-Allyl mercaptan
SAMC	*S*-Allyl mercapto cysteine
SAR	Structure-activity relationship
S-C	Sulfur-carbon
SD	Standard deviation
SDS	Sodium dodecyl sulfate
SLS	Sodium laureth sulfate
SMC	*S*-Methyl cysteine
S_N2	Bimolecular nucleophilic substitution
-S-S-	Disulfide
TBAI	Tetrabutylammonium iodide
TBS	Tris-buffered saline
ΔS	Entropy
tert-	Tertiary

TFA	Triflouroacetic acid
THF	Tetrahydrofuran
TLC	Thin layer chromatography
Tol	Toluene
Tris	Tris(hydroxymethyl)aminomethane
TWEEN 20	Polyoxyethyene (20) sorbitan
UCT	University of Cape Town
UGT	Glucuronosyltransferase
UT	Untreated
UV	Ultraviolet
WB	Western blot
WHCO1	Oesophageal cancer cell line

Chapter One: Literature Review

"Sith Garlic then hath powers to save from death,
Bear with it though it make unsavory breath:
And scorn not Garlic, like to some that think
It only makes men wink, and drink, and stink."
-The Englishmans Doctor by Sir John Harrington 1608

1.1 Historical use and medicinal significance of garlic

Garlic (lat. *Allium sativum*) is a popular seasoning and medicinal plant. The word garlic is derived from the Anglo Saxon word *gar-leac* meaning "spear plant",[1] and is thought to have originated in Central Asia after which it was taken to North Africa and Europe. In many cultures it has gained the medicinal reputation as a "cure-all" because the plant can strengthen the body's immune system to fight off disease, as well as acting directly on pathogens and cancer cells. In 1858, Louis Pasteur was the first to experimentally confirm garlic's antibacterial activity, which underpinned its common use during World War I and II in situations where antibiotics were scarce. This led to it being coined "Russian penicillin".[2,3] In light of the traditional use of garlic, it has been vastly researched in modern medicine, with over two hundred and fifty thousand scientific articles and books, making it one of the most researched medicinal plants. The scope of bioactivity spans several areas to include anti-microbial,[4] anti-parasitic,[5] anti-fungal,[6] anti-tumour,[7] and immunomodulatory activities,[8–11] which have been attributed to the plant's ability to form over twenty organo-sulfur compounds (OSC's) as part of its allelochemical defence repertoire.

1.2 Overview of the chemistry and biology of allicin

Within an intact garlic clove an analogue of the thiol-bearing amino acid cysteine, called *S*-allyl cysteine *S*-oxide, participates in a self-defence mechanism against pathogens and certain herbivores.[12] This defensive substrate, commonly known as alliin,[13] is compartmentalised in a mesophyll vacuole of the garlic clove, while its enzymatic counterpart, alliinase, is found within the cell wall. Upon crushing or damaging of the clove, alliin is enzymatically converted to 2-propensulfenic acid and 2-aminoacrylic acid by the S-C lyase, alliinase. The subsequent condensation of two 2-propenesulfenic acid molecules gives the pungent smelling allicin (see **Figure 1**).

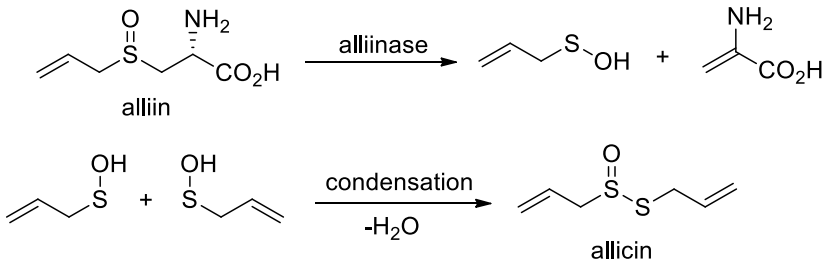

Figure 1: *Biosynthesis of allicin*

The structure of garlic's primary metabolite, allicin, was first elucidated in seminal work by Cavallito and Bailey in 1944.[14] Three years later in 1947, they demonstrated that the chemical oxidation of diallyl disulfide (DADS) with peracetic acid produces allicin synthetically (see **Figure 2**).

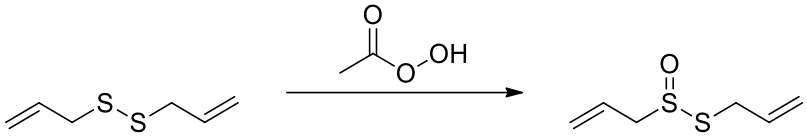

Figure 2: *Selective oxidation of DADS using peracetic acid*

Early studies on garlic were aimed at validating its traditional use as a natural antibiotic, and focused on its anti-microbial activity. Thus far, studies on allicin have demonstrated a wide range of anti-microbial activities against acid-fast *(mycobacterium tuberculosis*), gram-negative (*Escherichia coli* and *shigella dysentriae*) and gram-positive (*staphylococcus*) strains of bacteria.[15,16] Jalali *et al*. demonstrated *in vivo* anti-microbial effects of allicin on male rabbits with burn wounds by topically applying ethanolic garlic extracts. The treated rabbits showed significantly lowered bacterial contamination as well as a visible reduction in wound size.[17] It was stated that additional tissue regenerative and angiogenic effects were not linked to allicin, but to the secondary compounds that form from its degradation.[18] The poor chemical stability of allicin has made it an unreliable compound for medical research, and emphasis has thus been placed on investigating its more stable degradation products, which themselves, synergistically or individually, are toxic to pathogens and cancer cells.[19,20] **Figure 3** shows four distinct degradation pathways of allicin that were first described by Block in 1986.[14] The labile thiosulfinate functional group of allicin can undergo a Cope-type rearrangement to give 2-propenesulfenic acid and thioacrolein, via route **i)**. Route **ii)** involves hydrolysis to produce 2-propenesulfinic acid and allylmercaptan (SAM). The latter, in route **iii)**, can

undergo a substitution reaction with allicin to give DADS and 2-propenesulfenic acid. Lastly, shown in route **iv)**, the thioallylation of allicin with 2-propenesulfenic acid affords a sulfonium ion intermediate which forms the basis for the generation of multiple higher order OSC's.

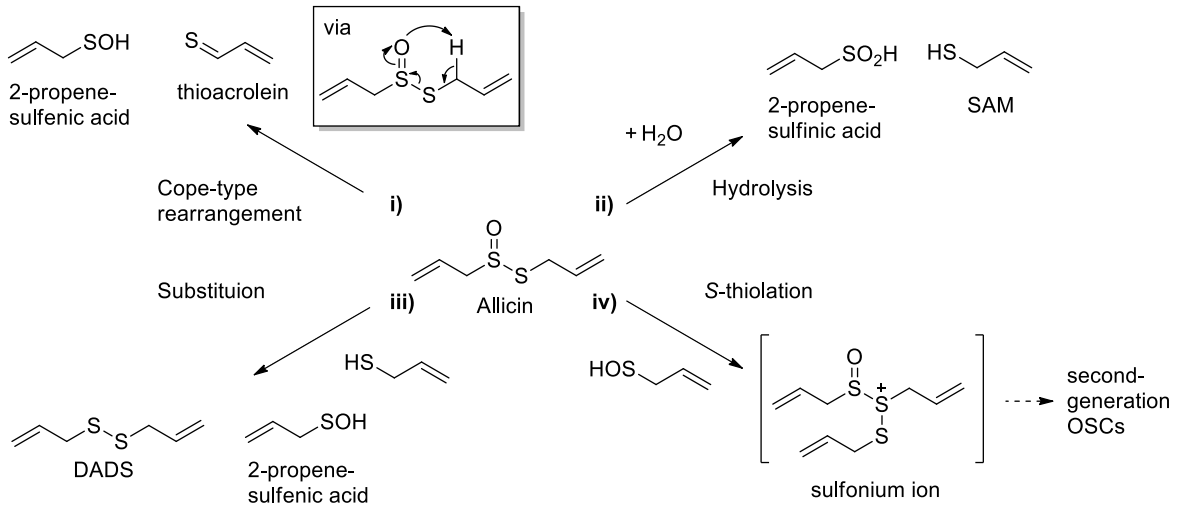

Figure 3: *Decomposition pathways of allicin*

Allicin and its degradation products, called first- and second-generation OSC's respectively, form the core of the plant's self-defence mechanism, and contribute to the wide scope of garlic's beneficial health effects. Shared commonalities in the mode of action and resulting bioactivity of these OSC's has led to their classification into distinct chemotype sub-sets according to structural features. The following section will provide a background on the sulfur chemistry that involves their formation and governs their biological activity.

1.3 Garlic organo-sulfur chemotypes

Allicin is a first-generation OSC and the plant's key chemical defence. It is the predominant thiosulfinate found in crushed garlic, while its propyl- and methyl-derivatives are present in much lesser amounts. For this reason, the majority of the second-generation garlic OSC's fall into the allicin-derived allyl-family. These allyl-sulfur compounds can be separated into water-soluble constituents such as *S*-allylcysteine (SAC) and *S*-allymercaptocysteine (SAMC), and lipid-soluble constituents, which include diallyl sulfide (DAS), diallyl di-, tri- and tetra-sulfides (DADS, DATS, DAS4), dithiins and *E/Z*-ajoene.[21,22] **Figure 4** shows the two principle cysteine-containing water-soluble

OSC's together with the general structure of the three principle lipid-soluble chemotypes that are produced from allicin's (thiosulfinate) chemical transformation.

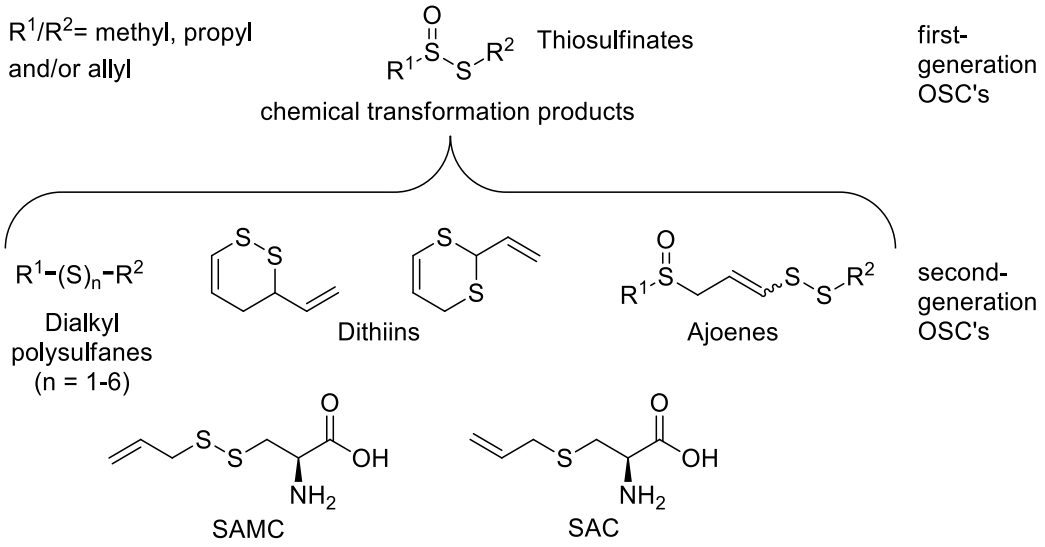

Figure 4: *Classification of first- and second-generation garlic OSC's*

The generation of allicin metabolites depends on the garlic preparation, the extraction method (i.e. choice of solvent, temperature and time) and the garlic cultivar.[19,23–25] For example, essential oil of garlic is rich in allicin, but a mere twenty hours at room temperature already sees its full conversion into second-generation products such as DAS, DADS and higher polysulfanes (where $S_{(n)}$ = 3-6).[26] Steam-distillates of crushed garlic contain DADS and DATS as the main products, whereas preparations that incubate crushed garlic in vegetable oil promote the conversion of allicin to *E*- and *Z*-ajoene and dithiins.[27,28] The culinary-savoured fermented or baked whole garlic cloves (at high temperatures of approximately 200 °C) is, in effect, devoid of any first or second-generation OSC's, as the allicin-forming enzyme (alliinase) is denatured, and the volatile OSC's escape. This results in the clove having a sweet flavour lacking the characteristic pungent odour and taste. Aged garlic extracts are traditionally prepared as part of Tibetan and Ayurvedic medicinal practices. Here macerated garlic is soaked in 20% ethanol in water at room temperature for twenty months. A lengthy storage such as this transforms the lipophilic OSC's into the more stable water-soluble SAMC, SAC and *S*-methylcysteine (SMC).[29]

The complicated rearrangement chemistry of garlic products and the difficulty in isolating single compounds from garlic preparations has highlighted the need for

synthetic access to these compounds in order to discriminate the specific bioactivities of individual OSC's. The sulfide or polysulfide backbone is a structural similarity and likely represents the pharmacophore that is shared in all OSC's found in garlic. The focus of this thesis is on ajoene, which is one of the lipophilic second-generation compounds, and thus the following section reviews literature on the synthesis and biology of its closest organo-sulfur relatives.

1.3.1 Dialkyl polysulfanes

Dialkyl polysulfanes (R^1-$S_{(n)}$-R^2 (n = 1-6), see F**igure 5**) constitute the largest group of garlic OSC's, in which bioactivity is due to sulfur's ability to form S-S bonds through redox reactions. In general, polysulfanes are similar or superior to allicin in bioactivity due to their enhanced stability and higher target specificity.[30] Diallyl disulfide (DADS) is a direct product of allicin degradation that is formed via an *S*-alkyl substitution pathway (see **Figure 3**, Reaction **iii)**), and represents the major dialkyl disulfane constituent found in crushed garlic (>50%).[26] For instance, garlic oil extracted from a particularly strong British garlic variety was found to contain 530 mg/g of DADS, followed by DATS (115 mg/g), DAS (106 mg/g), DAS4 (43 mg/g), DAS5 (11 mg/g) and DAS6 (0.1 mg/g) (see **Figure 5** for structures).[31] Dialkyl disulfanes can be synthetically accessed through standard disulfide methodology, (e.g. via sulfenate exchange methodology, *viz*. R^1-S^- + LG-S-R^2 → R^1-S**-**S-R^2 + LG^- for mixed disulfides). Studies on DADS have shown it to have anti-microbial,[32] anti-thrombotic and anti-cancer activities.[33]

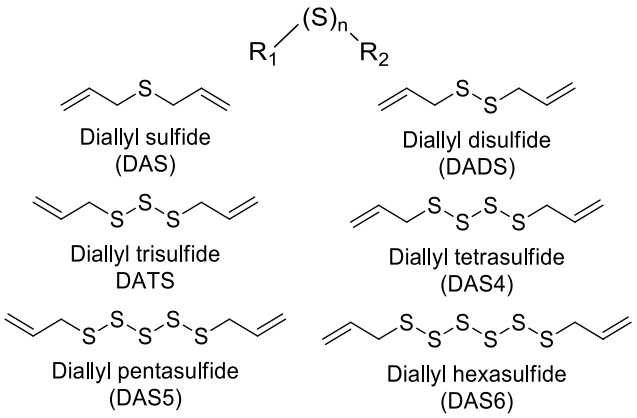

Figure 5: *General structure of dialkyl polysulfanes, and the six diallylpolysulfane constituents of garlic*

Diallyl sulfide (DAS) and its analogous mono-sulfide compounds are the simplest members of the dialkyl polysulfane family, and are formed in garlic preparations during polysulfide degradation or OSC metabolism (via SAM).[27] Lacking a cleavable disulfide, its biological activity is restricted to lipophilic membrane disruptions and ligation properties.[30]

The higher dialkyl polysulfanes (R^1-$S_{(n>2)}$-R^2) are related to DADS in that their polysulfide chains are able to undergo a thiol-disulfide exchange. As with DADS, a disulfide exchange reaction yields another disulfide (R-S-S-R'); however instead of liberating a free thiol (RSH), trisulfides and higher polysulfanes produce hydropersulfide (RSSH) or hydropolysulfide ($RS_{(x)}H$), respectively.[34,35] This so called perthiol or polysulfane is a highly reactive species that is able to illicit further activity by participating in redox-reactions, radical chemistry, catalysis and metal binding.[30] There is significant interest in DATS, as it exhibits excellent activity against platelet aggregation,[36] as well as activity against colon and gastric cancer.[37] Block hypothesised that the biosynthesis of DATS occurs through a series of additions and eliminations that can iteratively produce the higher polysulfane forms.[18] Hence, two allicin molecules self-react via sulfinylation of the thiosulfinate sulfenyl sulfur to give a sulfonium ion. Water-mediated desulfenylation produces a homoelongated sulfinate that iteratively undergoes a further sulfinylation, under acidic catalysis, with the loss of 2-propenesulfenic acid. The final step involves a desulfinylation to give DATS (**Figure 6**).

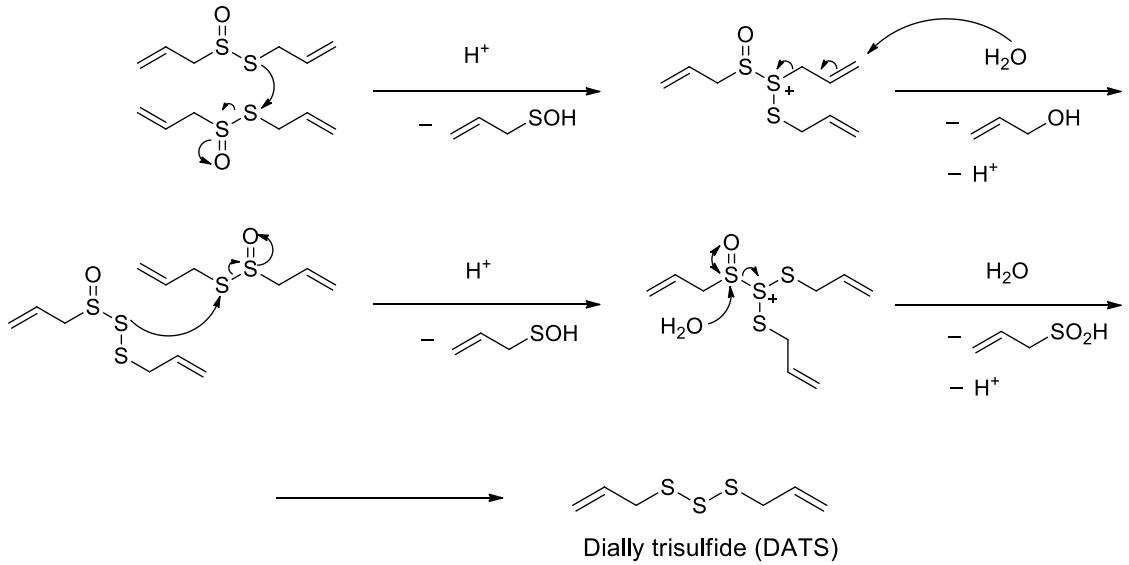

Figure 6: *Proposed biosynthesis of diallyl trisulfide (DATS)*

1.3.2 Dithiins

Dithiins are synthetically exciting targets as they are cyclic vinyl-sulfides. They are formed during allicin degradation in non-polar solvents and were first identified by Brodnitz in 1971 as a product of allicin's thermal degradation.[26] **Figure 7** shows Block's proposed mechanism for their formation, which involves a non-regioselective hetero-Diels Alder cycloaddition of two thioacrolein molecules to give 1,3- and 1,2-dithiins in a 9:2 ratio.[14] To date, little research has been conducted on their biological activity, but the disulfide 1,2-dithiin, in particular, presents an interesting lead for further work relating to our studies on ajoene due to its vinyl-disulfide (vide infra).

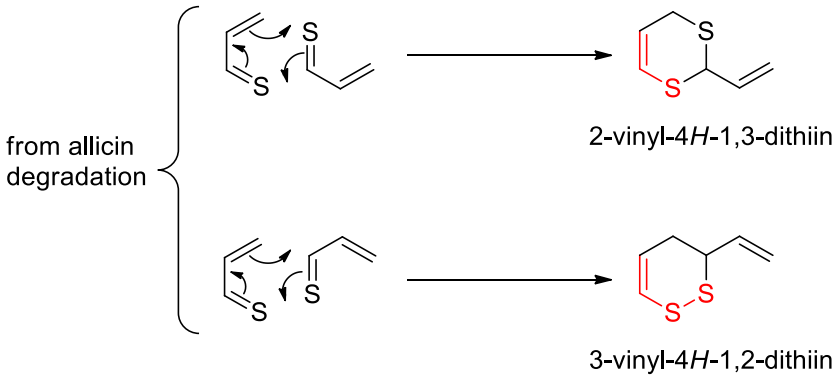

Figure 7: *Proposed formation of dithiins found in garlic preparations; suspected pharmacophores are highlighted in red*

1.3.3 Ajoenes

Ajoene, from the Spanish word *ajo* (pronounced "aho") for garlic, was first identified by Apitz-Castro *et al*. in 1983 whilst studying garlic's anti-thrombotic effects.[38] Two seminal papers by Block in 1984 and 1986, elucidated its structure as one containing a unique sulfoxide vinyl-disulfide backbone that is shown in red in **Figure 8**.[14,18] He postulated that ajoenes emerge from a *S*-thiolation reaction involving two allicin molecules. The resultant sulfonium ion undergoes a β-elimination and desulfinylation to form a thiocarbocation (thionium ion) that subsequently undergoes a Michael addition with sulfenic acid to yield *E*/*Z*-ajoene.

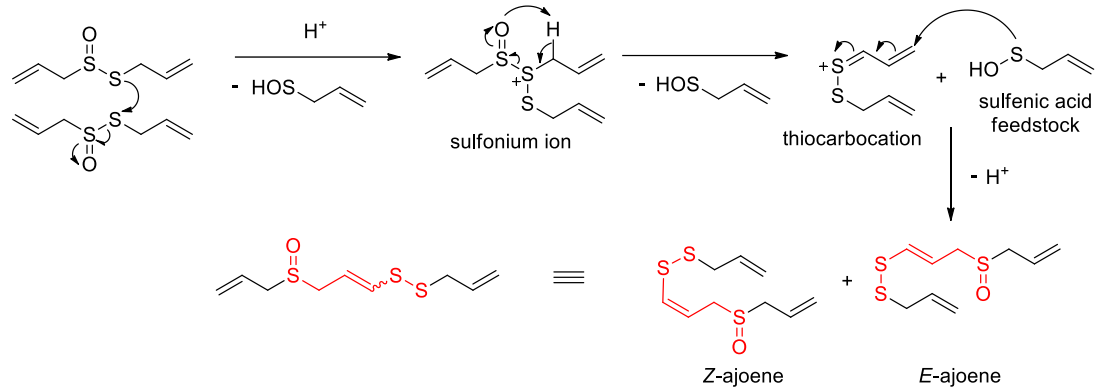

Figure 8: *Block's proposed ajoene biosynthesis*

The ajoene molecule occurs naturally as a mixture of *E*- and *Z*-isomers about the vinyl-disulfide bond. Naznin *et al.* demonstrated that freshly-crushed garlic does not contain ajoene until exposed to solvents.[28] In one study, a non-polar solvent was shown to favour the formation of *Z*-ajoene whereas a more polar system was found to favour *E*-ajoene.[39] In another study, fresh garlic preparations in vegetable oil revealed a 1:3 mixture of *E*/Z isomers, which following heating at 30 °C for three days shifted to a 1:1 ratio due to the *Z*-isomer being less thermodynamically stable (more reactive) than the *E*-isomer. Naznin *et al.* reported that the heating of garlic in rice oil for four hours gave the highest yield of ajoene (648 μg/g of garlic) in a 1:3 ratio of *E*/*Z* isomers. Lastly, it has been shown that temperatures above 100 °C lead to ajoene degradation (little *E*- and no *Z*-ajoene detected after four hours).[28] The first "total" synthesis of *E*/*Z*-ajoene was achieved by Block *et al.* in 1986 by refluxing allicin in aqueous acetone to obtain the natural product in 34% yield as a 4:1 mixture *E*/*Z*-isomers (**Figure 9**).[14] The non-selectivity of the reaction and large number of by-products renders this an inefficient synthesis. Moreover, it can't be used to access derivatives, but in spite of these limitations this low-yielding approach currently provides the only synthetic access to ajoene. The natural product displays broad-spectrum bioactivities that include the suppression of platelet aggregation *in vitro* and *in vivo,*[14] as well as activities against malaria,[40] obesity,[41,42] bacterial[43] and fungal infections[44–46] and cancer.[47–49]

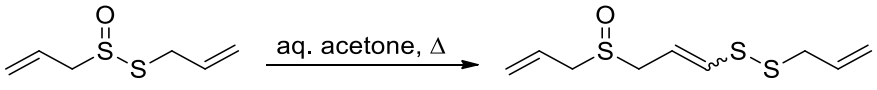

Figure 9: *Biomimetic ajoene synthesis involving the refluxing of allicin in aqueous acetone*

1.4 Garlic and cancer

Cancer is one of the leading causes of mortality worldwide and consequently there is much interest in garlic's cancer preventative and anti-cancer activity.[50] The pathogenesis of cancer was popularised by Hanahan and Weinberg (in 2000 and 2011) when they specified eight distinct cellular features that govern its development.[51,52] These include: self-sufficiency in growth signals, insensitivity to growth-inhibition signals, evasion of programmed cell death, limitless replicative potential, sustained angiogenesis, tissue invasion and metastasis, reprogramming of energy metabolism and evasion of immune destruction. The complex interplay between these cellular mechanisms implies that successful cancer therapies have to manipulate multiple targets in order to combat this adaptive and durable disease.

During the past thirty years epidemiological studies have looked into the nutraceutical potential of garlic as a cancer preventative agent in populations spanning from China and Europe through to the Americas. Many of the studies have demonstrated a reciprocal relationship between garlic intake and cancer incidence primarily of the gastrointestinal tract. Multiple meta-analyses of the pooled data, however, have exposed a lack of uniformity in the garlic preparations, heterogeneity in test groups and other biases.[7] It is well known that garlic OSC's can exert direct cytotoxic effects on cancer cells by inhibiting proliferation and inducing apoptosis.[53] Allicin[54], dialkyl sulfanes[55,56] and ajoene[57] have all been shown to illicit pro-apoptotic responses by causing mitochondrial perturbations that lead to caspase-mediated signalling events, as well as concurrently down-regulating anti-apoptotic pathways involving Bcl-2.[58] The anti-proliferative activity of garlic OSC's may in part be related to their ability to induce G_2/M cell cycle arrest.[59,60] Some investigations on ajoene[61] and DADS[62] have linked the generation of reactive oxygen species (ROS) to both of the aforementioned intercellular stress events.[63,64] Furthermore, studies have indicated that garlic OSC's may primarily act as oxidative thiolating agents that can form mixed disulfides with low molecular weight thiols, such as cysteine[65,66] and glutathione.[64,67] In a cellular context, a disulfide exchange with a key protein target, as seen in **Figure 10**, will lead to alterations in signalling pathways which in combination with secondary downstream events may affect the initiation, promotion and the progression of tumour cells.[30]

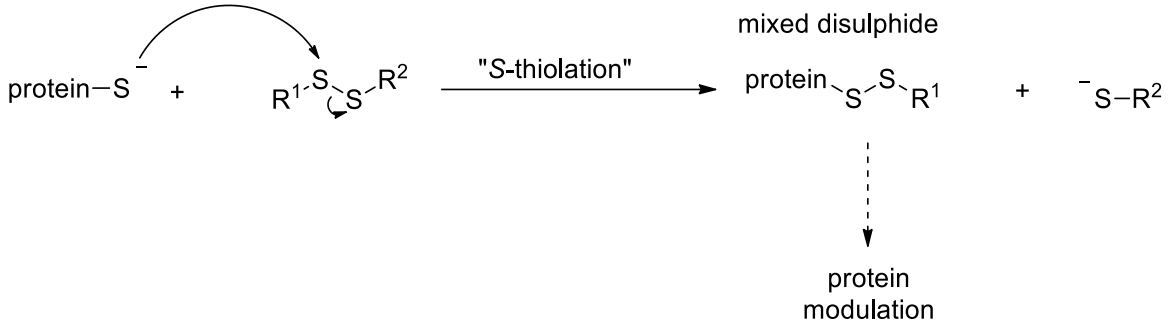

Figure 10: *Thiol-disulfide exchange between an OSC and a target protein*

1.5 The *S*-thiolation of protein targets by garlic compounds

Seminal work conducted by Wills in the 1950's showed that allicin rapidly *S*-thiolates and inhibits the plasma proteins papain and alcohol dehydrogenase via a mixed disulfide exchange reaction within the active site of the enzyme.[68] Seki *et al.* demonstrated that DATS can directly oxidise cysteine residues on *β*-tubulin, resulting in disruption of the microtubule network during early mitosis.[37,69] In each case the garlic compounds are proposed to *S*-thiolate a reactive cysteine residue on a protein.

This mixed disulfide reaction is well known in biological systems to involve the small molecule thiol glutathione (GSH) in which the tripeptide GSH represents the major thiol-disulfide redox buffer in eukaryotic and some prokaryotic cells. The glutathione-dependent redox cycle utilises GSH in its reduced form to scavenge ROS in which it forms the enzymatically-reversible disulfide conjugate GSSG. In addition, both GSH and GSSG are able to *S*-thiolate redox sensitive cysteine residues on proteins to form a GSH-protein adduct.[70] This process of *S*-glutathionylation, illustrated in **Figure 11,**[71] is an important post-translational modification involved in cell redox signalling while concomitantly protecting free thiol residues from irreversible oxidative damage.

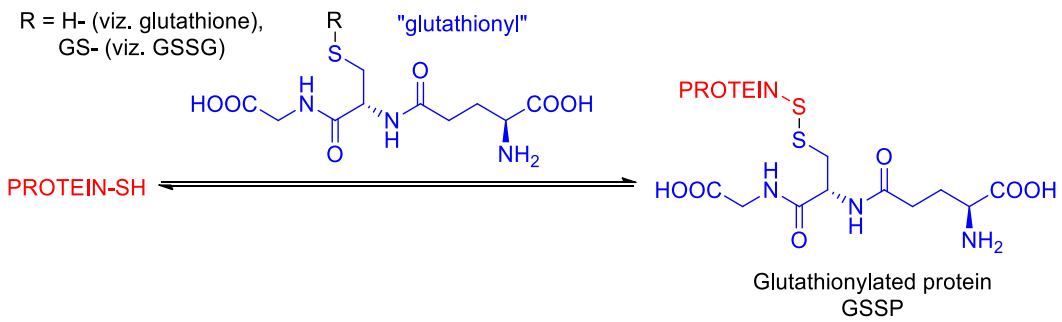

Figure 11: *Glutathionylation of a redox sensitive protein*

Although OSC's most probably affect the GSH:GSSG redox cycle by forming oxidative S-S adducts with the reduced GSH thiol, the high millimolar cellular concentration of GSH versus the micromolar cytotoxicity of OSC's are indicative of additional targets being involved other than GSH. Since OSC disulfide pharmacophores are able to *S*-thiolate proteins in an analogous manner to *S*-glutathionylation, there may be overlap between the protein targets. **Table 1** lists a selection of proteins that are targets of glutathionylation.[69,72]

Table 1: *Proteins which are S-glutathionylated by GSH/GSSG*

HSP70-9B (mortalin-2)	*Stress-induced phosphoprotein 1*	*Tubulin*
Theoredoxin-1	*HSP60*	*Peroxiredoxin 1*
Protein-disulfide isomerase	*Peptidylprolyl isomerase*	*RNA-binding protein regulatory subunit*
Glutaredoxin	*Profilin*	*Myosin*
Haemoglobin	*Aldolase*	*Triosephosphate isomerase*
Actin	*Cytochrome c oxidase*	*Vimentin*

Research at UCT has identified that garlic OSC's may act as GSSG mimics to affect the redox state of the cell. Experiments by Pinto *et. al.* demonstrated that the allyl-sulfur compound 2-propenyl thiosulfate can spontaneously react with GSH under physiological conditions to form *S*-allyl-GSH, which itself is able to inhibit proteins with cysteine (Cys) in their active or allosteric site. To date, only a handful of garlic OSC-protein interactions have been specifically identified and these are listed in **Table 2**:

Table 2: *Currently identified garlic OSC protein targets*

Protein target	Garlic compound(s)
β-tubulin[37,59,73]	DATS, SAMC, *Z*-ajoene
Glutathione reductase[74]	Ajoene
Sulfur transferase[64]	2-PTS
Rhodanase[75]	2-PTS
Gastric lipase[76]	Ajoene
Intergrin α4β1[77]	Ajoene
Phase II enzymes (GST, UGT)[78,79]	DATS

1.6 Ajoene – a superior thiolating agent

A paper by Gallwitz in 1999, highlighted ajoene as a potential glutathione disulfide (GSSG) mimic by reporting that ajoene covalently modifies the glutathione reductase enzyme by forming a mixed disulfide with its cysteine active site, which results in enzyme inhibition.[80] Based on this evidence it is hypothesised that garlic OSC's that contain a disulfide or polysulfide functional group, can undergo a thiolysis exchange with a suitable cysteine thiol. A thiol-disulfide exchange, aka. thiolysis, involves the nucleophilic attack of a thiolate (red in **Figure 12**) at the sulfur of a disulfide bond to form a trisulfide intermediate that shares the negative charge across all sulfur atoms. Thereafter, a disulfide is produced along with a thiolate leaving group (blue in **Figure 12**). The formation of the intermediate, which is governed by the nucleophilicity of the thiolate and the electrophilicity of the sulfur of the disulfide, is kinetically controlled, while the formation of the thiolate nucleophile and the expulsion of the leaving group are governed by thermodynamic principles.

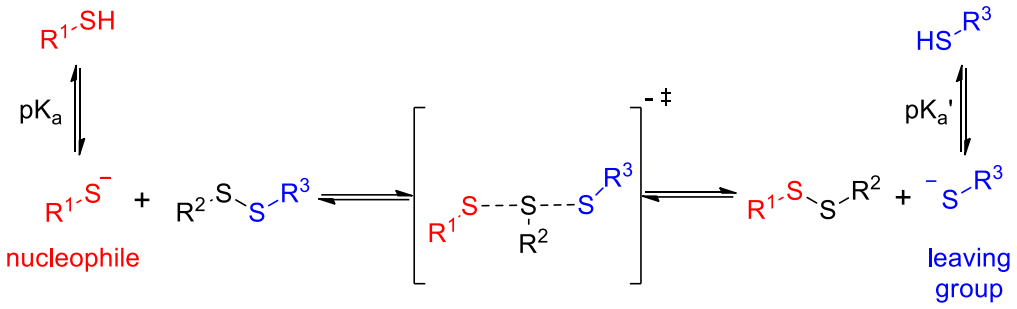

Figure 12: *Mechanism of a thiol-disulfide exchange reaction*

In **Figure 12** above the cysteine thiolate represents the reactive nucleophile, and its formation is governed by its ionizability (pK_a).[81] In the laboratory, the thiolate can be generated by the addition of a base, whereas within a cellular setting this is achieved by the basicity of the protein microenvironment. Free cysteine has a pK_a of 8.3-8.5, and is predominantly protonated at physiological pH (approximately 7), making it a poor nucleophile. Within a protein reactive cysteine thiol groups are influenced by adjacent electron-rich and charged amino acid residues. These can stabilise the thiolate anion and effectively lower its pK_a to shift the equilibrium towards the thiolate, which is a potent nucleophile.[82,83] In certain enzyme active sites, cysteine thiols are reported to have pK_a values as low as 3.4.[84] In spite of this, once the thiolate is formed it remains the protein's only reaction contributor (incoming nucleophile) and thus the electrophilicity and steric accessibility of the OSC disulfide is what actually governs the rate of reaction. Most garlic OSC's contain symmetrical disulfides which do not involve any regioselectivity in thiolate attack. In contrast, ajoene and 1,2-dithiin contain a vinyl-disulfide, which presents a regioselectivity question regarding the site of nucleophilic attack (See **Figure 13**).

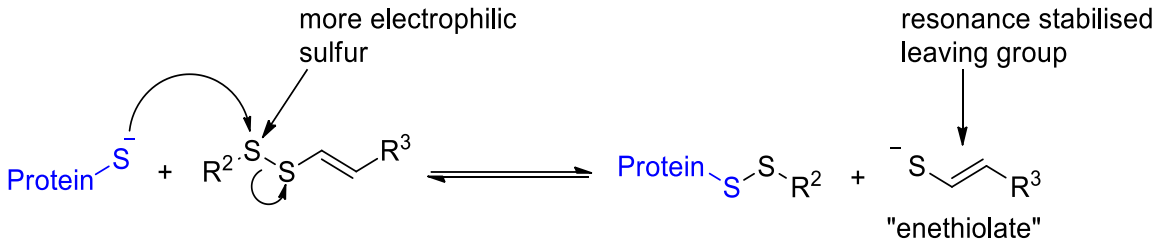

Figure 13: *Regioselectivity of the disulfide exchange with ajoene*

This regioselectivity is determined by the relative electrophilicities of the two sulfur atoms (non-vinyl and vinyl), which in turn links with thiolate leaving ability. With ajoene, the favoured leaving group is the resonance-stabilised enethiolate in preference to the

unconjugated sulfide; hence, regioselective attack proceeds at the non-vinyl sulfur. For this reason ajoene is a superior thiolating agent compared to other garlic OSC's because of the stabilised leaving group favouring the thermodynamics of the exchange. Furthermore, it is proposed that ajoene may also compete with GSSG in exchange reactions with site-specific redox sensitive cysteine residues in protein targets (See **Figure 13**). This aspect has a powerful bearing on the Results and Discussion section (Chapters Three and Four) of this thesis.

Chapter Two: Ajoene Research at the University of Cape Town

This Chapter will review previous work carried out in the University of Cape Town (UCT) group that has relevance to research work described in this thesis.

2.1 Synthesis of ajoene analogues

With a particular interest in the anti-cancer activity of potential ajoene analogues, in 2008 our laboratory at UCT published a four-step synthetic route to access end-substituted ajoene analogues in an overall 30% yield.[66,85] The synthetic route is displayed in **Figure 14** and will be described in the following section.

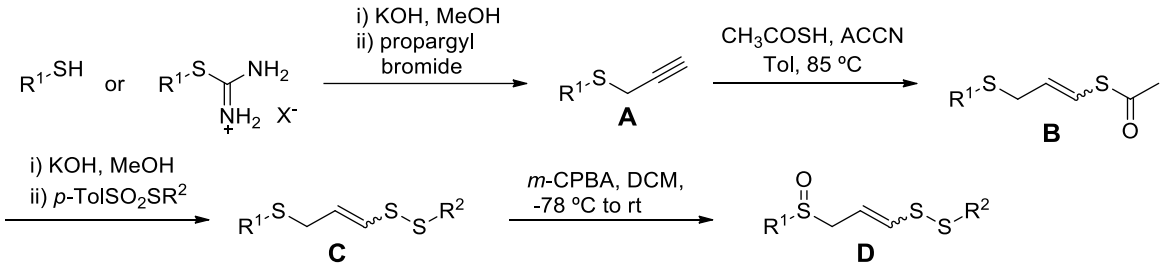

Figure 14: *Synthesis of doubly-end substituted ajoenes*

2.1.1 Step one: Propargylation

Figure 15 shows the first step involving the *S*-propargylation of an appropriately R^1-substituted thiolate in which the R^1-group ends up on the sulfoxide end (left-hand side) in the final ajoene molecule. In the case of a commercially available R^1-substituted thiol, standard propargylation conditions (KOH, propargyl bromide, MeOH) affords thioether **A**. Alternatively, it is possible to access the thiol by first preparing an isothiouronium salt by refluxing a suitable R^1-substituted alkyl halide and thiourea in acetonitrile, as depicted in **Figure 16**. The filtered and washed salt is then hydrolysed *in situ* to generate the thiolate, which is similarly propargylated to form the desired R^1-substituted thioether **A**. Yields in this step are high (> 90%).

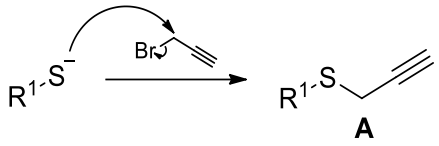

***Figure 15**: Thiolate propargylation*

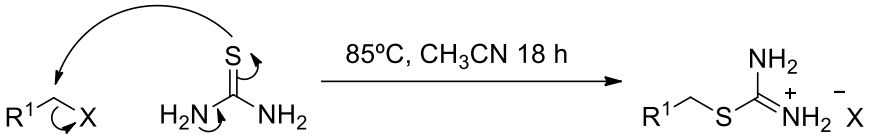

***Figure 16:** Isothiouronium salt preparation*

2.1.2 Step two: Radical addition

The second step was inspired by a reaction pioneered by Kampmeier[86] that was published in *JACS* in 1965 in which it was shown that thiolacetic acid undergoes a regioselective radical addition to the terminus of 1-hexyne due to the formation of the more stable vinyl radical intermediate (*vide infra*). The regioselective addition of thiolacetic acid to thioether **A** (**Figure 14**) was the key step of our sequence, as it generates a protected vinyl-sulfide relevant to the target. For the radical addition, ACCN (1,1′-azobis(cyclohexanecarbonitrile) is used as the radical initiator. It is a member of the azobis-family of radical initiators and by virtue of its labile 1,1'-azobis core undergoes thermal radical cleavage at 85°C to give an active α-cyano radical.[87] In the initiation step, this α-cyano radical abstracts a proton from thiolacetic acid. For the propagation steps the resultant thiyl radical then regioselectively adds to the alkyne terminus of the propargylic thioether **A** to form a vinyl thioacetate radical. The vinyl thioacetate radical then abstracts a proton from thiolacetic acid to afford the desired stereoisomeric vinyl thioacetate **B** as a mixture of *E*:*Z* isomers in a ratio of approximately 1:2. The predominance of the *Z*-isomer was welcomed in view of its higher bioactivity.[65] This step propagates the chain reaction, since it regenerates another thiyl radical. Reduction of the *Z*-thioacetate radical intermediate is sterically less demanding than that of the *E*- and thus the *Z*-isomer is formed faster than the *E*-isomer (kinetic control). Undesirable termination involves dimerization of two thiyl radicals to form a disulfide diacetate by-product, **B'**, as shown in **Figure 17**. Yields for this step of the sequence vary depending on the substrate, but are generally around 60-70%. The preparation of the natural product ajoene itself is not possible via this route owing to a suspected intramolecular

cyclisation (5-*exo*-trig or 6-*endo*-trig) involving the allyl-substituent (R^1 = allyl) during the radical addition step.

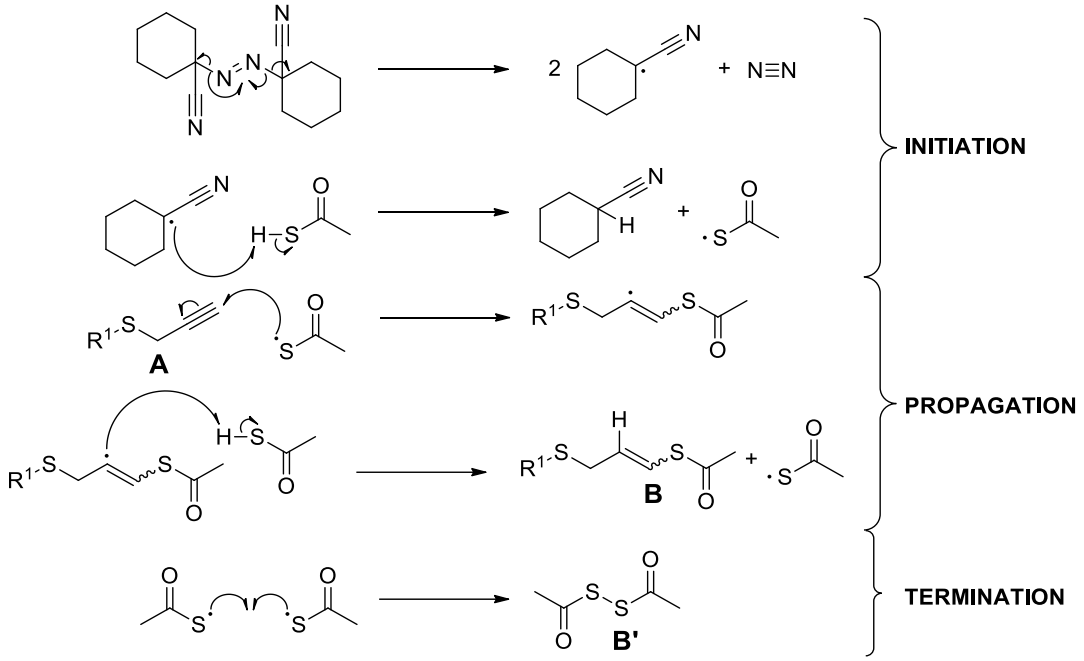

Figure 17: *Proposed mechanism of radical addition of thiol acetic acid to the terminus of alkyne* ***A*** *to form of thiolacetic acid* ***B***

2.1.3 Step three: Sulfenylation

The vinyl-disulfide formation step was inspired by work by Brandsma who demonstrated sulfenylation of a base-generated thiolate by an alkyl alkanethiosulfonate.[88] In the ajoene case a -SR^2 substituent is introduced into the right-hand side (disulfide end) of the ajoene molecule in the form of the vinyl-disulfide pharmacophore, **Figure 18**. This reaction represents the second key step in the synthetic sequence as it also influences the *E*:*Z* outcome of the ajoene product. From a practical perspective, thioester **B** is first hydrolysed with KOH to generate an enethiolate anion. Thereafter, the enethiolate is sulfenylated at its soft sulfur end with the R^2-substituted *p*-toluenethiosulfonate (sulfenylating agent) to afford vinyl-disulfide **C**. The ratio of *E:Z* (1:2 in **B**) doesn't change significantly towards favouring the *E*-isomer when the temperature is kept low (less than 0 °C). However, at higher temperature isomerization can occur, presumably via the thioaldehyde tautomer undergoing a bond rotation about the C_α-C_β axis to enrich the thermodynamically more stable *E*-isomeric form after enethiolate regeneration, as shown in **Figure 19**. Yields for the overall transformation to afford **C** were usually fairly acceptable in the region of >75%.

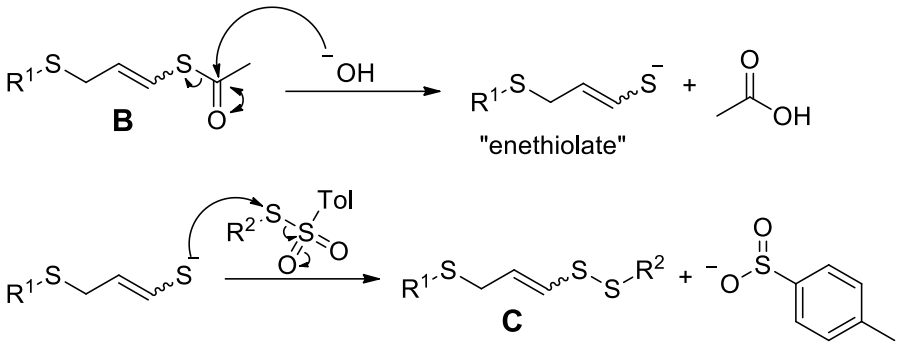

Figure 18: *Pharmacophore generation via low temperature S-alkylation*

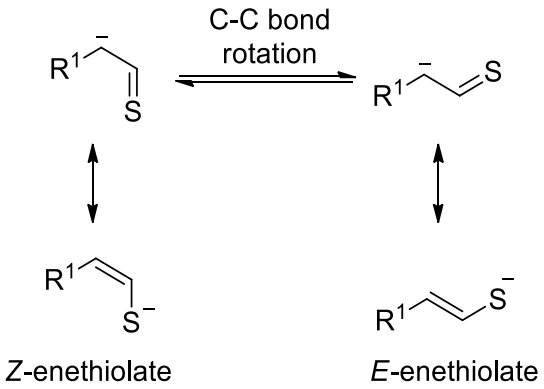

Figure 19: *Tautomeric shift of enethiolate*

2.1.4 Step four: Oxidation

The final step in the ajoene analogue synthesis involves a low-temperature chemoselective oxidation, as shown in **Figure 20**. By reacting **C** with a molar equivalent of *m*-CPBA at low temperature (-78°C), only its most nucleophilic (sulfide) sulfur is oxidised to afford the sulfoxide **D**. The sulfoxide is produced as a racemate, and its stereogenic nature is observed in the ^{1}H-NMR spectrum of the product **D** in form of diastereotopic splitting for its α-proton signals, which allowed unambiguous assignment of the chemoselective site of oxidation. The *E:Z* ratio was retained from **C** within experimental (column chromatography) consideration. Yields for this step were normally around 75%.

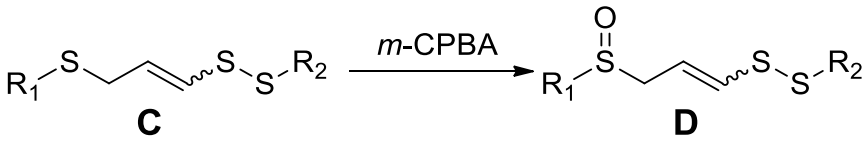

Figure 20: *Chemoselective sulfide oxidation*

2.2 Structure-activity relationships: cytotoxicity of ajoene in cancer cells

In the 2008 study, the ajoene analogues synthesised by the UCT route were tested for their anti-proliferative activity against WHCO1 oesophageal cancer cells and a structure-activity profile generated. The results revealed that activity was retained when varying the R^1/R^2 end-groups (**Figure 21**).

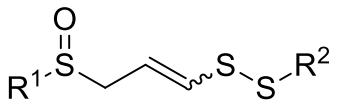

Figure 21: *General structure of substituted ajoenes developed at UCT* [66,85]

This important finding revealed that the pharmacophore does not reside within the terminal allyl groups of ajoene. Interestingly, it was also shown that end-group substitutions at R^1 and/or R^2 were found to modulate activity, with some analogues showing an improved activity compared to ajoene,[66,85] due to an increase in lipophilicity. Also, a stereochemical bias was observed, with the *Z*-isomers consistently showing a very moderate (about 1.5 fold) increase in activity over the corresponding *E*-isomers, supporting the importance of geometrically-specific protein-binding interactions in their bioactivity.[60] In some cases, it was not possible to separate the individual *E*- and *Z*-ajoene isomers by chromatography, particularly in compounds containing aromatic rings, and in these cases, the IC_{50} was reflected as the activity of the *E/Z*-mixture.[66] It is worth noting that these ajoene derivatives also showed an improved shelf-life stability over ajoene. The most active analogue was found to be a *bis*-paramethoxybenzyl substituted ajoene, called *bis*-PMB (R^1/R^2 = PMB), which displayed a twelvefold increase in activity compared to the natural product ajoene (**Table 3**). The modulatory role of the end-groups pointed towards the pharmacophore residing within the backbone of the ajoene molecule which was validated by synthesising a mini-library where each of its three functional groups, namely the sulfoxide, vinyl and disulfide, were varied individually. Owing to its improved stability and activity compared to ajoene, *bis*-PMB was chosen as the lead for this elucidation study. **Table 3** shows the cytoxicities against WHCO1 cells of the synthetically modified analogues (**Entries 6-10**).[66]

Table 3: *Structure activity pharmacophore analysis of bis-PMB regarding inhibition of WHCO1 cell proliferation*

Entry	Name/descriptor	Structure	WHCO1 IC_{50} ± SD (µM)
1	ajoene	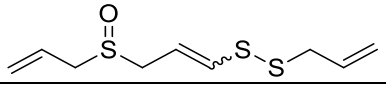	*Z*: 25.0 ± 2.8 *E*: 39.0 ± 7.8
2	propyl-allyl ajoene	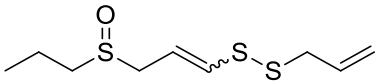	*Z*: 23.0 ± 4.2 *E*: 37.0 ± 4.5
3	propyl-propyl ajoene	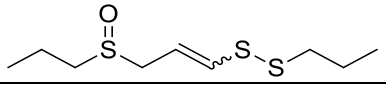	*Z*: 18.0 ± 4.1 *E*: 24.0 ± 2.8
4	PMB-allyl ajoene	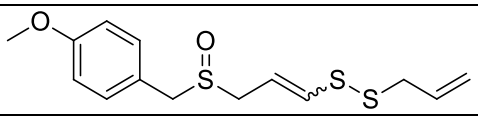	*E*/*Z*: 7.4 ± 0.7
5	*bis*-PMB ajoene	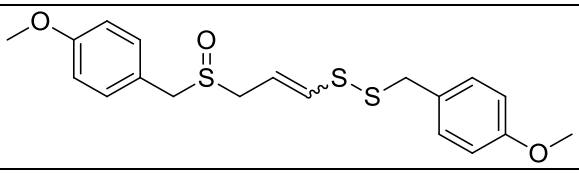	*E*/*Z*: 2.1 ± 0.4
6	*bis*-PMB sulfide ajoene	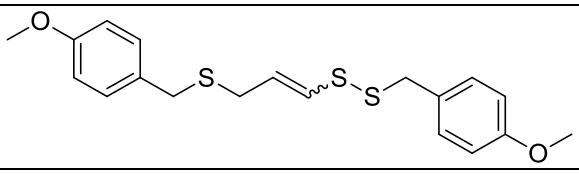	*E*/*Z*: 0.7 ± 0.3
7	*bis*-PMB dihydroajoene	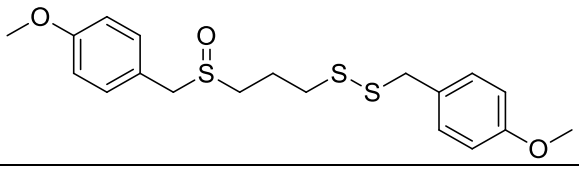	16 ± 3.7
8	*bis*-PMB sulfide dihydroajoene	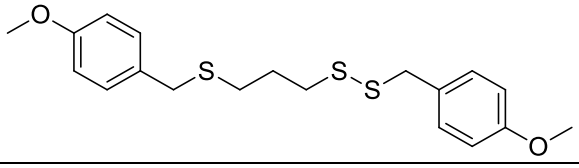	> 200
9	*bis*-PMB sulfoxide vinyl-sulfide	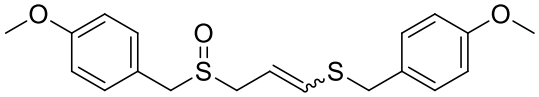	*Z*: >200 *E*: >200
10	*bis*-PMB sulfide vinyl-sulfide	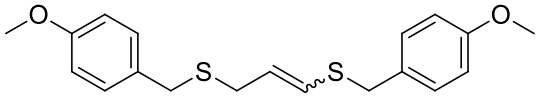	*E*/*Z*: > 200

Entry 6, the *bis*-PMB analogue with the sulfoxide removed, retained anti-proliferative activity indicating that the sulfoxide is not the pharmacophore. Surprisingly, this analogue showed the highest activity of the series (including its parent *bis*-PMB). The removal of the doubled bond (*bis*-PMB dihydroajoene) led to a decreased activity (**Entry 7**) due to less stabilization of the anion in the exchange. These results highlight that the sulfoxide and the double bond, on their own, play a modulatory role and are thus not essential for activity. The removal of both the sulfoxide and vinyl-disulfide resulted in

loss of activity below 200 μM which implies that there is synergism between the sulfoxide and the double bond that governs disulfide thiolysis. Substitution of the disulfide by a sulfide (**Entries 9-10**) resulted in a loss of activity below the highest tested concentration of 200 μM, proving that the disulfide is the pharmacophore.

In summary, the ajoene synthesis developed in our laboratory has enabled access to ajoene analogues such as "*bis*-PMB" that are more potent in their ability to kill cancer cells, with cytotoxicity comparable to that of current clinical cancer therapeutics.[66] The SAR study has laid the foundation for probing the mechanism of action of ajoene in cancer cells, as well as for developing further ajoene analogues with enhanced bioactivity in a medicinal chemistry context.

2.3 Development of *bis*-PMB as a cancer therapeutic lead

There are a number of studies that have previously looked into the bioavailability and metabolism of garlic in the context of a medicinal chemistry development. Lawson *et al*. conducted investigations on subjects who had ingested 25 g of raw garlic (~ 60 mg allicin). Following ingestion, no allicin was detected in either serum or urine from 1 to 24 hours after consumption.[27,89] Similarly, breath analysis of a 90 kg man who had ingested 38 g of raw garlic showed no detectable allicin upon exhalation. Various second-generation OCS's, such as DADS, DATS and other dialkyl disulfanes, as well as acetone, have been identified as the major metabolites.[90] In a study conducted by Egen-Schwind *et al*., allicin was perfused through an isolated rat liver and found to be completely metabolised to DADS and *S*-allyl mercaptan (SAM) after the first pass through the organ. The further breakdown products ajoenes and vinyldithiins were also recovered in the perfusion medium (Krebs-Henseleit buffer). Akin to the behaviour in the hepatic and gastrointestinal system, allicin rapidly disappears from the blood after injection.[91] In contrast, the second-generation OSC's showed higher half-lives in blood. Specifically, ajoene and DATS were recorded as 1 and 4 minutes, while 1,2-vinyldithiin, DADS and 1,3-vinyldithiin had half-lives of 15, 60, and >120 minutes, respectively.[92] These findings highlight that the introduction of garlic OSC's into a biological system results in a complex metabolic behaviour, and that allicin, owing to its blood instability and first pass effect through the liver, cannot be the bioactive principle from garlic, except if the bioactivity occurs before the compounds reach the liver or blood (i.e. in the GI tract).[91] Allicin contains a reactive thiosulfinate group which can be viewed as an activated disulfide,

implying that it is very susceptible to thiolysis *in vivo*. Its longer-lived *in vivo* metabolites are probably the bioactive principles of the systemic circulation.

Although it has been shown that ajoene has a low half-life in blood,[93] there are two reports in which ajoene is reported to be active at inhibiting tumour xenograft formation *in vivo.* In the first study, daily intraperitoneal injections of *Z*-ajoene into mice with hepatocarcinoma 22 (4 mg/kg) and sarcoma 180 (8 mg/kg) xenografts, over twelve days, showed a 42% and 32% reduction in tumour size respectively.[59] In the second study, mice with B16/BL6 melanoma cell xenografts showed a 90% reduction in tumour size after 28 days when *E/Z*-ajoene was administered intravenously (25 mg/kg of bodyweight, daily).[94]

With the ajoene analogue *bis*-PMB showing excellent *in vitro* cytotoxicity against cancer cell lines, as well as reports on the bioactivity of ajoene *in vivo*, in a previous project to this MSc it was decided to test *bis*-PMB in a preclinical animal model for cancer. In this experiment, nude mice with WHCO1 xenografts were treated with daily intraperitoneal injections of *bis*-PMB (8 mg/kg) in 20% DMSO/intralipid for four weeks. Interestingly, no significant change in tumour size was observed between the control and treated groups of mice. This result was surprising based on the excellent *in vitro* activity of *bis*-PMB as well as the literature reports supporting the *in vivo* activity of ajoene. Therefore the experiment was followed up by conducting a pharmacokinetic HPLC study of *bis*-PMB in a nude mouse. **Figure 22** illustrates how the blood concentration of *bis*-PMB was found to rapidly decrease following intravenous injection into a mouse, implying very poor metabolic stability. Furthermore, it was observed that the mice had difficulty breathing and that the blood samples had turned dark purple.

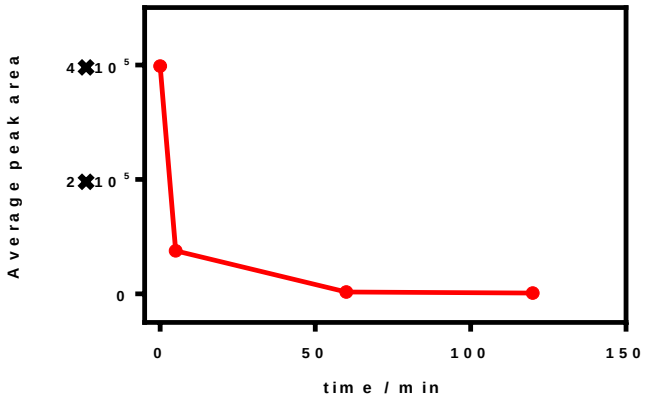

Figure 22: *Concentration of intravenously administered bis-PMB versus time in pharmacokinetic trails on a mouse as measured by HPLC*

In order to further probe the interactions between *bis*-PMB and blood, an *in vitro* blood stability test was conducted. Here, fresh blood was collected from mice and separated into plasma and red blood cell (erythrocyte) fractions. These different fractions were incubated with *bis*-PMB, and the resultant stability is shown in **Figure 23** as quantitated by LC-MS. The results revealed that *bis*-PMB had poor stability in the presence of erythrocytes but good stability in plasma.

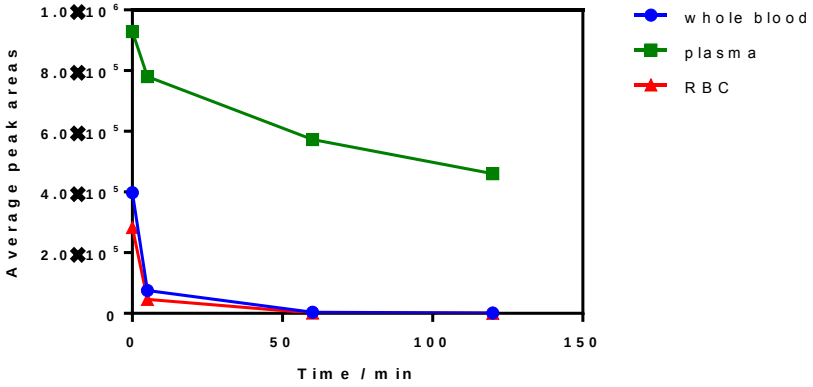

Figure 23: *Concentration of bis-PMB in whole blood, plasma and red blood cell (RBC) fractions over time*

Hence, in the first part of this thesis the aim was to better understand the pharmacokinetic profile of *bis*-PMB and to improve its blood stability while retaining its strong cytotoxicity.

2.4 Dansyl-labelled ajoene

In order to track the movement of ajoene in cancer cells, an ajoene probe with a fluorescent dansyl tag was synthesised by Cotton.[95] This derivative allowed visualisation and tracking within the cell using confocal laser spectroscopy, which revealed strong activity in the ER (Endoplasmic Reticulum). Crucial to the design of the probe was application of our mechanistic understanding of the regioselectivity in the disulfide exchange, resulting in placement of the dansyl label on the more electrophilic non-vinyl sulfur end of the molecule, as seen in **Figure 24**:

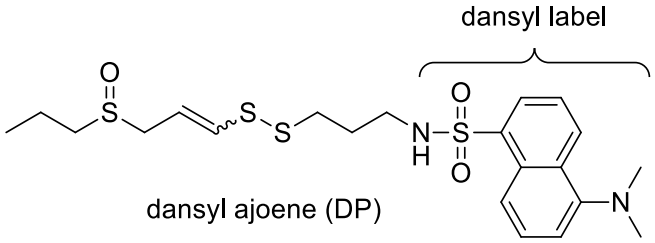

Figure 24: *Dansylated ajoene probe*

In agreement with the previous structure-activity findings, the dansyl-ajoene (DP) was found to be fully active at inhibiting proliferation and inducing apoptosis in MDA-MB-231 human breast-cancer and in WHCO1 human oesophageal-cancer cells with an IC_{50} similar to that for ajoene. The transfer of the dansyl label during protein-ajoene exchange was envisioned to proceed as illustrated in **Figure 25**:

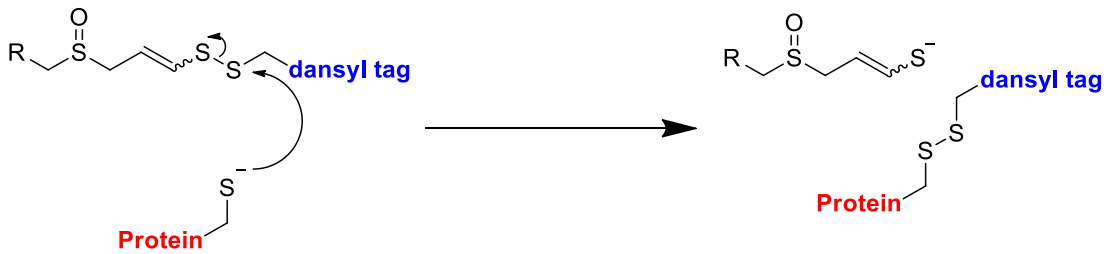

Figure 25: *Transfer of dansyl tag to a protein target by S-thiolation*

In addition, an analysis of the cell lysate by western blot (WB) analysis allowed a cursory insight into the protein targets involved. As expected, lysates collected from MDA-MB-231 cells treated with the dansyl-ajoene probe (DP) (25 μM), for 6 and 24 hours, were found to contain many dansyl-labelled protein targets under non-reducing conditions only. **Figure 26** shows the presence of dansylated targets as distinct protein bands for

both time points when probed with an anti-dansyl antibody. The control of untreated cells (UT) showed no labelled protein bands. To test whether the dansyl label was attached to the protein through a disulfide linkage, the lysate was treated with the reducing agent β-mercaptoethanol, which confirmed the presence of a disulfide linkage since no anti-dansyl active protein bands were observed in these samples. These experiments thus confirmed our hypothesis by showing that DP is able to *S*-thiolate multiple protein targets, and furthermore illustrated the reversibility of *S*-thiolation under reducing conditions.

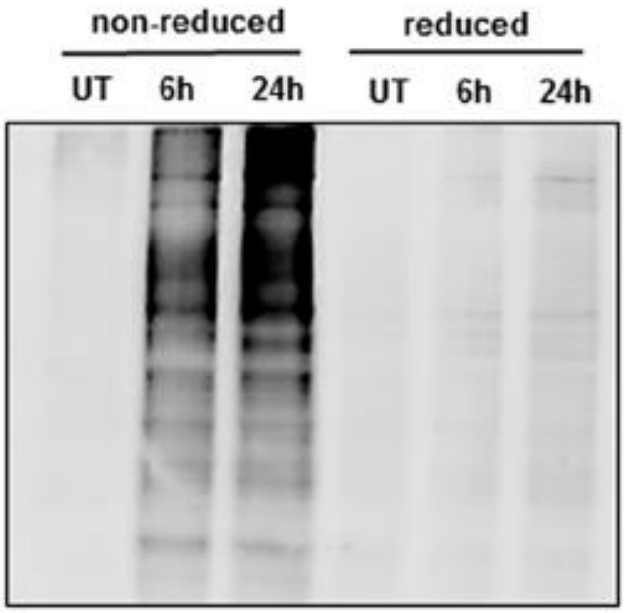

Figure 26: *Western blot showing multiple dansylated proteins in DP-treated cell lysate*[95]

These findings confirm the ajoene regioselectivity in disulfide formation with cysteine residues of cancer proteins. In order to identify the actual targets, this project envisions an alternative labelling strategy that allows for the isolation of the proteins targeted by ajoene.

2.5 The design of the biotinylated probe

In order to isolate and identify the ajoene labelled proteins in cancer cells we chose to use a more direct approach involving the synthesis of a biotinylated ajoene probe. Biotin is exploited in diverse biotechnological applications due to its stability, solubility in physiological media as well as its high affinity and specificity towards avidin.[96] The probe design took into account our understanding of the biotin / ajoene system based on an Honours project (C. Pike 2013) as well as recent literature on biotin conjugation

chemistry.[97] Based on the previously established regioselectivity of *S*-thiolation, the biotin tag was placed on the *S*-allyl side of the ajoene. It is proposed that the biotinylated protein adduct could be captured from a treated cell lysate with an appropriate avidin conjugate bound to a magnetic bead or in the form of immobilised streptavidin. Streptavidin is a tetrameric protein in which each monomer has an eight-stranded β-barrel secondary structure. Biotin binds to the interior of the respective binding pocket and therefore a spacer group is recommended between biotin and the active compound,[98] see **Figure 27**:

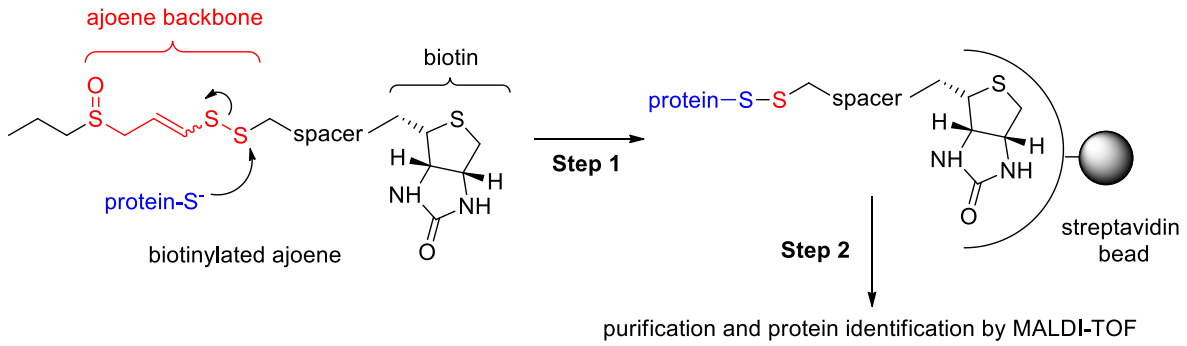

Figure 27: *Protein S-thiolation by ajoene in cancer cells*

For the synthesis of the probe, in order to avoid a potential reaction between biotin and ajoene, it was envisioned to use a convergent strategy in which the biotin and ajoene fragments would be separated by a spacer and coupled in the final step using a "Click"-strategy.[98]

In 2001, Sharpless *et al.* defined "Click chemistry" as: "reactions that are high yielding, wide in scope, create only by-products that can be removed without chromatography, are stereospecific, simple to perform, and can be conducted in easily removable or benign solvents."[99] The copper(I)-catalysed alkyne-azide cycloaddition (CuAAC) is the most successful and versatile "Click"-reaction currently available. It involves a Cu(I) catalysed regioselective [3+2]-dipolar cycloaddition between a terminal alkyne and an azide to form the 1,4-regioisomer of 1,2,3-triazole, as illustrated in **Figure 28**. The reaction may be classified formally as a cycloaddition, but is not pericyclic in nature as with the original Huisgen thermal cycloadditions. In short, the cycle starts with the formation of a copper acetylide, followed by coordination of the azide reaction partner to the copper via ligand displacement. Thereafter, an unusual six-membered copper(III) metallacycle is formed.

The ring then contracts to a triazolylcopper derivative followed by protonolysis that ends the cycle to afford the triazole product regioselectively.[100]

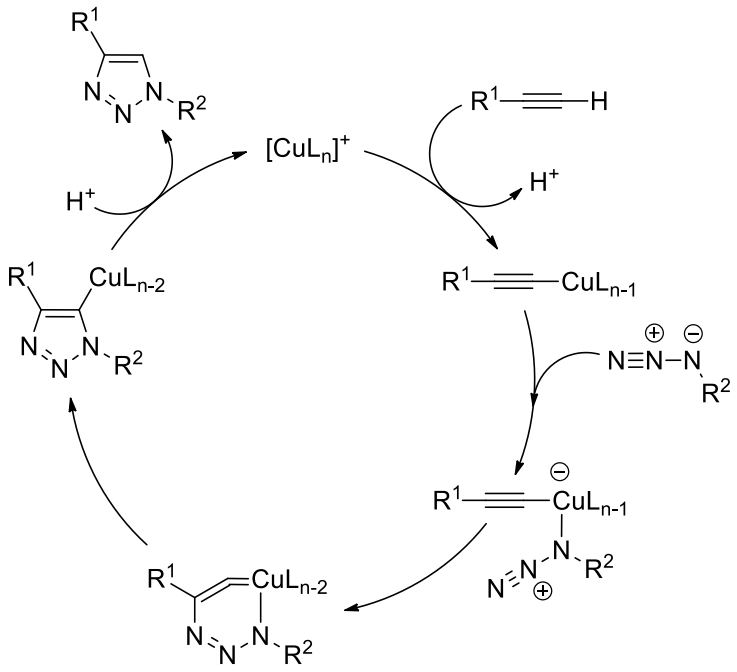

Figure 28: *Mechanism of the Copper-Catalysed Azide-Alkyne Cycloaddition (CuAAC)*

The triazole linkage is extremely stable, as it not susceptible to hydrolysis, or facile oxidation or reduction, as well as surviving MS ionization. The presence of the copper(I) catalyst increases the rate of reaction by more than 10^6-fold, compared to the uncatalysed non-regioselective Huisgen azide-alkyne 1,3-dipolar cycloaddition. In accordance with other "Click"-labelling technologies, CuAAC employs bioorthogonal reactive chemistry with high target specificity, as the azide and alkyne reaction partners have no endogenous representation in biological cells or organisms. Owing to the small size of an alkyne or azide attachment the modified molecules can be processed by enzymes while some larger labels may cause functional perturbations.[101,102] The copper(I) catalyst has proven problematic in *in vivo* studies due to its cytotoxicity. During *in vitro* trials however, the cells can be conveniently pre-treated with one reaction partner, then lysed and treated with the other "Click"-counterpart, using Cu(I) generated *in situ* by the sodium ascorbate reduction of $CuSO_4$ (Cu(II)). This strategy enables the labelling of various biological targets in their native environment. In 2012, Jezowska showed that a biotin linker equipped with an activated triple bond donor could successfully biotinylate oligonucleotides and peptides via CuAAC (Shown in **Figure 29**).[98]

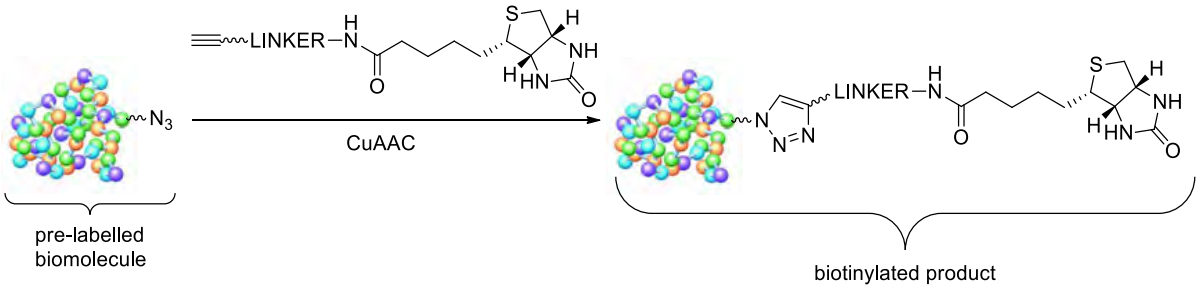

Figure 29: *In situ biotinylation of azide-labelled biological molecules*[98]

We chose to incorporate this alkyne-linker-biotin idea as part of our probe design, which required us to synthesise a suitable azide-ajoene reaction partner, full details on which will be described in the chapter on Results and Discussion (Chapter Four). **Figure 30** shows a workflow describing the two approaches of biotinylation. In the first approach the plan was to add the probe to cancer cells, hoping to biotinylate directly via a regioselective disulfide exchange. In the second approach, the plan was to pre-treat cancer cells with the azide-bearing ajoene to promote disulfide exchange followed by lysis of the cells and only then addition of the alkyne partner to the lysate to bring about the "Click"-reaction *in situ*. The use of the fully assembled probe on intact cells was thought could potentially result in compromised activity due to its large size and possible solubility issues. For this reason both approaches were considered.

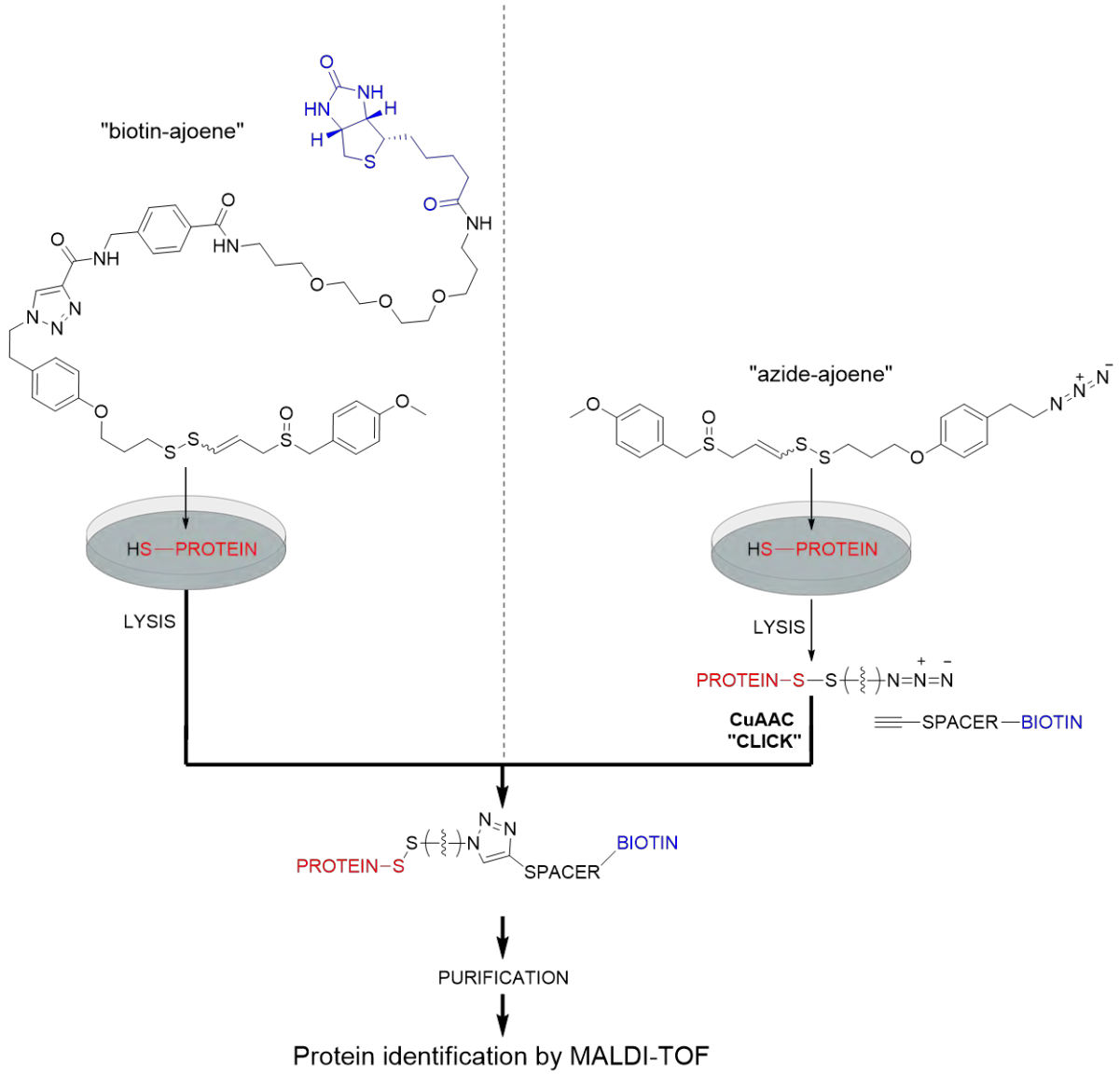

Figure 30: *The two biotinylation approaches*

2.6 Thesis hypothesis

The cytotoxicity of ajoene in cancer cells and its rapid degradation by erythrocytes is due to thiolysis exchange with reactive cysteines on target proteins within the erythrocyte or cancer cell.

Aim

To investigate the structure-blood stability relations in ajoene and to synthesise a biotinylated ajoene probe to identify the protein targets of ajoene in the cancer cell.

Objectives

- Structure-Activity Relationships of *bis*-PMB Analogues:
  - Design and synthesise a library of ajoene analogues with increased water solubility and blood stability;
  - Biological testing of the library for *in vitro* cancer cell cytotoxicity and blood stability.
- Synthesis of a Biotin-labelled Ajoene Probe:
  - Design and synthesise of a biotinylated ajoene probe using "Click"-chemistry;
  - Confirmation of biotin-ajoene cytotoxicity in cancer cells;
  - Demonstrate that biotin-ajoene is able to *S*-thiolate proteins in cancer cells directly or through its azide precursor

Chapter Three: Structure-Activity Relationships of *bis*-PMB Analogues

3.1 Introduction

The *in vitro* cancer cell anti-proliferation activity of the ajoene derivatives invited a number of mechanistic questions, as well as the possibility of evaluating their potential in drug-discovery, since the most active derivative, *bis*-PMB was about twelve times more active than the parent ajoene against an oesophageal cancer cell-line as shown in **Figure 31**:

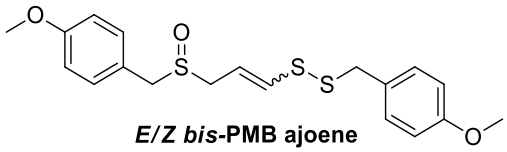

***E/Z bis*-PMB ajoene**

IC_{50} WHCO1 oesophageal cancer cells = 2.1 ± 0.4 μM
IC_{50} Z-ajoene = 25.0 ± 2.8 μM

Figure 31: *Structure of bis-PMB*

Our SAR studies on ajoene derivatives identified that end-group modifications allow retention of *in vitro* bioactivity against cancer cell lines, in which there was a correlation between the IC_{50} and the substituent lipophilicity, and it was from this study that *bis*-PMB had emerged as the lead compound for further *in vivo* experiments, with a greatly enhanced activity compared to that of ajoene. We had previously shown that synthetic ajoene analogus have up to threefold higher cytoxicity towards tumour cells than the corresponding normal counterpart.[60] The literature had reported that ajoene reduced tumour growth in mice[59,94], which prompted us to explore the activity of *bis*-PMB. However, a failure in a study by us to observe a decrease in tumour size using *bis*-PMB-treated mice, compared to the control group, necessitated a follow-up pharmacokinetic evaluation, focusing on solubility and drug half-life as likely causes of the inactivity. Although the lipophilic *p*-methoxybenzyl (PMB) substituents enhanced the *in vitro* activity their lipophilic character posed solubilisation difficulties when trying to solubilise the compound in a polar medium for administration in the *in vivo* study. A suitable injection mixture was developed using Chondroitin, PEG and DMSO, but nevertheless left the possibility that *bis*-PMB could have precipitated out once introduced into the circulatory system, rendering it "biologically unavailable" and thus undetectable. The second likely cause of inactivity was considered likely to be due to the lability of *bis*-PMB's disulfide pharmacophore by it reacting with cysteine thiol groups of blood

proteins. Hence, an SAR study was carried out designed to address the influence of these two parameters on the bioavailability.

3.2 Design of *bis*-PMB analogues

The two likely causal factors relating to inactivity were addressed by modifying the pharmacophore for the reactivity issue, and one of the end groups for the polarity, as indicated in **Figure 32**:

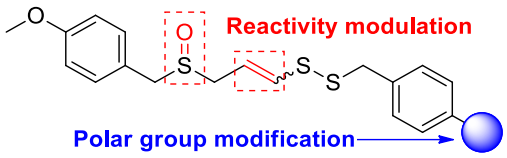

Figure 32: *Ajoene modification with respect to polarity and reactivity modulation*

3.2.1 Solubility parameter

For enhancing the aqueous solubility it was decided to replace the methoxy group of one of the *bis*-PMB groups with one having an improved hydrogen-bonding capability. Drastic changes were avoided for fear of introducing other activity issues such as conformational changes and lipopholicity changes. To this end, the methoxy methyl group was replaced by H (eg. **6**, **7**, **11** and **12** in **Figure 33** below) and an amidomethylene moiety (CH_2CONH_2) (eg. **8**, **9**, **13** and **14** in **Figure 33** below) that was expected to result in the more soluble derivative of the two. We expected the two derivatives to increase water solubility compared to ajoene while retaining the attractive lipophilic character due to the other PMB group.

3.2.2 Reactivity parameter

The reactivity parameter involved removing the double bond in order to create a dihydroajoene series. This was expected to reduce the reactivity of the disulfide as a thiolating agent in the disulfide exchange in view of reduction in stabilisation of the resultant thiolate versus the enethiolate (ajoene) leaving group. In this regard the sulfoxide functionality was considered to still provide an inductive stabilisation of the thiolate leaving group. Hence, the redox level at sulfur as sulfide or sulfoxide was also included as part of the study. The library of derivatives targeted, and ultimately synthesised, is shown in **Figure 33**:

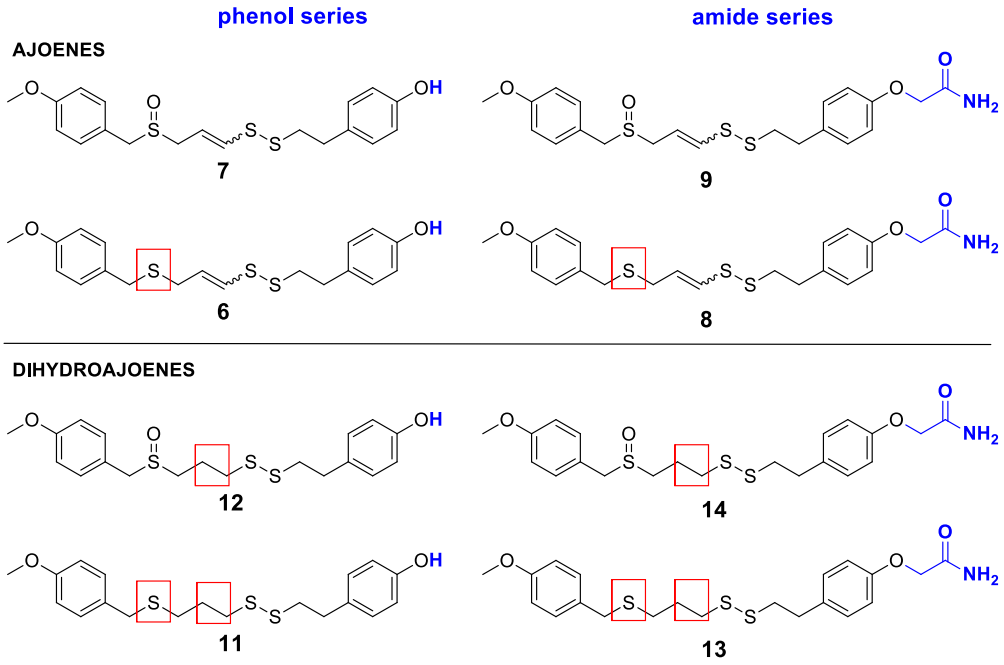

Figure 33: *bis-PMB-analogue library, showing reactivity modulations in red*

The solubility tag was most conveniently incorporated into the sulfenylating agent to be used in the UCT synthesis already described, rather than into the vinyl thioacetate segment. The dihydroajoene series was prepared using an independent sequence to the UCT ajoene derivative synthesis. The synthesis of compounds in the two series will now be independently described:

3.3 Derivative Synthesis

3.3.1 Ajoene derivatives

The retrosynthetic plan for preparing the "water-soluble" ajoenes is shown in **Figure 34**. It envisaged synthesis of fragment **2**, a *para*-methoxybenzyl analogue of the previously described (Chapter 2) vinyl thioacetate. Similarly, the ajoene vinyl disulfide pharmacophore would be obtained from disulfide bond formation between thioacetate **2** and the phenolic sulfenylating agent **5**, which in turn would be accessed from methyl (4-hydroxyphenyl)acetate in three functional group interconversion steps. The disulphide formation would be followed by divergent modification involving alkylation of the phenol hydroxyl group and/or oxidation of the sulfide to the sulfoxide.

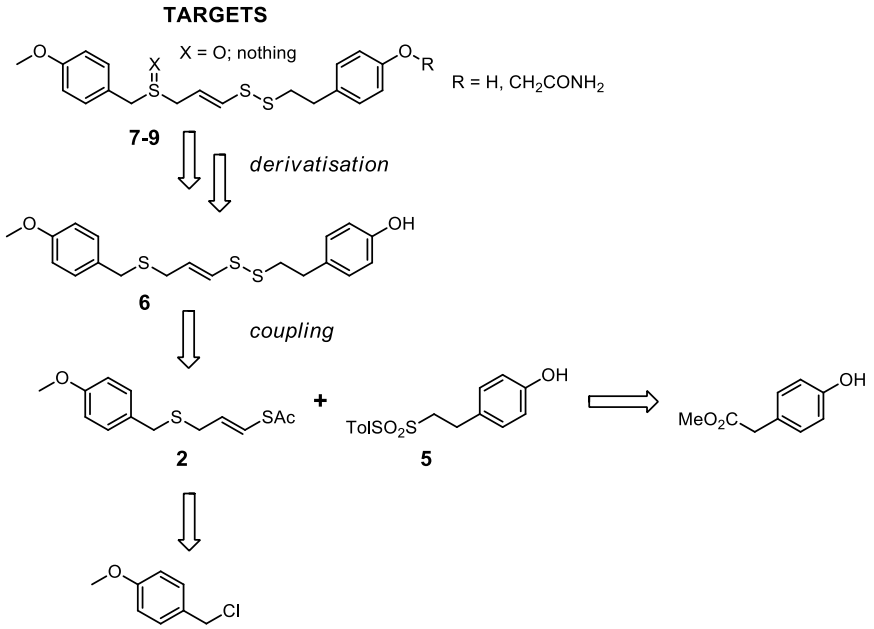

Figure 34: *Retrosynthesis of ajoene analogues with polarity modification*

3.3.1.1 Synthesis of coupling fragment **2**

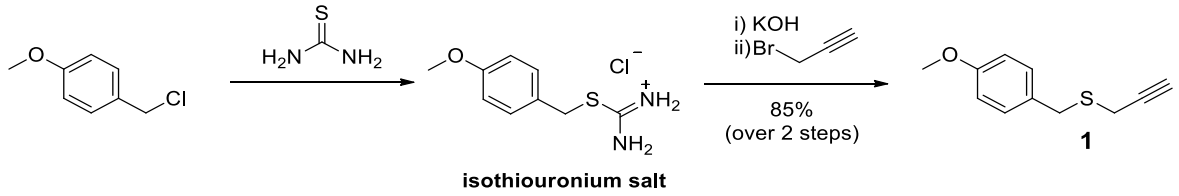

Figure 35: *Synthesis of propargylic thioether,* ***1***

The first step towards the synthesis of coupling partner **2** involved the formation of the isothiouronium salt shown in **Figure 35** by refluxing PMBCl with thiourea (1.2 eq) in acetonitrile for fourteen hours. Following cooling of the solution, the product precipitated, and this was filtered and washed with chilled acetonitrile. Without any further purification the salt was taken up in methanol, and hydrolysed with KOH (2 eq, for 2 hours at -20 °C) to generate the thiol *in situ*, which was subsequently alkylated using an excess of propargyl bromide (1.5 eq) at 0 °C to form the desired thioether **1** within 30 minutes. Purification by silica gel column chromatography afforded **1** as a clear-yellow oil in an overall 85% yield.

The ^{1}H-NMR spectrum of **1** showed propargylic methylene and terminal alkyne proton resonances as a doublet at 3.80 ppm (2H) and a triplet (1H) at 2.28 ppm, respectively. The eleven carbon atoms of **1** could be observed in the ^{13}C-NMR spectrum as nine resonances due to symmetry in the benzene ring. The diagnostic quaternary alkyne carbon (**C-8**) signal appeared at 80.1 ppm.

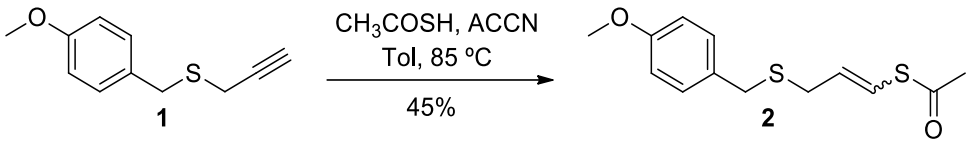

Figure 36: *Synthesis of vinyl thioacetate,* ***2***

The regioselective radical addition step proceeded as normal (Page 16) when dissolving **1** in toluene and heating the solution to 85 °C before adding the radical initiator ACCN (0.1 eq) followed by thiolacetic acid dropwise (**Figure 36**) The mixture was then refluxed for three hours. TLC analysis showed the formation of a more polar spot that was isolated by silica gel column chromatography to afford the odiferous vinyl thioacetate oil, **2**, as a 1:2 mixture of *E/Z*-isomers in 45% yield.

The IR spectrum of **2** showed a C=O stretch at 1700 cm^{-1} for the thioacetate group. Importantly, disappearance of the propargylic system in the ^{1}H-NMR spectrum was observed and the appearance of two vinylic resonances with *cis* (9.6 Hz) and *trans* (15.6 Hz) vicinal couplings, indicating that regioselective addition of the thioacetyl group had taken place to the alkyne terminus (**Figure 37**). The complete assignment of resonances (eleven for each) for each isomer in the ^{13}C-NMR spectrum could be achieved with the help of HSQC. Notably, the carbonyl carbon (**C-10**) resonated far downfield at 191.4 ppm (*Z*) and 193.1 ppm (*E*), while the vinyl carbon signals were observable at 130.3 (*Z*), 128.7 (*E*) for the α-vinyl carbon **C-9**, and 119.7 (*E*), 119.5 (*Z)* for the β-vinyl carbon **C-8**. In total, twenty two carbon resonances could be observed for the two isomers.

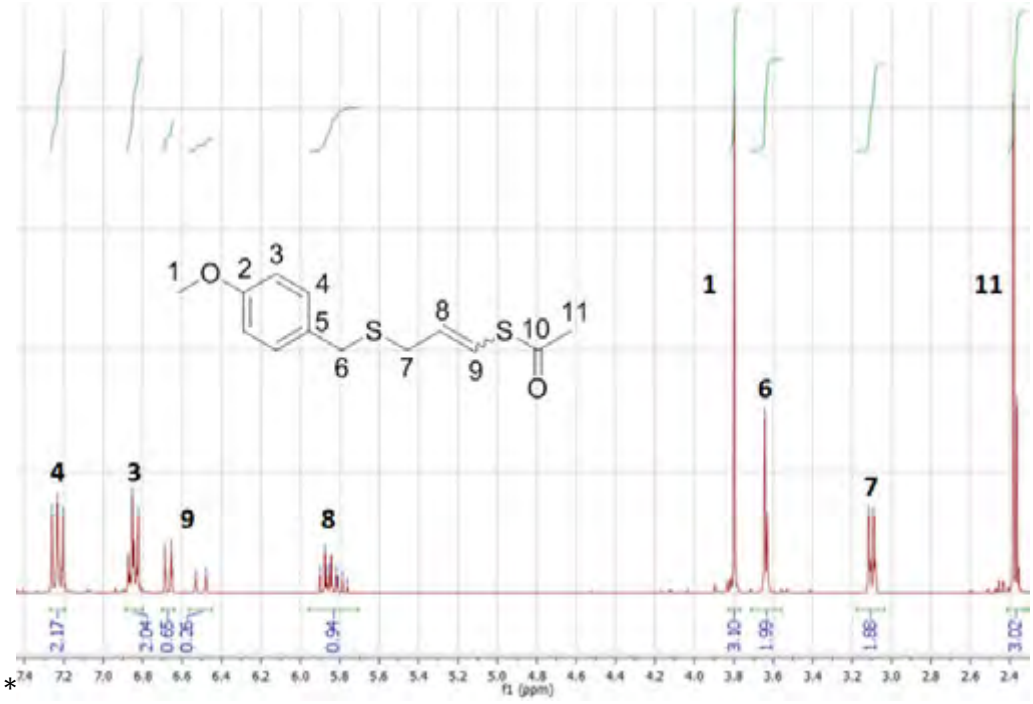

Figure 37: *^{1}H-NMR spectrum of PMB-vinyl thioacetate,* ***2***

3.3.1.2 Synthesis of coupling fragment **5**

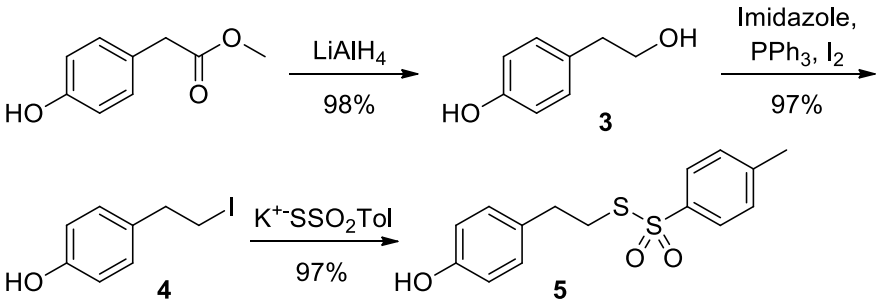

Figure 38: *Synthesis of hydroxyphenethyl thiotosylate,* ***5***

Synthesis of the coupling partner, **5**, involved applying standard functional group conversion reactions (**Figure 38**) starting with the $LiAlH_4$ (2.2 eq) reduction of commercially available methyl (4-hydroxyphenyl)acetate. This was achieved in dry THF at 0 °C, and the reaction was complete after two hours as monitored via TLC, with the formation of a single UV-active spot of higher polarity. The reaction was quenched under acidic conditions to liberate the product from the aluminium-alkoxide salts. A subsequent work-up and purification by flash chromatography yielded **3** as a colourless crystalline solid in 98% yield that could be recrystallised from EtOAc/Hexane. Its resulting melting point range of 91-93 °C corresponded sufficiently well with the literature value of 90 °C.[103]

Formation of the primary alcohol was confirmed by the ^{1}H-NMR spectrum of **3** which revealed the disappearance of the methoxycarbonylmethylene functionality (as two singlets). This was replaced by two triplets for the two vicinal methylene groups. Similarly, the ^{13}C-NMR spectrum confirmed the presence of all six expected resonances in a 4:2 aromatic:aliphatic split.

The next step involved an Appel reaction to convert the primary hydroxyl group of **3** into its iodide **4**. The reaction proceeds by activation of triphenylphosphine by reaction with iodine to give an iodophosphonium salt. The hydroxyl group oxygen attacks phosphorus to generate an oxyphosphonium intermediate with loss of HI to the imidazole. This transforms the oxygen into a leaving group, and an S_N2 displacement by iodide takes place to form the final alkyl iodide and triphenylphosphine oxide as a byproduct (**Figure 39**).

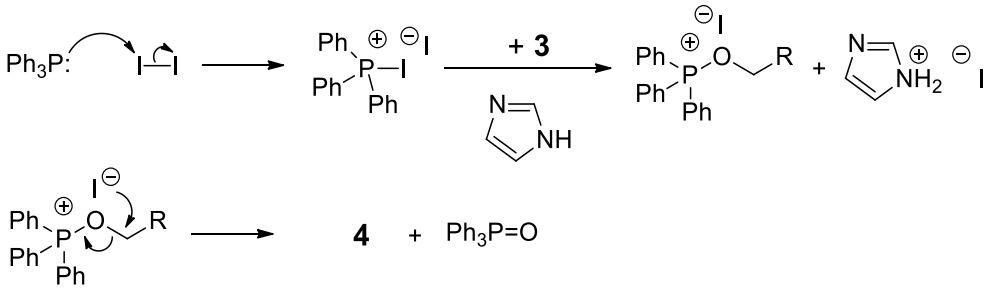

Figure 39: *Mechanism of the Appel transformation of **3** to iodide, **4***

According to TLC the reaction in THF was complete within two hours at room temperature. Purification by silica column chromatography successfully removed the triphenylphosphine oxide by-product to obtain **4** as a yellow crystalline solid in 97% yield.

The ^{1}H-NMR spectrum of **4** showed the disappearance of the alcohol hydroxyl signal of **3** together with an upfield shift of the methylene group bearing the heteroatom. In the ^{13}C-NMR spectrum the signal at 6.4 ppm represented a characteristically highly shielded iodo-alkyl carbon.

The sulfenylating agent **5** was obtained by the S_N2 reaction of **4** with an excess of potassium thiotosylate (2 eq) in DMF at room temperature overnight. Diluting the resulting reaction mixture with EtOAc and subjecting it to copious washings with H_2O

successfully removed the DMF and any inorganic by-products. Purification by silica gel column chromatography afforded **5** as a clear-yellow oil in 97% yield.

Its ^{13}C-NMR spectrum displayed eleven resonances that were assigned to the fifteen carbon atoms in the molecule. The addition of a tosyl group showed an extra set of double doublets at 7.82 and 7.34 ppm and a methyl singlet at 2.45 ppm in the ^{1}H-NMR spectrum (**Figure 40**). Lastly, the IR spectrum showed the retention of the phenolic group by virtue of an O-H stretch at 3436 cm^{-1}.

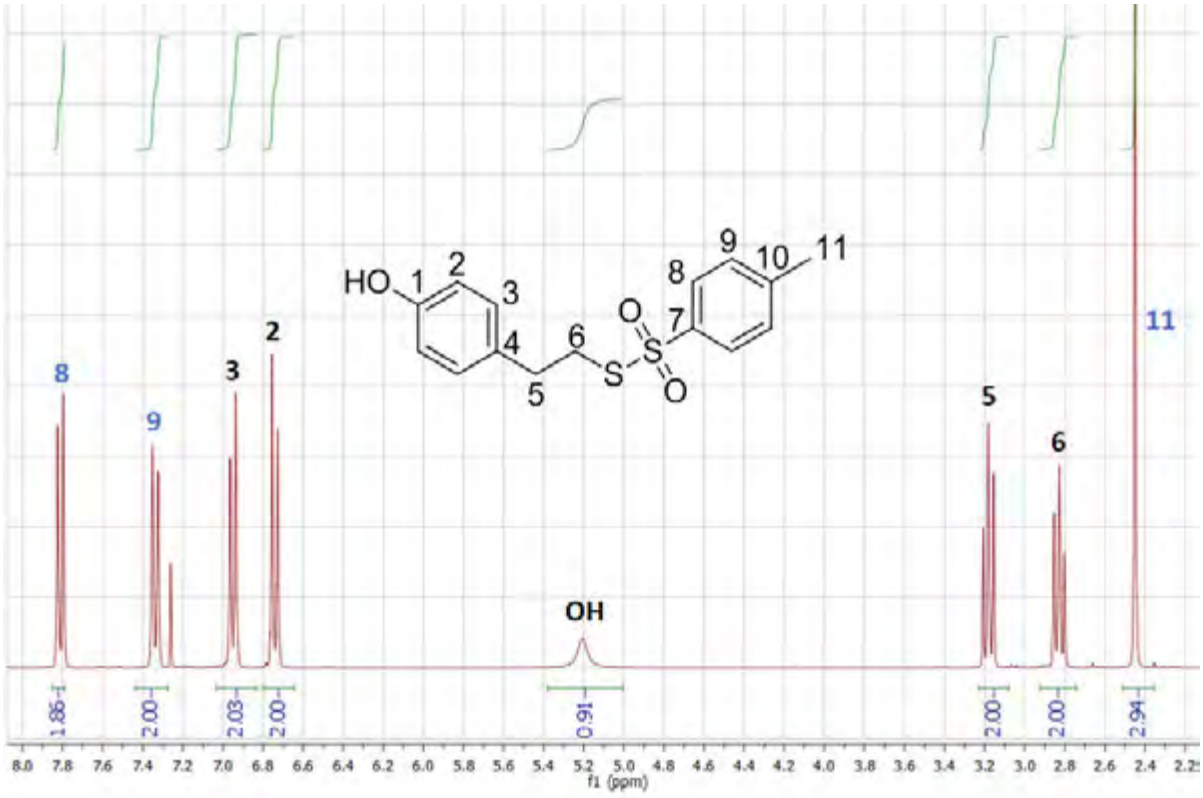

Figure 40**: ^{1}H-NMR spectrum of sulfenylating agent, **5

3.3.1.3 Coupling of **2** and **5** to the disulfide, **6**

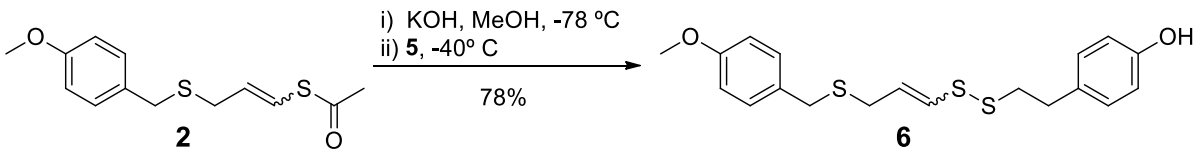

***Figure 41:** Fragment coupling by sulfenylation*

The coupling of **2** and **5** was achieved using the UCT synthesis (described in section 2.1) which involved treating **2** with potassium hydroxide (MeOH, -78 °C) to generate its

enethiolate followed by sulfenylation with **5** at the soft end of the enolate. Isolation by silica column chromatography gave **6** (**Figure 42**) in 72% yield and as a 3:5 mixture of E/Z isomers according to the ^{1}H-NMR spectrum.

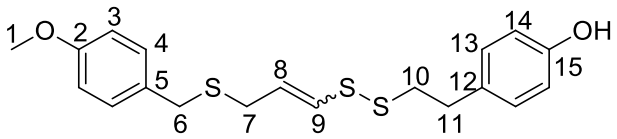

Figure 42: *Phenol-ajoene* ***6***

Support for formation of **6** was given by the appearance of characteristic signals for both coupling fragments in its ^{1}H-NMR spectrum, with the exception of the thioacetyl methyl singlet (the IR also lacking the carbonyl stretch) as well as thiotosylate signals. *Cis* and *trans* isomers were detected by virtue of the appearance of two distinct geometric sets of doublets of triplets at 6.24 and 6.09 ppm for the H_{α} proton (**H-9**) of the *Z*- and *E*-isomers respectively. The triplet arose due to an allylic coupling with the allylic methylene hydrogens (**H-7**) while a vicinal coupling of 9.3 Hz could be assigned to the Z-isomer at 6.24 ppm and a 14.6 Hz coupling for the *E*-isomer at 6.09 ppm. Similarly the H_{β} (**H-8**) hydrogen appeared as two sets of doublet of triplets at 5.88 and 5.70 ppm, with the same *cis* and *trans* couplings with **H-9** but a larger vicinal coupling of 7.3 Hz with **H-7**, as shown in **Figure 43**:

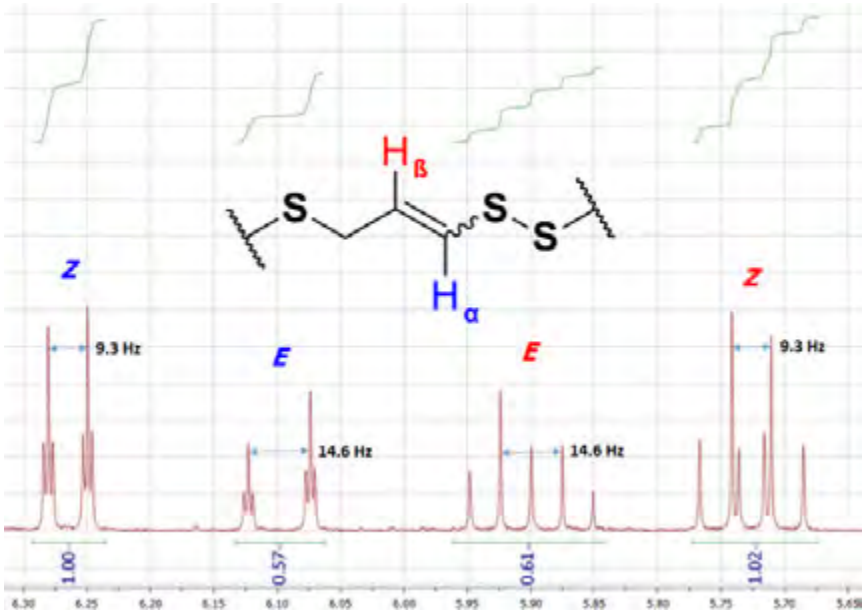

Figure 43: *Expansion of ^{1}H NMR vinylic signals of* ***6***

The ^{13}C-NMR spectrum of **6** showed resonances for all 19 carbon atoms for each isomer, in which some carbons away from the stereogenic axis resonated at the same chemical shift. Two downfield signals at 158.8 and 154.3 ppm could be assigned to the deshielded quaternary aromatic carbons, **C-2** and **C-15** respectively. The remaining two quaternary centres, **C-5** and **C-12**, were identified at 132.2 and 130.7 ppm. Although **H-10** and **H-11** were indistinguishable in the ^{1}H-NMR spectrum, HSQC analysis of the ^{13}C-NMR spectrum revealed **C-10** as having distinct *E*- and *Z*- signals (39.9 and 40.6 ppm), while the benzylic **C-11** appeared as a single resonance at 34.8 ppm for both isomers, as seen in **Figure 44**:

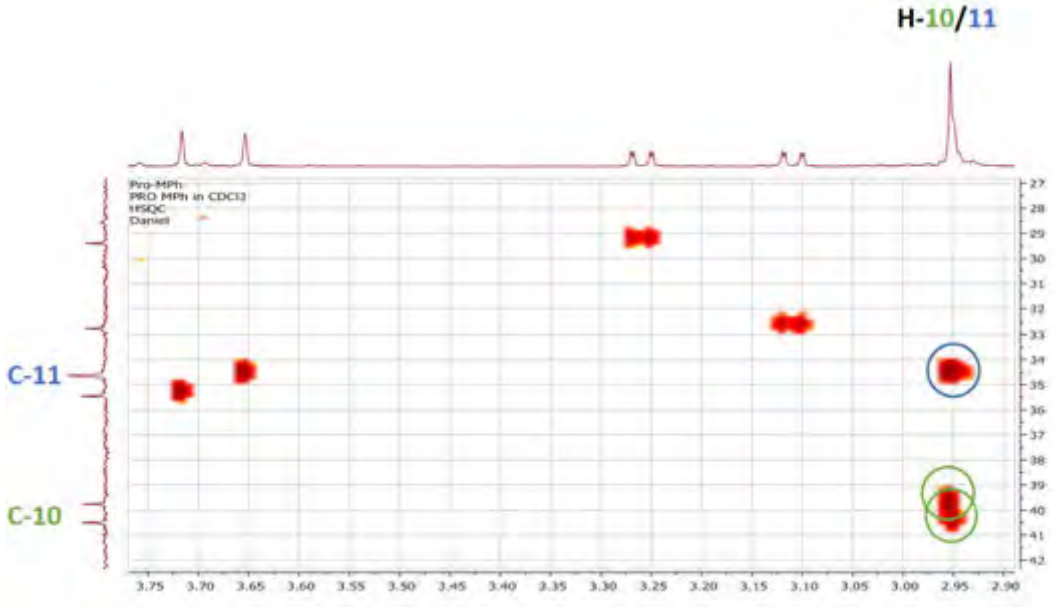

Figure 44: *Expansion of HSQC for* ***C-10/-11*** *of* ***6***

3.3.1.4 Final derivatisations

The various options for final derivatisations are shown in **Figure 45**:

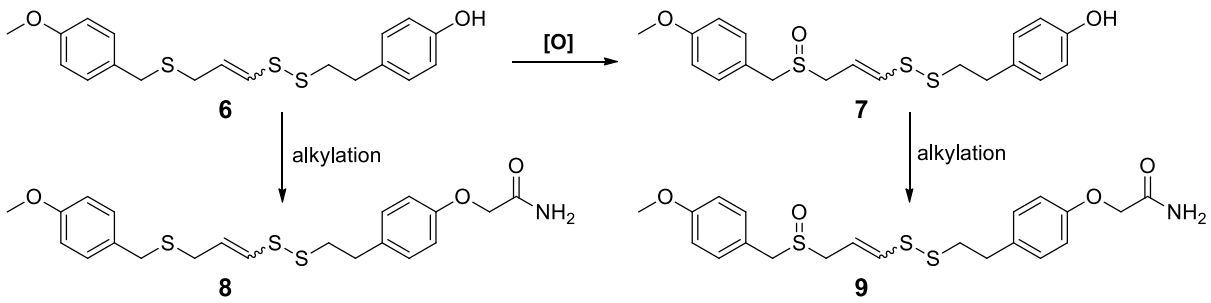

Figure 45: *Derivatisation sequence, depicting oxidation and alkylation steps*

Hence, chemoselective oxidation as previously accomplished (Page 18), of the more nucleophilic sulfur of **6** with *m*-CPBA in DCM at -78 °C afforded the ajoene-phenol

derivative **7**. Following a basic work-up to remove the benzoic acid by-product as well as excess *m*-CPBA, isolation by chromatography produced **7** as a 1:2 mixture of *E*/*Z*-isomers in 60% yield.

Formation of the sulfoxide as opposed to the sulfone was indicated by the presence of diastereotopic **H-7** hydrogens due to the adjacent chiral sulfoxide centre, with a large geminal coupling of about 13 Hz. **Figure 46** illustrates the diastereotopic splitting of the proton alpha to the chiral sulfoxide and highlights their corresponding coupling constants with each of the vinylic proton. The full ^{1}H-NMR spectrum of **7** is presented in **Figure 47**.

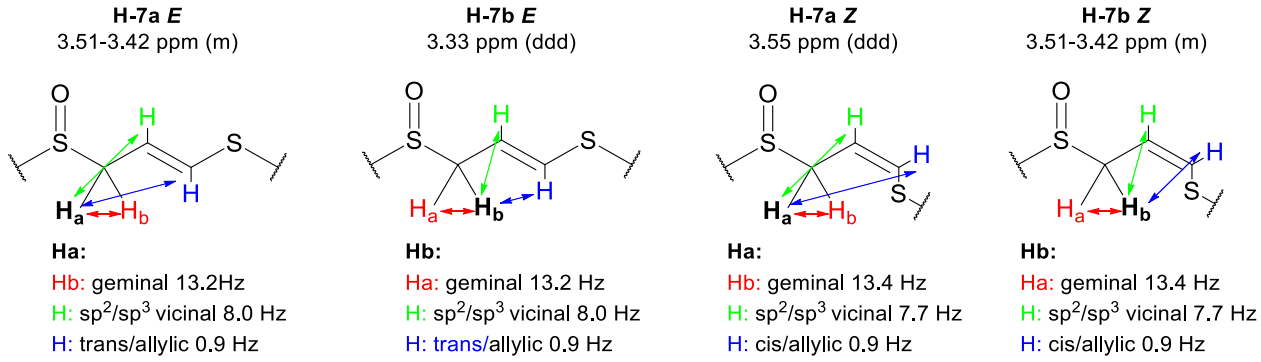

***Figure 46: H-7** coupling patterns for **7** (J-values of multiplets are estimated)*

While taking overlapping signals and geometric isomerism into account, all 38 carbon atoms (19 per isomer) could be identified by the aid of ^{13}C-NMR and HSQC analysis. The ^{13}C-NMR spectrum revealed the strong deshielding effect of the sulfoxide on adjacent carbon atoms, **C-6** and **C-7**. The *E*- and *Z*-isomers of **C-6** in **7** resonated higher at 56.4 and 57.0 ppm, compared to at 34.8 and 35.6 ppm in **6**. Similarly, the two isomeric signals for **C-7** had shifted from 32.9 and 29.5 ppm (in **6**) to 52.9 and 49.6 ppm, for *E* and *Z* respectively in **7**.

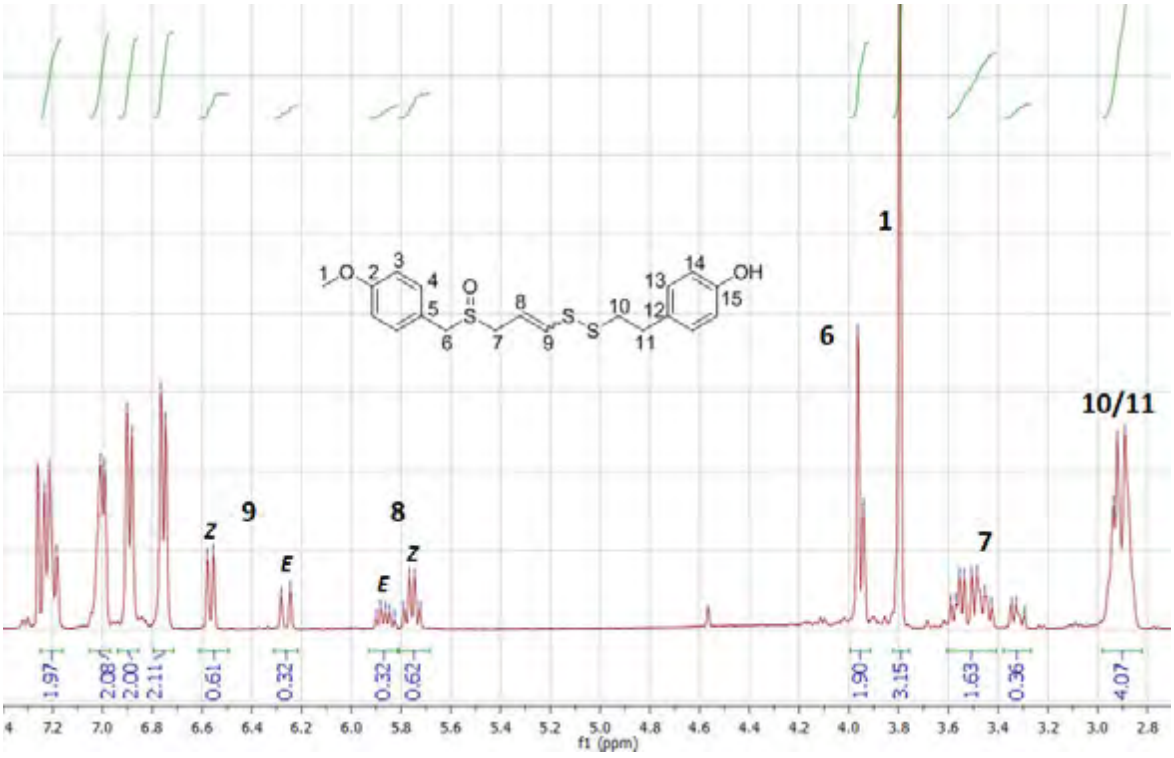

Figure 47: *^{1}H-NMR spectrum of phenol-ajoene,* ***7***

As shown in **Figure 45** introduction of the amide functionality was required at the two different oxidation levels. This could be achieved by using potassium carbonate (2 eq) as base with 2-chloroacetamide (2 eq) and TBAI (0.1 eq) in acetonitrile for twelve hours at reflux. The TBAI was used to generate iodoacetamide *in situ*. **Figure 48** summarises the S_N2 reaction involved. For ajoene-amide **9** it was more efficient to introduce the amide functionality after the sulphide had already been oxidised.

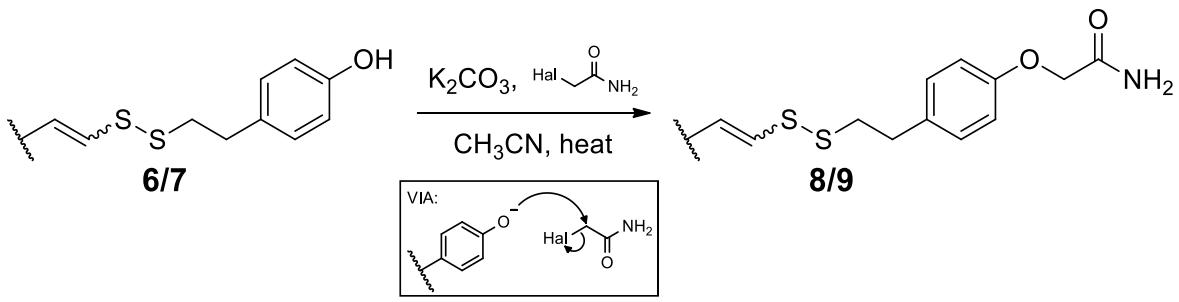

Figure 48: *Phenol alkylation*

Application of this methodology afforded the sulfide-amide **8** as a 3:4 mixture of *E*/*Z*-isomers in 40% yield, and the sulfoxide-amide, **9**, in 48% and an *E*:*Z*-ratio of 3:2. Interestingly inversion of the ratio from 1:2 in **7** to 3:2 in **9** implies that the reaction in

some way enriched in the *E*-isomer, presumably via deprotonation of one of the acidic α-sulfoxide protons, followed by double bond isomerisation to the more stable *trans*-isomer and finally reprotonation.

The ^{1}H-NMR spectra of **8** and **9** were analogous to those of **6** and **7**, namely the diagnostic *E/Z* splitting observed in the vinylic protons (order of chemical shift = *Z-E-E-Z*), the presence of two sets of aromatic signals (dd x 2) and the five methylene proton signals accounting for the methoxy, benzylic (x2) and alpha-sulfide (x2) (sulfoxide for **7** and **9**) positions. However an extra methylene singlet at around 4.5 ppm in both spectra (**8/9**) for each isomer could be observed for the newly introduced amidomethylene moiety (**Figure 49**). Moreover, a pair of N-H resonances at ~6.6 and 6.0 ppm (*E*- and *Z*-coincidental here) could be observed for the non-equivalent amide hydrogens. Two N-H stretching bands in the IR at around 3200 and 3400 cm^{-1} as well as an amide carbonyl stretch at 1700 cm^{-1} confirmed the presence of the primary amide. The ^{13}C-NMR spectrum provided further evidence as it showed two additional acetamide carbon signals for **C-16** and **C-17** at 67.5/67.4 ppm (-CH_2-) and 171.2/171.1 ppm (carbonyl) for **8/9** respectively. The HRMS data for **8** gave a molecular ion $(M+H)^+$ at 436.1068 $(M+H)^+$, in which $C_{21}H_{26}NO_3S_3$ requires 436.1080, thus further corroborating that successful amide modification of these analogues had been achieved.

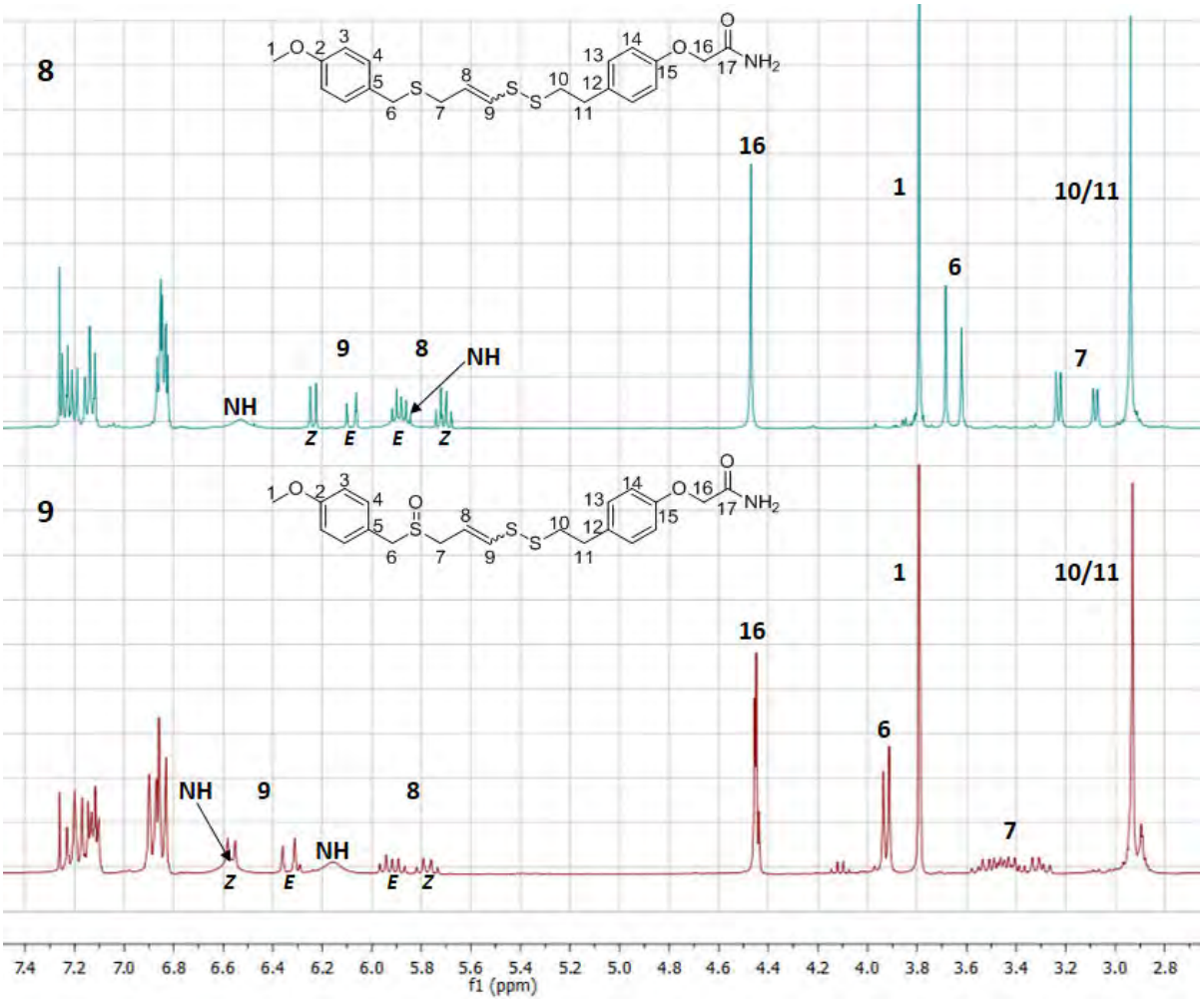

Figure 49**: [1]H-NMR spectrum of amide-ajoene analogues, **8** and **9

With the *bis*-PMB ajoene analogues in hand attention was turned towards accessing the analogous compounds in the dihydroajoene series, which will be described in the following section.

3.3.2 Dihydroajoene derivatives

The synthesis envisioned (**Figure 50**) proceeding via the mono-alkylation of 1,3-propanedithiol in which it was realised that care in respect of reagent equivalents would need to be taken in order to avoid over-substitution to afford the dialkylated product. Thereafter, the remaining thiol would be sulfenylated with **5**, to obtain **11**. Subsequent chemoselective oxidation of the more nucleophilic sulfur of **11** was expected to afford the sulfoxide disulfide, **12**. Finally, alkylation of **11** and **12** with caesium carbonate, 2-chloroacetamide and TBAI as in the ajoene series was expected to afford the targets **13** and **14**.

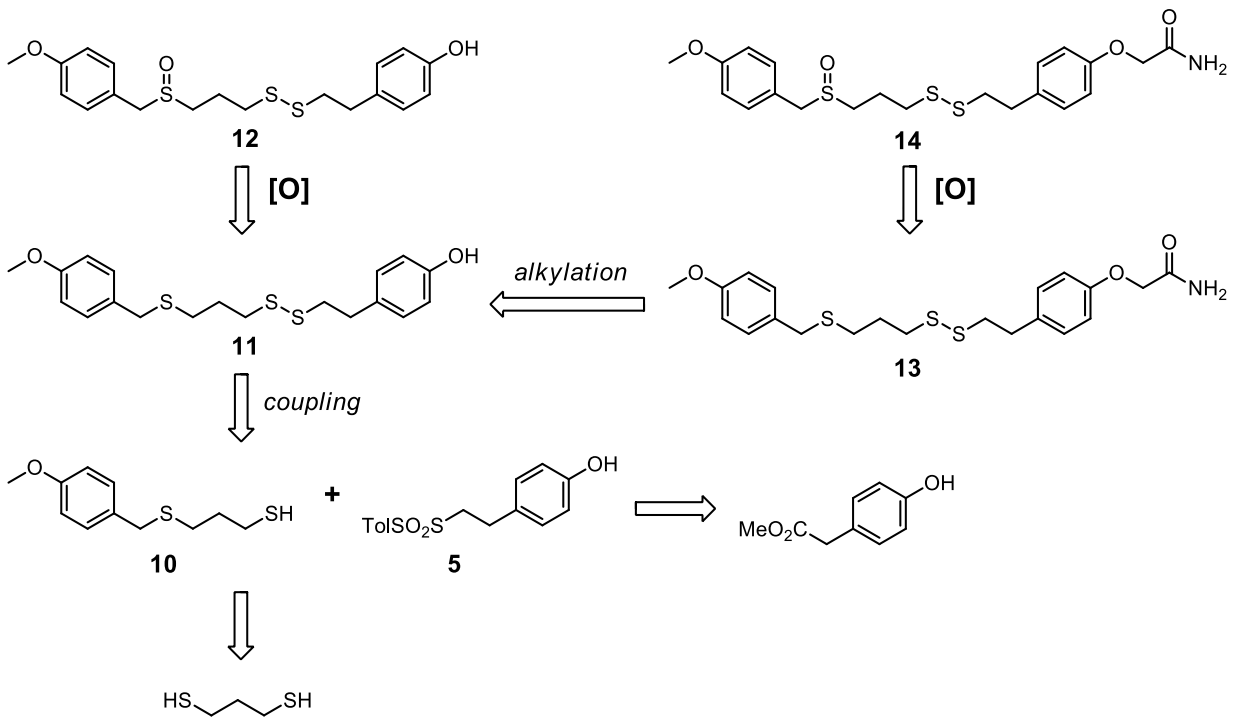

Figure 50: *Retrosynthesis of dihydroajoene analogues with polarity modification*

3.3.2.1 Synthesis of **11** and **12**

The following sequence summarises the two substitution and oxidation steps just described, **Figure 51:**

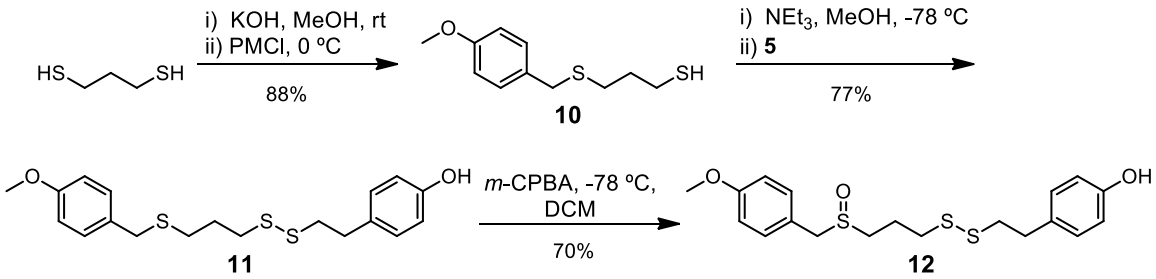

Figure 51: *Synthesis of PMB-S-propanethiol,* ***10***

Optimal conditions for the first step involved mixing an excess of 1,3-propanedithiol (1.2 eq) with potassium hydroxide (1.4 eq) in anhydrous methanol at 0 °C and then adding PMBCl (1 eq) dropwise. After two hours, TLC analysis showed that PMBCl had been completely consumed, and the reaction was neutralised with 1M HCl. Purification by silica gel column chromatography afforded the desired mono-alkylated thiol **10** in 88% yield.

Two pairs of aromatic doublets at 7.23 and 6.85 ppm together with two methylene triplets at 2.52 and 1.84 ppm from the propanedithiol partner with an integration ratio of 2:2:2:2 in the ^{1}H-NMR spectrum of **10** indicated a successful mono-alkylation. In addition a triplet for the thiol hydrogen was observed at 1.33 ppm.

The second thioalkylation proceeded by sulfenylating **10** with **5** in MeOH at -78 °C using triethylamine (1.5 eq) as a base catalyst. Warming the reaction mixture to room temperature over one hour followed by an acidic work-up and purification gave the sulfide disulfide, **11**, as a colourless waxy solid in 77% yield.

A successful coupling could be discerned by the appearance of signals for the sulfenylating agent into the ^{1}H-NMR spectrum and integrating correctly to the signals for the starting material **10.** The IR of **11** showed the appearance of a S-S stretching band at 550 cm^{-1} and the phenolic hydroxyl showed a strong O-H stretching band at 3433 cm^{-1}. All 15 carbon signals could be accounted for in the ^{13}C-NMR spectrum. Lowfield signals resonating at 158.8 and 154.3 ppm, respectively, represented the quaternary aromatic signals adjacent to the methoxy and hydroxyl groups respectively.

Analogous to the ajoene synthesis, the last step in this sequence involved a regioselective oxidation of **11** at the benzylic sulfur with *m*-CPBA (1.5 eq) in DCM at -78 °C. The reaction proceeded over one hour and gave the sulfoxide, **12**, in 70% yield.

Figure 52 confirms previous observations regarding the effects of the chiral sulfoxide on the prochiral hydrogens, **H-6** which were observed as a diastereotopic pair of AB doublets at 3.99 and 3.95 ppm, shifted downfield from 3.67 ppm in **11**. The multiplet at 2.77-2.58 ppm contained the **H-7** hydrogens towards **H-9**, which in **11** were separated as two distinct signals at 2.51 and 2.73 ppm. This was due to the deshielding effect of the sulfoxide through an inductive effect. Similarly, all 15 carbon signals were accounted for in the ^{13}C-NMR spectrum in which notably **C-6** experienced a strong deshielding shift from 35.8 ppm (in **11**) to 57.7 ppm in **12**, as well as **C-7** seen to 49.0 ppm from 29.9 ppm, both shifts caused by the electron-withdrawing sulfoxide. Lastly, the HRMS data supported formation of **12**, with the molecular parent ion $(M+H)^{+}$ found at 397.0966; $C_{19}H_{25}O_3S_3$ requires 397.0960. Generally, the NMR spectra in this series were much easier to assign than in the ajoene series because of the absence of *E/Z*-geometrical isomers.

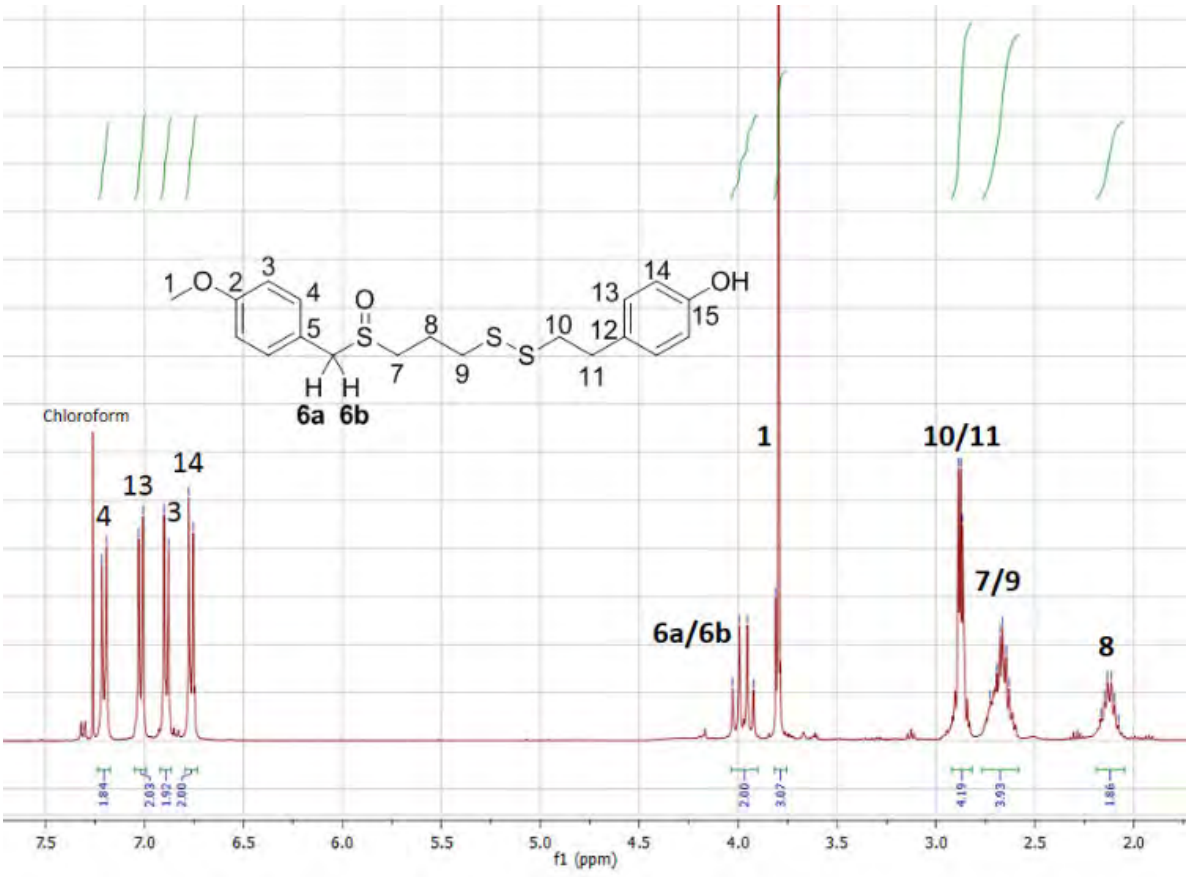

Figure 52: *^{1}H-NMR spectrum of phenol-dihydroajoene,* ***12***

3.3.2.2 Synthesis of **13** and **14**

The last two compounds of the dihydroajoene compounds were accessed divergently via their phenol parent, **11**, through first alkylation followed by oxidation to **14**, **Figure 53**:

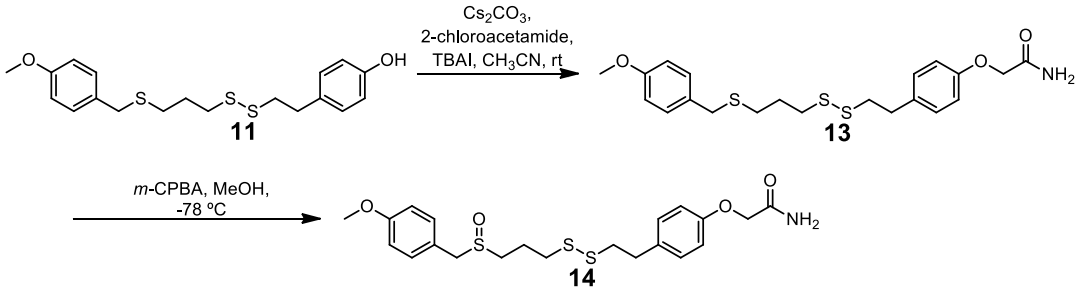

Figure 53: *Synthesis of amide-dihydroajoenes,* ***13*** *and* ***14***

For **13**, sulfide **11**, caesium carbonate (1.5 eq), 2-chloroacetamide (1.5 eq) and TBAI (0.1 eq) were reacted in acetonitrile at room temperature for eighteen hours. Compared to the alkylation of the ajoene analogues **8** and **9** the dihydroajoene compound, **13**, was obtained in a much higher yield of 77% as a more polar spot on TLC.

A singlet at 4.48 ppm in its ^{1}H-NMR spectrum for the newly introduced amidomethylene group together with two broad non-equivalent (due to amide resonance) amide hydrogen singlets at 6.53 and 5.71 ppm indicated a successful alkylation. The ^{13}C-NMR spectrum of **13** showed further evidence of the new functionality in form of a strongly deshielded carbonyl carbon at 171.1 ppm as well as a much less deshielded methylene carbon neighbour resonating at 67.5 ppm. The infrared spectrum showed characteristic amine N-H stretches and a carbonyl C=O stretch at 3160/3380 cm^{-1} and 1666 cm^{-1}, respectively.

The amide sulfoxide sulfide, **14**, was obtained via the regioselective oxidation with *m*-CPBA in 72% yield, as previously described for **12.**

A diagnostic diastereotopic pair of AB doublets at 3.96 and 3.93 ppm in the ^{1}H-NMR spectrum for **H-6** proved that oxidation had taken place at the sulfide sulfur only, **Figure 54**. Seventeen distinct carbon resonances were detected and accounted for. The successful synthesis of **14** was lastly confirmed via its HRMS data, where its parent ion $(M+H)^{+}$ was found at 454.1187, $C_{21}H_{28}NO_4S_3$ requires 454.1186.

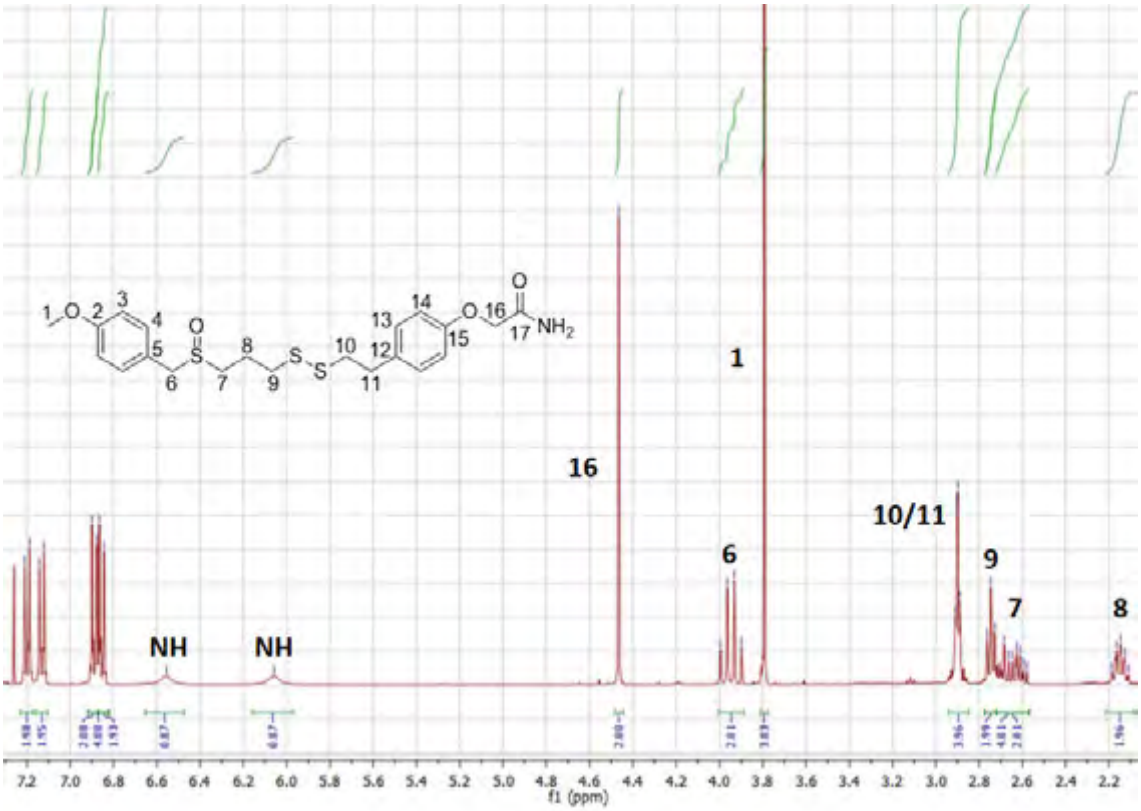

Figure 54**: ^{1}H-NMR spectrum of amide-dihydroajoene, **14

3.4 Biological evaluation of *bis-PMB* analogues

3.4.1 Anti-proliferative activity

The synthesised library of *bis*-PMB and its 8 analogues were first tested for cytotoxicity against WHCO1 cancer cell proliferation using the MTT cell viability assay.[104] This colorimetric assay quantitates viable cells by detecting residual reductase enzyme activity in the cells after treatment. The viable enzyme is able to convert yellow MTT (3-(4,5-dimethylthiazol-2-yl)-2,5-diphenyltetrazolium bromide) to purple formazan. In brief, WHCO1 cells were treated in 96-well plates with varying concentrations of the ajoene analogue for 48 hours, the treated cells were then incubated with the MTT reagent for four hours after which the reaction was stopped by the addition of a denaturing solubilizing reagent. To show that the compounds do not directly disrupt the assay, a control included the incubation of compound and the MTT reagent without cells present. The resulting colour change (yellow to purple) is colorimetrically quantified using a multiwall scanning spectrophotometer, from which, a dose-response curve could be generated and an IC_{50} value determined. The IC_{50} is a quantitative measure of the concentration of drug found to inhibit the growth of 50% of the cells. **Table 4** shows the IC_{50} values obtained for *bis*-PMB and its eight structural analogues. Each IC_{50} determination represents an average of between three and five independent determinations. It can be seen that the standard deviations are small and that the data obtained from these experiments is reproducible.

Table 4: *Activity of bis-PMB and its analogues against WHCO1 cell proliferation*

Name/#	Structure	WHCO1 $IC_{50} \pm SD$ (μM)	n
bis-PMB	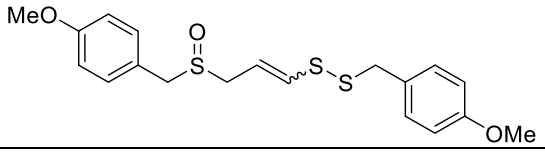	2.1 ± 0.4 [60]	
7	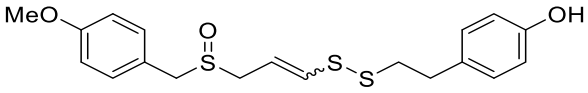	2.7 ± 0.5	5
6	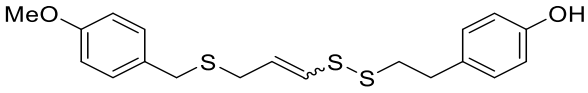	0.5 ± 0.3	4
12	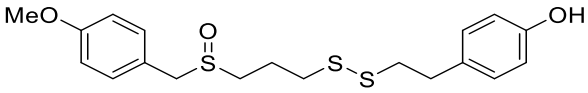	4.9 ± 0.6	4
11	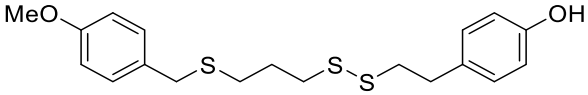	14.3 ± 3.1	3
9	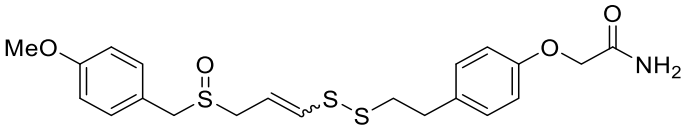	7.4 ± 1.7	5
8	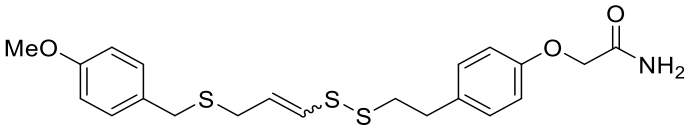	8.6 ± 4.2	3
14	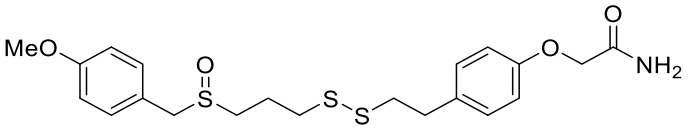	13.6 ± 0.7	3
13	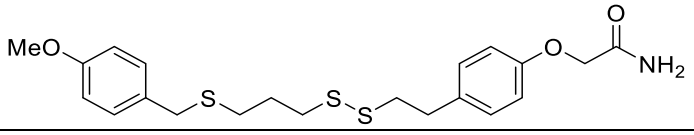	23.2 ± 0.9	3

n = number of independent repeats

In previous work,[66] the ajoene disulfide was identified as the pharmacophore. Its vinyl group was shown to enhance activity by labilising the disulfide and its removal in *bis*-PMB dihydroajoene demonstrated an eightfold decrease in activity. The removal of the sulfoxide, in the presence of the vinyl group, was found to actually enhance activity threefold. However, the ajoene analogue that lacked the double bond and the sulfoxide

(sulfide dihydroajoene) remained inactive at a concentration of 200 μM (cut-off), which implied some synergism between the (two functionalities) sulfoxide and vinyl-disulfide.

In this study, we found that our library of ajoene analogues all had comparable activity to the parent, *bis*-PMB regardless of whether a full vinyl-disulfide or sulfoxide group was present, with all compounds falling into the strongly active IC_{50} range of 0.5 – 23 μM. All compounds were found to be more active against WHCO1 cancer cells than the natural product ajoene (allyl parent: IC_{50} = 39.2 μM (*E*) and 25.2 μM (*Z*)).[60] The phenol analogue **6**, lacking the sulfoxide**,** was the most active with an IC_{50} in the nanomolar range of 0.48 μM, which was in agreement with our previous findings for the methoxy analogues (*bis*-PMB series) where the sulfide vinyl-disulfide was found to be more active than the sulfoxide.[66] The amide **8** did not however reflect this trend. Although the phenol **11** and amide **13** dihydroajoenes were the least active in their respective series, they are still considered to be strongly active, with IC_{50}'s in the 15-25 μM range, and show substantially higher activity compared to the previously inactive *bis*-PMB sulfide dihydroajoene (<200 μM). Overall, the phenol-substituted analogues were 2-3 fold more active than their amide counterparts and of similar activity to the *bis*-PMB series (methoxy derivatives).

The removal of the double bond resulted in a twofold drop of activity, when comparing the ajoene with its dihydroajoene (saturated vinyl disulfide) partner in both the phenol and amide series (**7** versus **12** and **9** versus **14**) although this was found to be more pronounced in the *bis*-PMB series (eightfold decrease). In support of a thiolysis mechanism, the double bonds stabilises the enethiolate anion leaving group through resonance delocalisation, which effectively drives the disulfide exchange as demonstrated in our recent publication.[105] The loss of the double bond in the dihydroajoene series, lacking disulfide activation, may therefore explain the observed reduced cytotoxicity. When however comparing **12** and **14** to an analogous dialkyl disulfide such as dipropyldisulfide, it can be seen that the dihydroajoenes are still very active (4.9 and 13.6 μM, respectively, versus 50000 μM).[105] The ten thousand-fold increase in activity implies a very important role for the sulfoxide/sulfide and the aromatic side groups.

In both the dihydroajoene series (**11**-**14**) removal of the sulfoxide in **11** and **13** caused an increase in activity (threefold phenol and twofold amide). This is in agreement with our group's previous paper where it also found that the sulfoxide restored the activity of the methoxy dihydroajoene (sulphide version).[66] The role of the sulfoxide moiety appears more subtle, though, where it may produce a long range inductive withdrawing effect through the molecule's sigma framework to make the sulfur distal to the sulfoxide more electrophilic. The increased electrophilicity of the sulfur in the disulfide would be expected to promote thiolysis and thus effectively lower the IC_{50}. However it must be stressed that the sulfoxide overall probably plays a minor role, as the presence of the disulfide alone (in the sulfide dihydroajoenes **11** and **13**) yields analogues which are strongly active, and in some cases (phenol **6** and the *bis*-PMB analogue from previously published data[66]) the sulfide is the more active compound. The findings that the amide series is overall less active than the phenol and methoxy analogues may lend some support to our previous observations that increased lipophilicity may contribute to increased activity.

In summary, the sulfoxide does not appear to play much of a role in enhancing the activity of the vinyl-disulfide series (and in some cases it is favourable to not have it at all), although it does increase the activity of the sulfide dihydroajoenes. This presumably occurs through an increase in the electrophilicity of the disulfide due to inductive electron-withdrawal via the σ-framework, which in turn enhances the leaving ability of the thiolate. It has been previously proposed that the sulfoxide may promote hydrogen bonding to adjacent amino acid residues in the cysteine peptide microenvironment.[74] However, this argument does not appear to apply here for the ajoene series. Importantly, however, in line with our previous findings on ajoene and its analogues, this study supports the disulfide being the pharmacophore, in which the double bond plays an activating role by stabilising the leaving group anion in thiolysis.

3.4.2 Stability studies of ajoene analogues in blood

The series of ajoene analogues in this thesis were designed to probe structural features affecting the blood stability of the ajoene pharmacophore. The previous *in vivo* and *in vitro* blood stability experiments of the *bis*-PMB parent showed that it is not bioavailable in a mouse as no *bis*-PMB was detected in the blood even after 5 minutes following intravenous administration. It would appear that a specific erythrocyte (red blood cell) interaction is involved as the rapid disappearance of *bis*-PMB was only observed *in vitro* in whole blood and in the erythrocyte fraction but not in plasma. Owing to the high cytotoxicity of *bis*-PMB against cancer cell lines and in view of being an efficient *S*-thiolating agent, we hypothesised that it may rapidly *S*-thiolate erythrocyte proteins or glutathione (GSH) thereby leading to its *in vivo* instability. In the current study we aimed to synthetically modify the *bis*-PMB pharmacophore in an attempt to lengthen its half-life in blood and therefore increase its bioavailability.

The *in vitro* half-life experiments were performed by Dr Carmen de Kock in the Department of Pharmacology, UCT. Freshly collected mouse blood was incubated with the compounds at 37 °C for the indicated time points. The compound remaining was then quantified by liquid chromatography-mass spectrometry (LC-MS) as the peak area and compared to a calibration curve. The obtained results are preliminary as the experiment was only performed twice and the conditions were not yet optimised. Nevertheless, obvious trends are consistenly observed and are reported in this thesis. In corroboration with previous observations for the *bis*-PMB series, the stability trends of phenol analogues (R = OH) in mouse blood are shown in **Figure 55**:

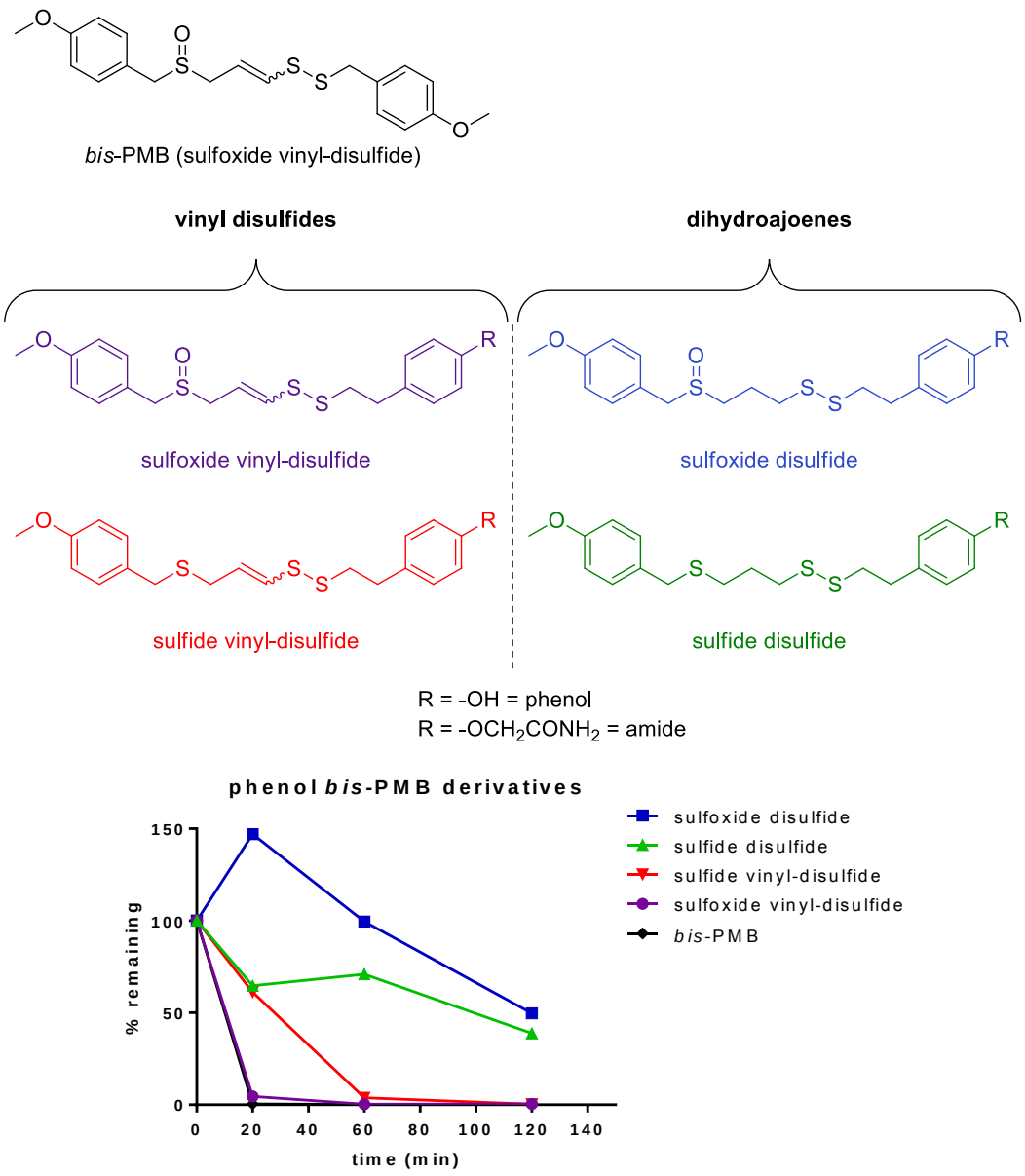

***Figure 55**: in vitro blood stability of phenol bis-PMB analogues in mouse blood at 37 °C*

In agreement with previous findings for *bis*-PMB, it was not detected at the 20 minute time point following *in vitro* incubation in whole mouse blood. Similarly, the phenol sulfoxide vinyl-disulfide (purple in **Figure 54**), displayed a very similar profile to that of *bis*-PMB. This finding was not surprising as both contain the sulfoxide vinyl-disulfide backbone of *bis*-PMB. The sulfide vinyl-disulfide (red) was found to have slightly improved stability with detectability up to 60 minutes fitting in with our ideas of thiolation (sulfoxide enhancing the reactivity of the double bond). In comparison, the two phenol dihydroajoenes (green and blue) showed greatly improved stability with good detectability at the maximum time point (120 minutes), with the sulfoxide (blue) showing

the greatest stability of the series. It is immediately evident that the phenol dihydroajoenes (green and blue) have enhanced blood stability compared to the vinyl-disulfides (black, red and purple).

Similarly the stability trends of the amide *bis*-PMB (R = OCH_2CONH_2) series are shown in **Figure 56**:

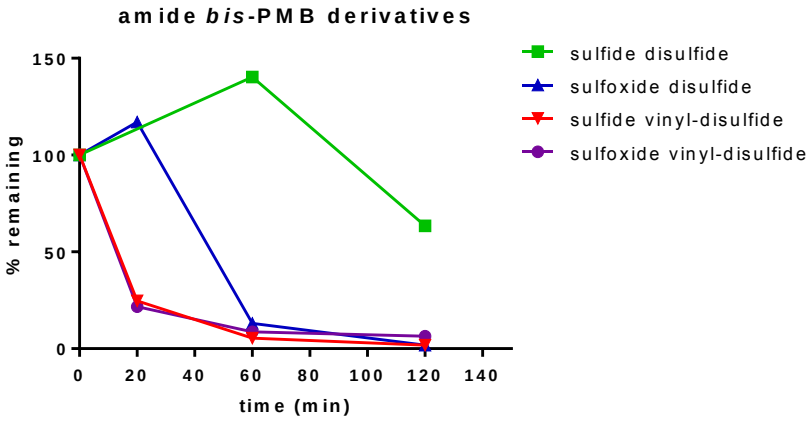

Figure 56*: *in vitro blood stability of amide bis-PMB analogues in mouse blood at 37 °C

Here, comparable trends were observed. The dihydroajoenes (green and blue) were detectable for significantly longer time periods compared to the vinyl-disulfides (red and purple). Interestingly, approximately 20% of both amide vinyl-disulfides (red and purple) were still detectable at 20 minutes post-incubation, compared to 0% at the same time point for the phenol vinyl-disulfides as well as *bis*-PMB. As expected intuitively, stability and cytotoxicity were found to be inversely related, i.e. the less cytotoxic (higher IC_{50}) the greater the stability. Interestingly, in the dihydroajoene series, the sulfide (green) was retained in blood the longest with 50% remaining after 120 minutes, compared to the sulfoxide (blue) – this was the reverse of the trend for the phenol series.

A striking trend in the blood stability SAR data is that the four dihydroajoenes synthesised were found to have acceptable retention (stability) in whole blood at 40 minutes (green and blue), whereas their respective vinyl-disulfide analogues were far less stable being either undetectable (phenol) or weakly detectable (amides) at 20 minutes. These data further support that the vinyl-disulfide in ajoene enhances its reactivity in a biological context by causing cancer cell cytotoxicity and poor *in vitro* blood-stability. The role of the sulfoxide in blood stability is not so clear although its

presence appears to enhance blood instability in most cases. It is evident though, that the sulfoxide does not play as much of a modulating role as the presence of the vinyl group, where in both series the dihydroajoenes were found to be significantly more stable than their respective vinyl-disulfide counterparts.

The correlation between WHCO1 cytotoxicity and blood-instability fits with our ideas on thiolysis exchange as being the cause, in which the more activated disulfide (i.e. vinyl disulfide) promotes the exchange reaction.

3.4.3 Ajoene metabolism within blood

It is well established that garlic compounds are toxic to erythrocytes and furthermore we found that the ajoene analogue *bis*-PMB is only unstable in whole blood and not in plasma. It would therefore appear that ajoene is either *S*-thiolating GSH or targeting a thiol group on an erythrocyte protein. Owing to the darkening of the blood and the difficulty in breathing in the treated mice, we hypothesised that ajoene may be interacting the oxygen-carrying protein, haemoglobin (Hb).

It is well known in the literature that garlic and onions are toxic to farm animals causing haemolytic anaemia.[34,106] It has also been shown that allicin is able to rapidly enter erythrocytes to spontaneously react with GSH which decreases the cells ability to counteract the production of ROS.[67] Haemolytic anaemia is characterised by the production of Heinz bodies in erythrocytes which follows from the oxidative degradation of Hb.[107] Munday *et al.* offered a mechanism for the oxidative degradation of Hb by garlic disulfides which is shown below (**Figure 57**). Here a one-electron oxidation of a thiolate ($R\text{-}S^-$) at the iron(II) centre of haemoglobin is proposed to generate H_2O_2 (a ROS), Met-haemoglobin (MetHb – iron(III)) and a thiyl radical. The resulting formation of oxidative species (H_2O_2 and thiyl radicals) then leads to depletion of GSH which may lead to oxidative damage of Hb and possible formation of Heinz bodies.

$$RSSR + 2GSH \rightarrow 2RSH + GSSG \quad (1)$$

$$RS^- + Fe^{II}HbO_2 \rightarrow RS^{\cdot} + Fe^{III}Hb + H_2O_2 \quad (2)$$

$$2RS^{\cdot} \rightarrow RSSR \quad (3)$$

$$RS^{\cdot} + RS^- \rightleftharpoons RSSR^{\cdot -} \quad (4)$$

$$RSSR^{\cdot -} + O_2 \rightarrow RSSR + O_2^{\cdot -} \quad (5)$$

$$RS^- + O_2 + Fe^{III}Hb \rightarrow RS^{\cdot} + Fe^{II}HbO_2 \quad (6)$$

$$RSSR^{\cdot -} + O_2 + Fe^{III}Hb \rightarrow RSSR + Fe^{II}HbO_2 \quad (7)$$

Figure 57: *Mechanism whereby an eliminated thiolate is oxidised at the iron(II) centre of Hb to form ROS and MetHb*[34]

If Munday's hypothesis holds true, a direct interaction between ajoene and the metalloporphryrin (heme) rings in Hb would reveal a change in the redox state of iron centre, as Hb is oxidised to MetHb. In UV-Vis experiments this oxidation (from iron(II) to iron(III)) results in a characteristic flattening of two diagnostic absorption bands for the heme-iron centre at 541 (β-band) and 577 nm (α-band).[108] **Figure 58** shows the shift in the spectra that would be expected if Hb were oxidised to MetHb.[109]

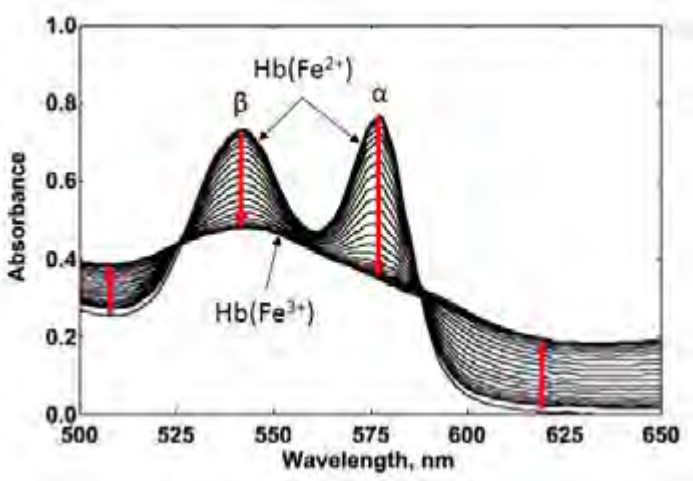

Figure 58: *Disappearing α- and β- bands of metalloporphyrin absorption in Hb upon oxidation of the iron(II) centre (Hb→MetHb)*[109]

Hence, to test if ajoene directly interacts with the Hb iron centre and as a result forms MetHb, we performed a spectrophotometric analysis by titrating mouse blood with *Z*-ajoene up to 200 μM. The resulting overlaid UV-Vis spectra can be seen in **Figure 59**:

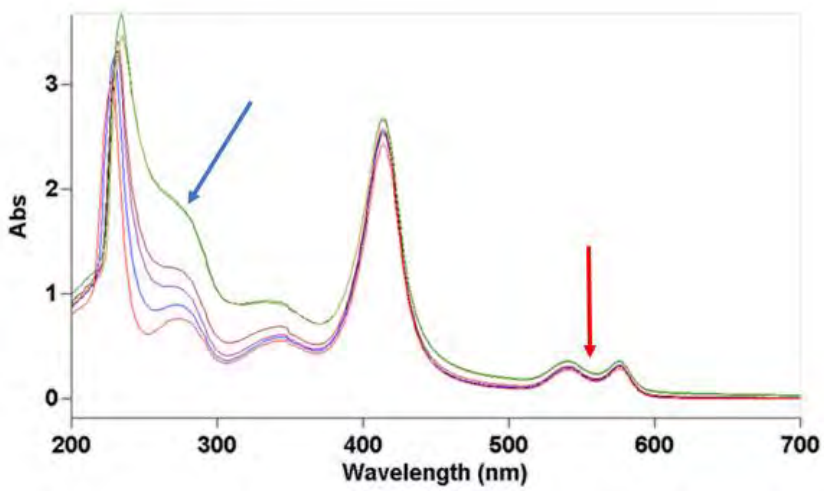

Figure 59: *UV-Vis spectra of haemoglobin titrated against bis-PMB*

No disappearance of the α- and β-bands (at 577 and 541 nm respectively) was observed (red arrow in **Figure 59**) and this implies that *bis*-PMB is not oxidising the Hb iron centre at the concentrations used in the experiments. Although ajoene did not cause oxidation at the iron(II) centre, the spectrum did however show a distinct red shift in the protein absorption region (blue arrow in **Figure 59**). This change in the 250 nm absorption region is the protein region of the spectrum and could imply interaction with the protein or the formation of a new chemical species. To investigate whether ajoene covalently modifies the Hb protein, a proteomics study was conducted.

3.4.4 Proteomic study of ajoene-Hb interactions

In the first step of the proteomic assay (Step **i** in **Figure 60**, two samples of purified human haemoglobin protein were prepared by incubation without (control) or with 100 μM *Z*-ajoene and sent for proteomics analysis at the Centre for Proteomics and Genomics Research (CPGR), Cape Town, South Africa.

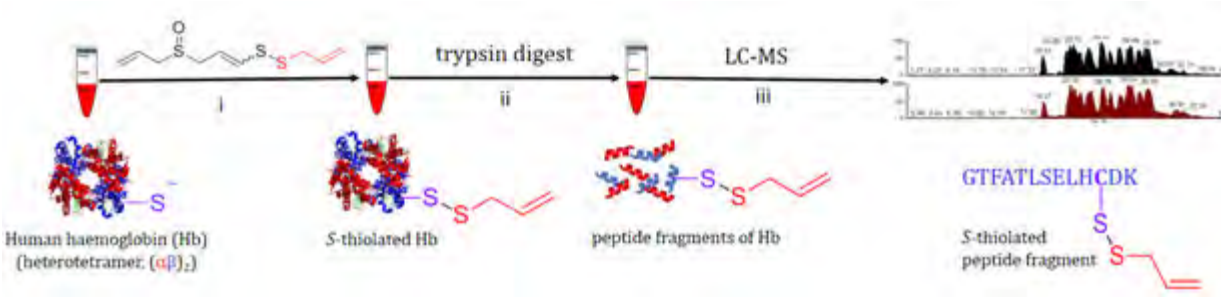

Figure 60: *Workflow of sample preparation for proteomic analysis*

The proteomic analysis is a sensitive analytical technique that allows for the detection of modifications on proteins by comparing the mass change of peptide fragments in treated and untreated samples. The Cys (**C**) β-93 residue of the haemoglobin β-subunit has been previously identified to be particularly sensitive to oxidation and *S*-glutathionylation.[110] We wondered whether ajoene, by mimicking GSH/GSSG, may also *S*-thiolate Hb at this cysteine residue. The Cys β-93-containing peptide fragment (GTFATLSELH**C**DK) was obtained by overnight trypsin digestion of the two Hb samples (Step **ii** in **Figure 60**). The protease, trypsin, site-specifically hydrolyses protein amide bonds at the carboxylic ends of lysine (**K**) and arginine (except if followed by proline) to afford tryptic peptide fragments, as shown in **Figure 61**:

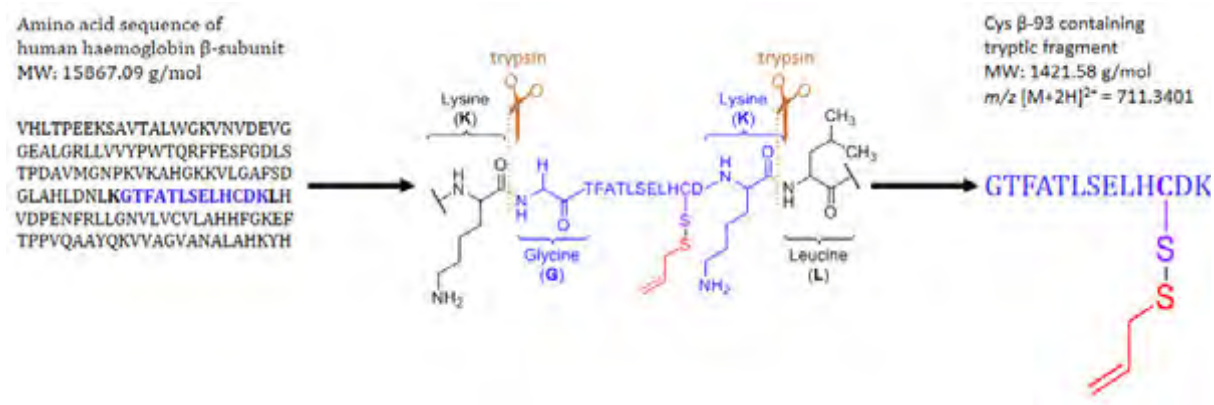

***Figure 61**: Site-specific digestion of human haemoglobin β-subunit by trypsin to obtain the Cys β-93-containing tryptic fragment (GTFATLSELH**C**DK)*

The resulting trypsin-digested samples were run through an LC-ESI-MS system to obtain a "three-dimensional" spectrum in which each LC elution time point provided a corresponding mass spectrum (Step **iii** in **Figure 60**).

According to the Expasy peptide prediction software, the predicted mass to charge ratio (m/z) of the haemoglobin fragment containing Cys β-93 (GTFATLSELH**C**DK) was 1421.6729 for the $[M+H]^+$ ion and 711.3401 for the $[M+2H]^{2+}$ ion. This fragment was detected in both ionic forms as shown in **Figure 62**:

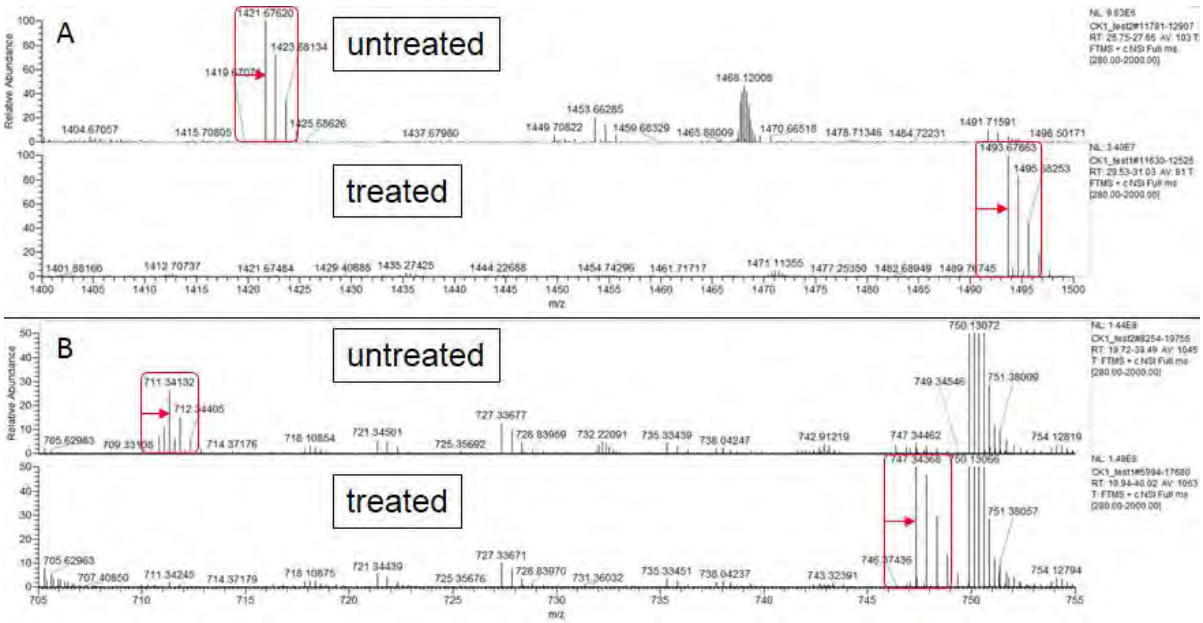

Figure 62: *Mass spectra of untreated and Z-ajoene-treated Hb samples.* ***A*** *showing the* $[M+H]^+$ *and* ***B*** *showing the* $[M+2H]^{2+}$

Both spectra show two distinct differences (highlighted in red). The top spectra of the control samples (**A** and **B**) shows the expected ion peaks of the GTFATLSELH**C**DK fragment. The treated spectra on the other hand were found to lack the ion peaks at 1421.67620 (in **A**) and at 711.34132 (in **B**), but shows a new peaks at m/z = 1493.67863 and at m/z = 747.34368, in **A** and **B** respectively. If ajoene successfully *S*-thiolated the Cys β-93 residue on GTFATLSELH**C**DK, the treated fragment mass increase would equal that of the added *S*-allyl group (based on regioselectivity). One must take into consideration that the fragment (-SH) loses one proton upon adduct formation (-S-S-). The calculations of the exact mass differences between the treated and untreated fragments for both the $[M+H]^+$ and $[M+2H]^{2+}$ ions are as follows:

For $[M+H]^+$:

$$Mass[adduct] = Mass[fragment(-SH) - H^+] + Mass[difference]$$

$$Mass[difference] = Mass[adduct] - Mass[fragment(-SH) - H^+]$$

$$Mass[difference] = 1493.67863 - (1421.67620 - 1.0078)$$

$$Mass[difference] = Mass[adduct] - Mass[fragement(-S^-)]$$

$$Mass[difference] = 1493.67863 - 1420.6684 = \mathbf{73.01023}$$

For $[M+2H]^{+2}$: $Mass[adduct] = Mass[fragment(-SH) - H^+] + Mass[difference]$

$where\ Mass[X] = (peak\ \times\ 2) - 2H$

$\therefore Mass[adduct] = (747.34462\ \times\ 2) - 2\ \times 1.0078\ = 1492.67364$

$\therefore Mass[fragment(-S^-)] = ((711.34132\ \times 2) - 2\ \times 1.0078) - 1.0078 = 1419.65924$

$\therefore Mass[difference] = Mass[adduct] - Mass[fragement(-S^-)]$

$Mass[difference] = 1492.67364 - 1419.65924 = \mathbf{73.01440}$

Table 5 lists the m/z ratios of the predicted and observed ions together with the calculated mass differences:

Table 5: *Mass/charge ratio of Cys β-93-containing ions and their respective calculated mass difference*

		Fragment (GTFATLSELH**C**DK)	**Adduct** (GTFATLSELH**C**DK-*S*-*S*-allyl)	**Difference in mass** (-*S*-allyl)
predicted	$[M+H]^+$ (**A**)	1421.67290	1493.67632	73.01174
	$[M+2H]^{2+}$ (**B**)	711.34010	747.34257	73.01174
actual	$[M+H]^+$ (**A**)	1421.67620	1493.67863	73.01023
	$[M+2H]^{2+}$ (**B**)	711.34132	747.34462	73.01440

It was pleasing to see, that the mass difference between the treated and untreated fragments for the $[M+H]^+$ and $[M+2H]^{2+}$ ion corresponded to 73.01023 and 73.01440 Da, respectively, In both cases, these masses corresponded to the predicted mass of one *S*-allyl$^-$ group (73.01174 Da) to two decimal points accuracy. This is highly convincing data that *Z*-ajoene regioselectively *S*-thiolates Hb at its Cys β-93.

In support of our findings, a study by Beuzard *et al*. showed that thiol reagents, unrelated to alliums, interact directly with Cys β-93.[111,112] It was later demonstrated that Cys β-93 is also targeted by glutathione via *S*-glutathionylation. The resulting GSS-Hb adduct has further been shown to cause a structural change in the protein thereby leading to increased affinity for oxygen, termed the alkaline Bohr effect.[113,114] Together, the reports on garlic induced haemolytic anaemia as well as the alkaline Bohr Effect support a likely direct interaction *in vivo* between Hb and the garlic compound.

These findings provide new evidence into the mechanism of erythrocyte toxicity of garlic compounds. It is highly likely that a combination of both GSH and Hb thiolysis may lead to the observed oxidative stress and toxic effects (**Figure 63**). Haemoglobin is the most

abundant protein in erythrocytes, and therefore *S*-thiolation of Hb would lead to an effective trapping of ajoene in the erythrocyte, where the expelled enethiolate leaving group may lead to further downstream events. These aspects as well as ajoene's role as a glutathione mimic will need to be investigated in the future.

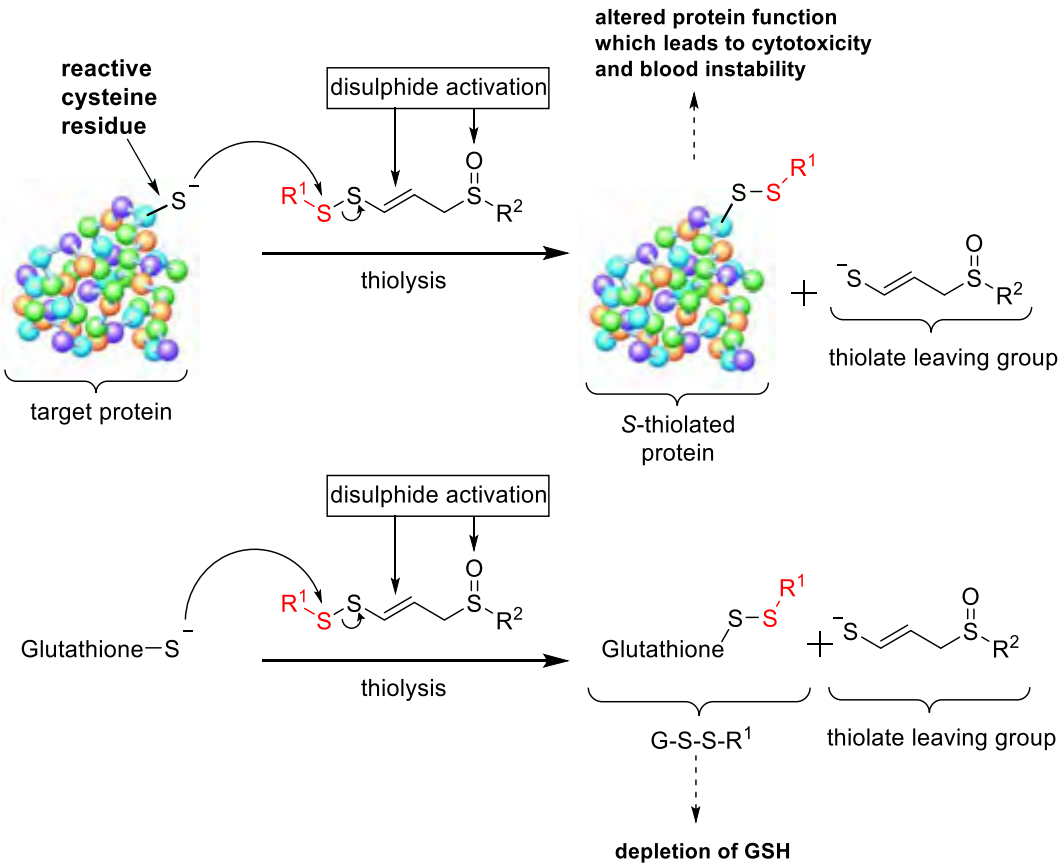

Figure 63: *Proposed governing principle of ajoene cytotoxicity and blood instability*

3.5 Summary and Outlook

In this chapter, two divergent synthetic routes were used to produce a small library of eight *bis*-PMB ajoenes with enhanced solubility and variations in the reactivity modulating backbone. The previously developed UCT ajoene synthesis allowed access to the vinyl-disulfide series (**6**-**9**), in which the key *S*-thiolation step between the vinyl thioacetate **2** and the phenolic sulfenylating agent **5** integrated the pharmacophore and the handle for polar modifications into the molecule. Synthesis in the dihydroajoene series (**10**-**14**) also utilised the modified sulfenylating agent and was accomplished via the dialkylation of 1,3-propanedithiol. The amide derivatives of both series were accessible through alkylation at the phenol moiety.

The subsequent structure-activity relationship study of the analogues demonstrated that the more cytotoxic molecules showed decreased blood stability, where it is proposed that the observed cytotoxicity and blood instability is directly correlated to ajoene's susceptibility towards thiolysis exchange (better leaving group), which is in agreement with our group's previous findings on garlic-related disulfides. The double bond of the vinyl-disulfide group showed to have the most pronounced effect as it greatly increased the stability of the resulting leaving group (enethiolate), and hence the dihydroajoenes which lack the double bond showed greatly enhanced *in vitro* blood stability. The presence of the sulfoxide group enhanced the activity of the dihydroajoenes, but decreased activity in the vinyl-disulfides which implies a long-range inductive electron-withdrawing effect on the disulfide through the σ-framework of the molecule. The phenol and methoxy functionalities had similar effects on cytotoxicity, whereas the amide functionality decreased cytotoxicity but enhanced blood stability.

A striking and important observation from this study is that although an inverse relationship between cancer cell cytotoxicity and blood stability is observed, it is weighted. Although the dihydroajoenes are slightly less cytotoxic than their vinyl-disulfide counterparts, they are still strongly active with an IC_{50} of 20 μM. Their improvement on blood stability is, however, very acceptable which has increased to around 50% remaining at 120 minutes. These findings provide a good lead for future therapeutic development of the dihydroajoenes.

Furthermore, it was demonstrated that *Z*-ajoene interacts with Cys β-93 of Hb by both proteomics and UV-Vis spectroscopy which provides a possible explanation for the blood instability and known cytotoxicity to erythrocytes.

We have previously found that the cytotoxicity of disulfides in cancer cells originates in the *S*-thiolation of protein targets. Strategies to identify these targets will be addressed in the upcoming chapter.

Chapter Four: Synthesis of a Biotin-labelled Ajoene Probe

4.1 Introduction

Our group's recent work on the cytotoxicity mode of action of ajoene in killing cancer cells *in vitro* used laser microscopy to track the movement of a fluorescent dansyl-tagged ajoene analogue inside a live cancer cell (MDA breast) (Page 23).[115] The study revealed that accumulation of the tagged ajoene occurs in the Endoplasmic Reticulum (ER), and a western blot of the lysate revealed that many proteins are the *S*-thiolation targets of ajoene. The literature demonstrated that the *S*-thiolation of proteins using biotinylated GSSG[116] and isothiocyanates[117] had shown to successfully label and identify reactive cysteine residues on cellular targets. Based on their mode of action (thiolysis), it is expected that ajoene's targets will overlap with those of GSSG and isothiocyanates. These results and analogous studies supported our undertakings to identify the protein targets of ajoene in cancer cells using the technique of biotinylation. This required the need to synthesise a biotinylated ajoene analogue, which on *S*-thiolation would result in the transfer of the biotin tag to the target. Subsequent isolation of the relevant proteins was then envisaged through the use of biotin's affinity for streptavidin beads, with subsequent protein identification by MALDI-TOF mass spectrometry analysis.

4.2 Probe design

The probe design was based on an important reactivity principle in context established in our work,[95] which had shown that the site of disulfide exchange in the *S*-thiolation process is at the non-vinyl sulfur of the ajoene disulfide pharmacophore as illustrated in **Figure 64**:

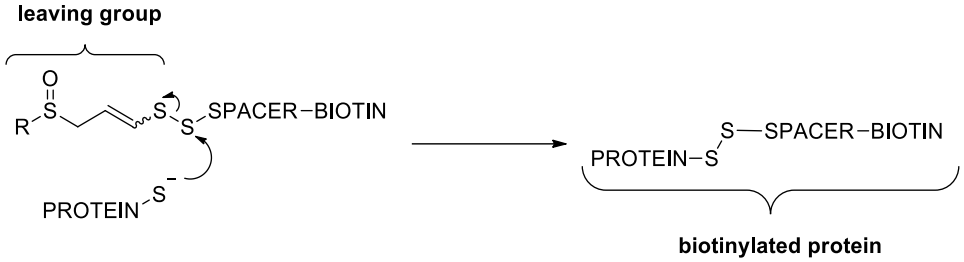

Figure 64: *Regioselectivity of protein S-thiolation by ajoene*

Therefore a crucial design element as it indicated that the biotin tag needed to be attached to the non-vinyl sulfur. Applying this design principle resulted in the structure (on paper) of our first prototype, which is shown in **Figure 65**:

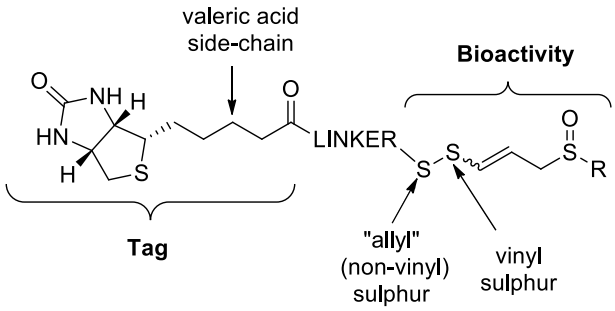

Figure 65: *Envisioned biotinylated ajoene analogue design, highlighting key synthetic aspects*

Previous synthetic endeavours directed towards the synthesis of the first prototype by Pike indicated that the biotin tag might be too close in proximity to the ajoene pharmacophore warhead,[118] so a second prototype was designed whose synthesis is described in this thesis. This second-generation target probe was designed based on the work of Jezowska *et al.*, on the biotinylation of peptides and oligonucleotides[98], and its structure is shown in **Figure 66** together with a convergent retrosynthesis (in red and blue) that was translated into a successful synthesis:

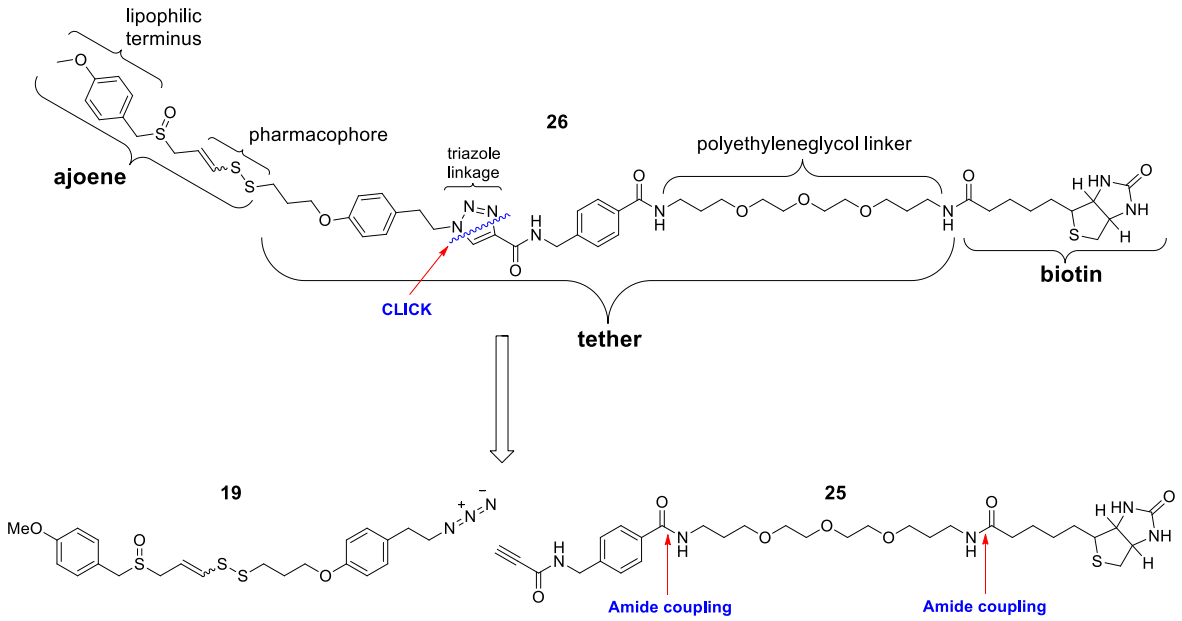

Figure 66: *Second-generation biotinylated ajoene probe with its retrosynthesis*

Hence, the synthesis involved bringing together two separately synthesised pieces, **19** and **25**, using "Click"-technology, in which the two "Click"-synthons were generated from a combination of amide couplings and substitution chemistry. A crucial advance from the first prototype synthesis was the finding that a much cleaner amide coupling for incorporation of the biotin fragment could be achieved using the *N*-hydroxysuccinimidyl biotin ester as coupling partner, which could be readily prepared from the commercially available biotin acid using a conventional DCC coupling with *N*-hydroxysuccinimide (NHS). With these insights the synthesis of fragments **19** and **25** could proceed and these are now discussed.

4.3 Synthesis of the "Click"-partners

4.3.1 Synthesis of azide-ajoene, **19**

The retrosynthesis plan for **19** is shown in **Figure 67:**

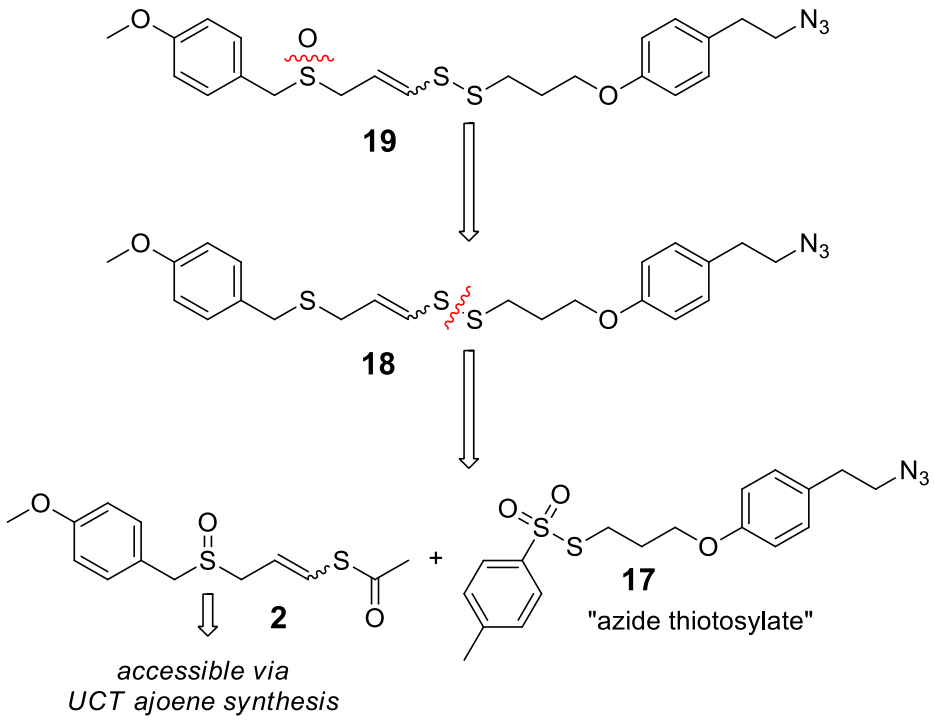

Figure 67: *Retrosynthesis of fragment* ***19***

The established UCT synthesis was well suited for obtaining the azide-ajoene fragment, **19**, using azido thiotosylate **17** as the sulfenylating agent, whose synthesis is given in **Figure 68**:

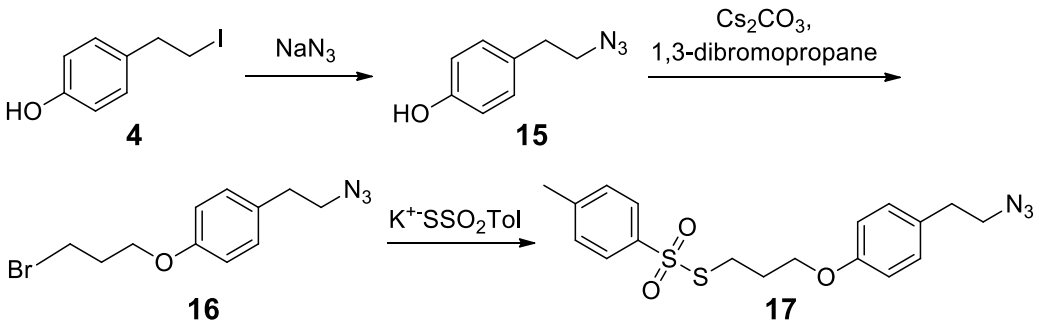

Figure 68: *Synthesis of azide sulfenylating agent **17***

The synthesis of sulfenylating agent **17** conveniently started from the previously described iodide **4**. In the first step **4** was subjected to an S_N2 substitution with sodium azide (1.5 eq) in DMF at 100 °C behind a blast shield. The reaction was left to proceed over three hours after which TLC indicated the formation of a closely running but distinct product. A conventional isolation and chromatography gave **15** as a clear-yellow oil in 96% yield.

The infrared spectrum of **15** showed a characteristic N=N stretching frequency of the azide at 2092 cm^{-1}. The azido methylene protons in the ^{1}H-NMR spectrum revealed the anticipated deshielding compared to the signal in the iodide **4**, together with a downfield shift in the ^{13}C-NMR spectrum from 6.4 ppm in **4** to 52.8 ppm in **15** due to the electron-withdrawing character of the azido group. Finally, a downfield broad singlet for the phenolic proton could also be discerned in the ^{1}H-NMR spectrum.

Incorporation of the bromopropyl side chain made use of a second S_N2 reaction by slowly adding **15** to a stirring solution of an excess of 1,3-dibromopropane (3 eq) to minimise disubstitution, together with caesium carbonate (1.1 eq) as base. The reaction was held at 50 °C for six hours to achieve completion. Any remaining base was quenched by aqueous ammonium chloride in the work-up, and the bromide, **16**, was obtained by silica column chromatography in 68% yield.

An important observation in regard to higher reaction temperatures and/or higher concentrations of base was made. During chromatography one could observe a faint spot that ran very close in R_f to that of the product by TLC and which also showed up as an impurity in the NMR spectra of the product. The spot was isolated via a slow silica gel column, and the ^{1}H-NMR spectrum revealed it to be the allyl ether as shown in **Figure 69**,

presumably derived via an E2 elimination of HBr in keeping with the high temperature (-TΔS as a driver to the ΔG).

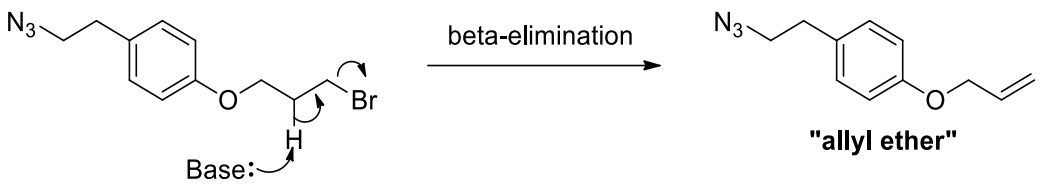

Figure 69: *Observed elimination reaction on* ***16***

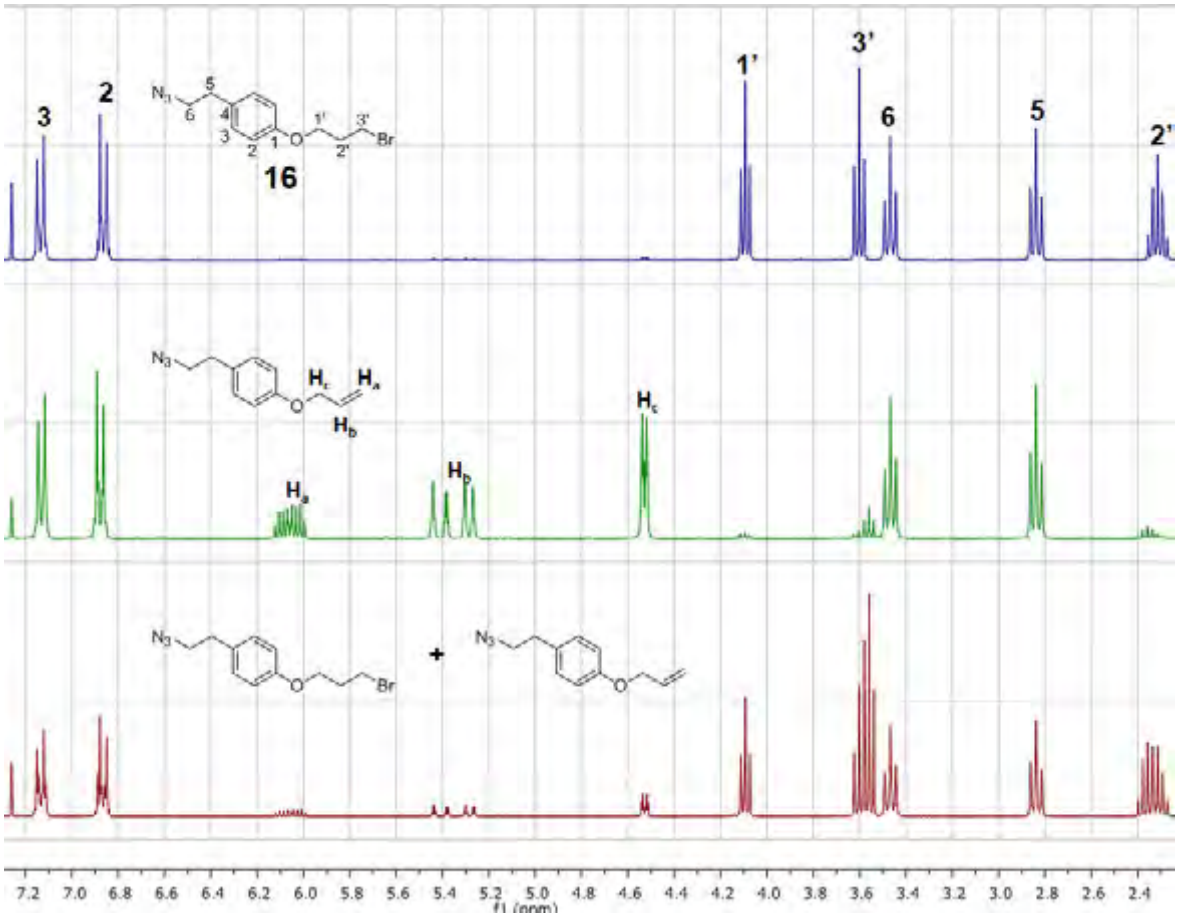

Figure 70: *[1]H-NMR of* ***16*** *(blue), its elimination by-product (green) and mixture (red)*

The [1]H-NMR spectrum (**Figure 70**) in blue shows the desired ether product, while the spectrum in green shows the elimination product, in which the downfield allyl triad can be clearly discerned. Finally, the spectrum in red reflects a mixture as isolated from an initial purification attempt. An IR spectrum run on pure **16** indicated successful ether formation by showing the azide N=N stretching peak at 2091 cm^{-1} and the disappearance of the aromatic O-H stretch, which was observed in compounds **2** and **15** at ~3200 cm^{-1}.

For the final step towards obtaining the sulfenylating agent **17**, bromide **16** underwent a third S_N2 reaction, using potassium *p*-toluenethiosulfonate (potassium thiotosylate; 2 eq) as nucleophile by heating the mixture (60 °C) in acetonitrile for eighteen hours to achieve a full conversion of starting material by TLC. The reaction proved to be low yielding (38%) though, and showed a variety of side products on TLC.

All 14 resonances of the 18 carbon atoms (symmetry) in the molecule were accounted for in the ^{13}C-NMR spectrum of **17**. The ^{1}H-NMR spectrum of **17** is shown in **Figure 71**, which, compared to **16**, showed an additional set of deshielded AA'BB' doublet of doublets at 7.82 ppm (**H-2''**) and 7.12 ppm (**H-3''**)-as well as a new methyl (**H-5''**) singlet at 2.44 ppm, all consistent with the introduction of the thiotosylate group. The IR spectrum showed the retention of the azide functionality by virtue of an azide N=N stretch at 2090 cm^{-1}. Lastly, the high-resolution mass spectrometry (HRMS) data showed a correct molecular mass as an M+H peak: (ES) *m/z*: Found 392.1103, $C_{18}H_{22}O_3N_3S_2$ $(M+H)^+$ requires 392.1108, which confirmed product formation.

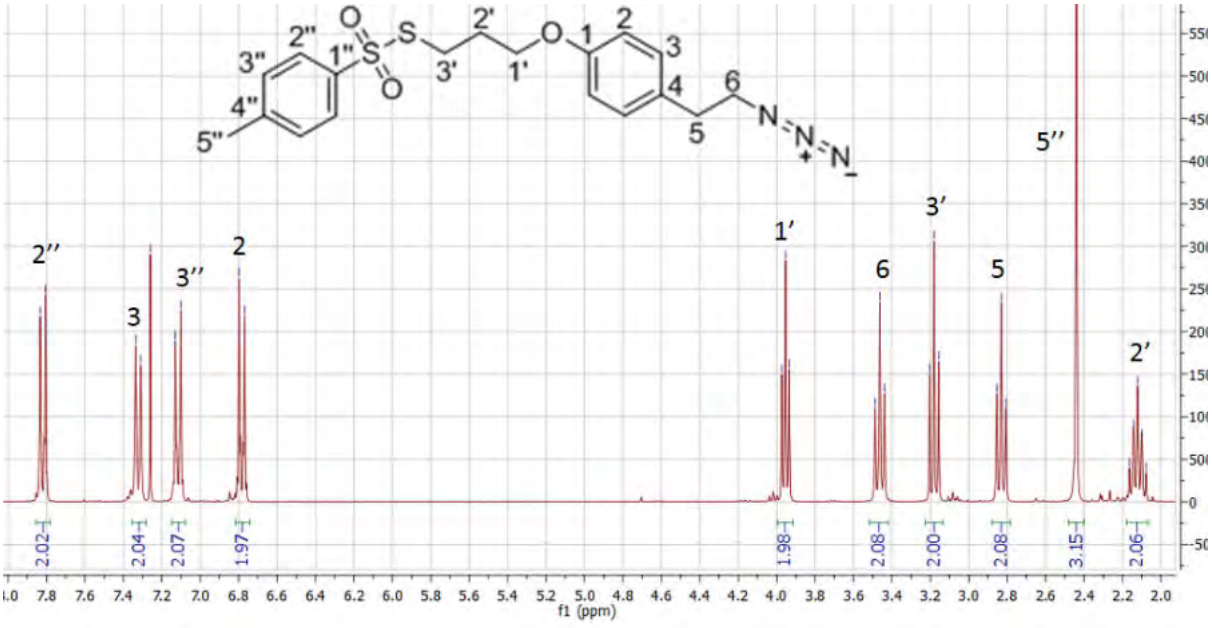

Figure 71: *^{1}H-NMR spectrum of azide sulfenylating agent,* ***17***

With the sulfenylating agent **17** in hand the coupling to vinyl thioacetate **5** previously described (Page 17) proceeded according to the previously established methodology to give vinyl-disulfide **18**, shown in **Figure 72**:

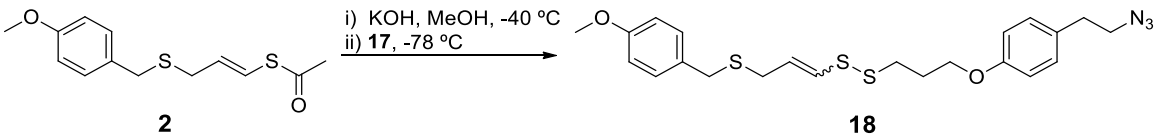

Figure 72: *Synthesis of* ***18***

Here, the low temperature base hydrolysis of **2** afforded the enethiolate *in situ* which was subsequently sulfenylated by **17** to afford **18.** Purification via silica gel column chromatography gave the vinyl-disulfide **18** in 85% yield as a 2:3 mixture of *E*/*Z*-isomers.

Proof of retention of the vinylthio moiety in the product was given by the presence of four vinyl signals in the ^{1}H-NMR spectrum of **18** for the two vinyl hydrogens of each geometrical isomer, as seen in **Figure 73.** These provided the characteristic pattern going from lowfield to highfield of *Z, E, E*, *Z*, here at 6.25 ppm (**H-9*Z***), 6.09 ppm (**H-9*E***), 5.89 ppm (**H-8*E***) and 5.71 ppm (**H-8*Z***) respectively, in which typical coupling constants could be discerned of ~15 Hz for *trans* and ~10 Hz for *cis*. The propyl tether featured as three separate signals at 2.91 ppm (**H-10**), 2.91 ppm (**H-11**) and 4.07-.4.02 ppm (**H-12**), integrating for 2:2:2 protons respectively. Collectively the analysis of ^{13}C-NMR and HSQC data identified all 18 carbon resonances of which some showed a splitting due to their proximity to the stereogenic axis. The infrared spectrum of **18** showed the presence of the azide moiety in the product through an N=N stretch at 2086 cm^{-1}. Conclusive evidence of success was given by the HRMS, where the molecular ion $(M+H)^{+}$ was found at 462.1344, in which $C_{22}H_{28}N_3O_2S_3$ requires 462.1349.

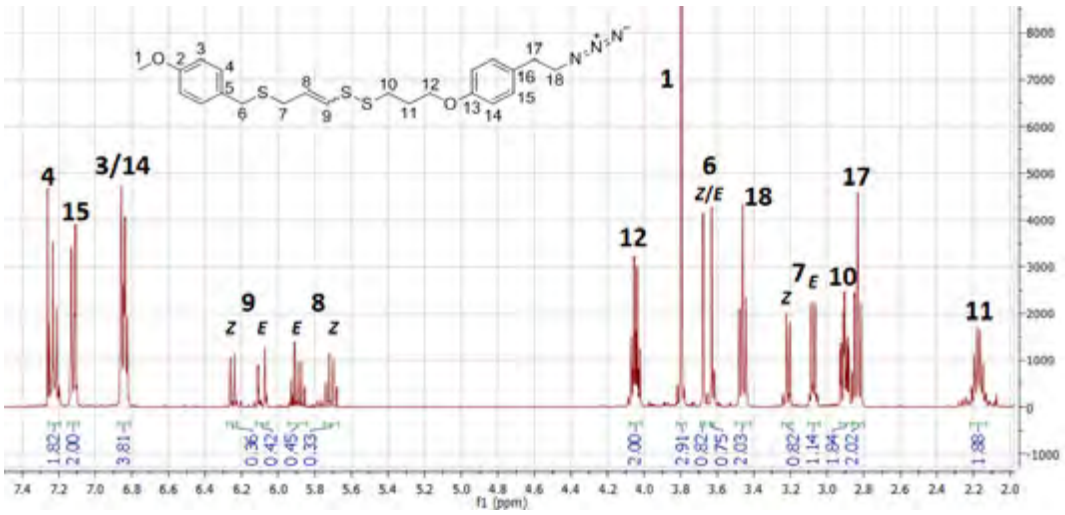

Figure 73: *^{1}H-NMR spectrum of* ***18***

The final step towards obtaining the ajoene analogue involved the chemoselective oxidation of the sulfide **18** to its sulfoxide **19** using *m*-CPBA as an oxidant at low temperature (-78 °C). Analogous to previously described oxidations (towards **7**,**9**,**12** and **14**), the reaction proceeded over one hour and the product was observed as a more polar spot on TLC. Subsequent chromatographic purification afforded the azide-ajoene analogue **19** as a 2:3 mixture of *E/Z*-isomers, in 62% yield.

In its role as an advanced intermediate, the microanalysis of **19** was diligently performed. The newly formed chiral sulfoxide resulted in diastereotopicity in the adjacent (vicinal) methylene hydrogens that was observed in the geminal couplings of **H-6** and **H-7**. All 14 proton signals and 18 carbon signals were successfully assigned via ^{1}H-NMR, COSY, ^{13}C-NMR and HSQC spectra are shown in **Figures 74** and **75**, with nuclei distal to the stereogenic double bond axis, as with previous ajoene derivatives, showing up as a single resonance.

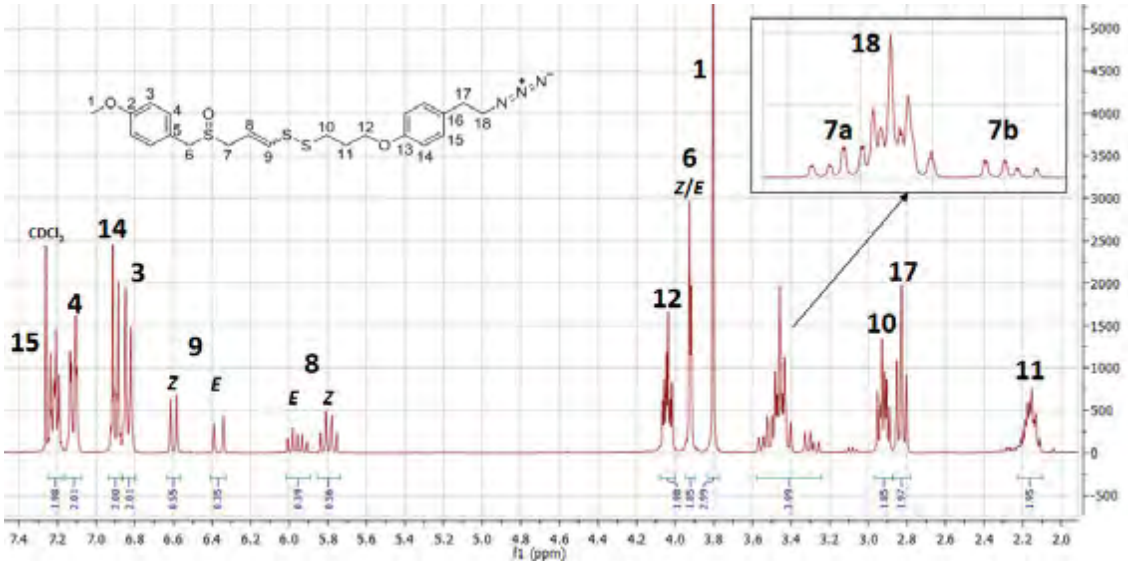

Figure 74: *^{1}H-NMR spectrum of azide-ajoene,* ***19***

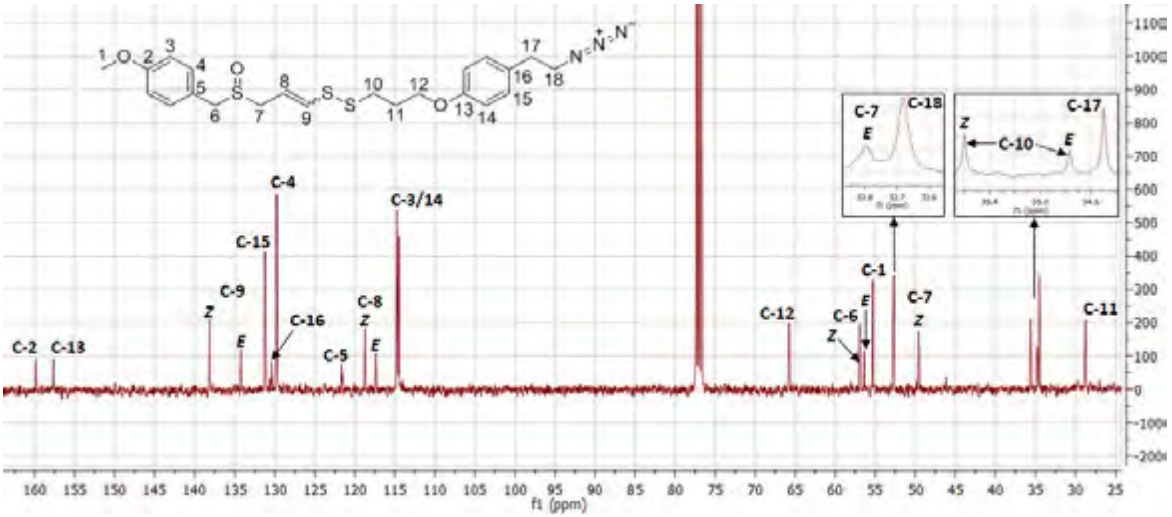

Figure 75: *^{13}C-NMR spectrum of azide-ajoene,* ***19***

The S=O stretch at 1031 cm^{-1} and the N=N stretch at 2094 cm^{-1} in the IR spectrum highlighted the formation of the sulfoxide and the retention of the crucial azide moiety respectively. Lastly, the HRMS data, displayed in **Figure 76**, revealed the correct molecular ion $(M+H)^+$ at 478.1303, where $C_{22}H_{28}N_3O_3S_3$ requires 478.1293, thus consolidating a successful formation of **19**.

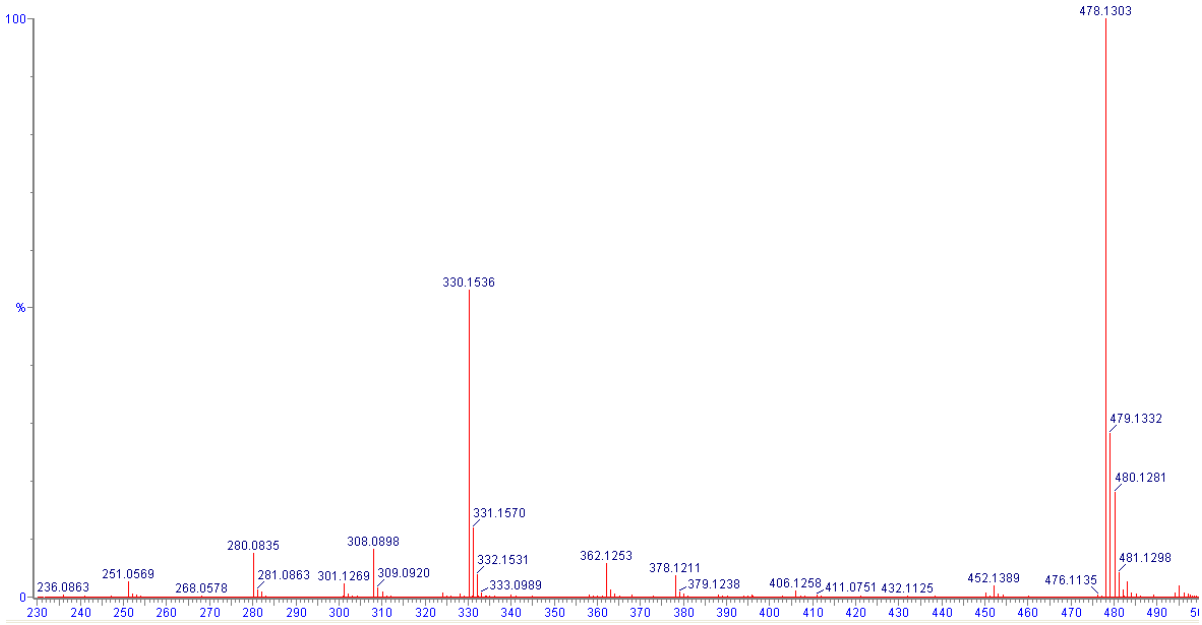

Figure 76: *High-resolution mass spectrum of* ***19***

With the successful synthesis azide-ajoene coupling partner completed, the following section will describe the route towards the alkyne-biotin "Click"-coupling partner, **25**.

4.3.2 Synthesis of alkyne-biotin linker, ***25***

The retrosynthesis plan for **25** is shown in **Figure 77**. The key design element was to insert a water-soluble tether between the biotin tag and the alkyne functionality for "Click" coupling to the ajoene pharmacophore. The cheaply available diamine tether was suitable in that it could be mono-protected, coupled to the alkyne source **21**, deprotected and then coupled with the biotin tag in the last step. Due to its polar nature biotin is notoriously difficult to work and was thus placed at the end of the sequence.

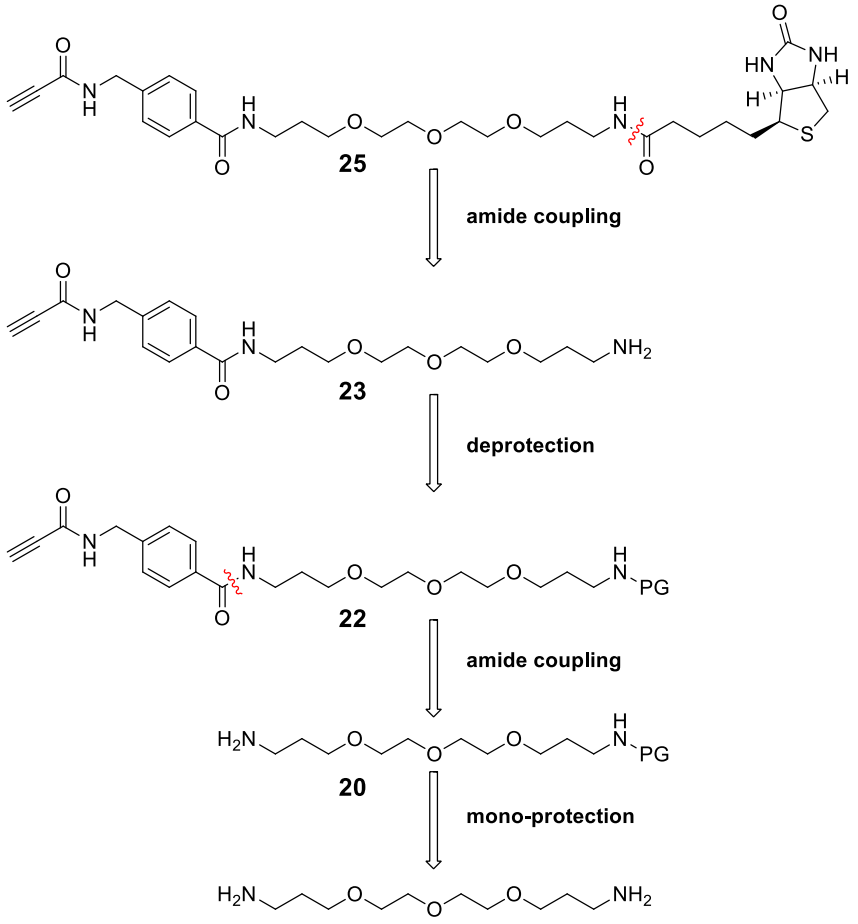

Figure 77: *Retrosynthesis of fragment* ***25***

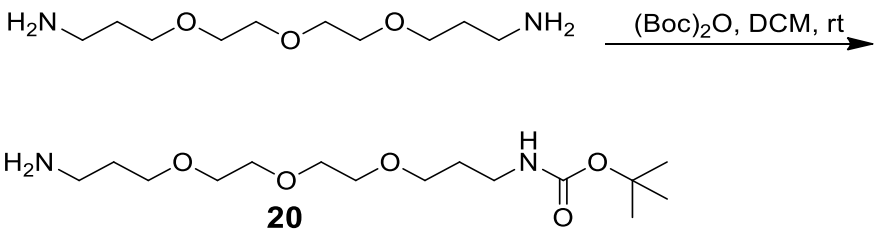

Figure 78: *Synthesis of* ***20***

The synthesis of the alkyne fragment proceeded via the mono-Boc-protection of commercially available 4,7,10-trioxatridecane-1,13-diamine. To this end, the diamine (1.5 eq) and Boc anhydride (1 eq) were reacted in DCM at room temperature, as presented in **Figure 78**. The appearance of an additional spot above the suspected mono-substituted product run on TLC at two hours, as seen in **Figure 79**, led to the termination of the reaction. Subsequent purification of the "middle" spot gave the mono-Boc-protected diamine linker **20** in 46% yield. Due to the affordability of the starting material we could get away with this low yield, but future optimisations would include increasing its equivalence to three or more to reduce di-substitution.

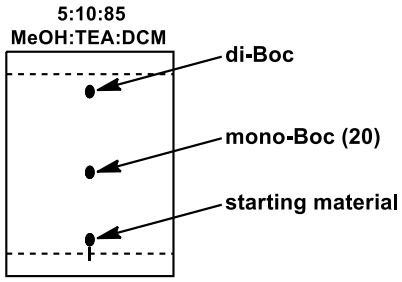

Figure 79: *TLC reaction profile of the protection of the diamine*

The integration ratio of 9:2 between the *tert*-butyl and deshielded α-methylene quartet to the carbamate in the ^{1}H-NMR spectrum suggested the successful mono-substitution in the product. Further evidence was given in the ^{13}C-NMR spectrum in terms of the observation of a single carbamate carbonyl carbon signal as well as a quaternary carbon for the *tert*-butyl moiety at 156.2 and 77.9 ppm, respectively.

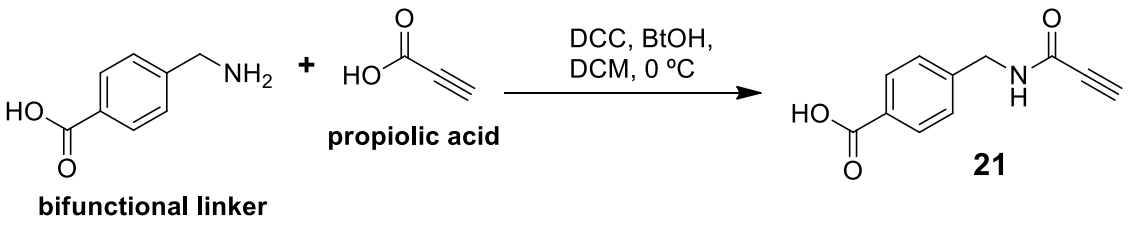

Figure 80: *Synthesis of **21***

The crucial choice of alkyne source was made according to the strategy used by Jezowska previously referred to.[98] Here, propiolic acid was used, not only because of its commercially availability but also because it provided a more reactive alkynyl partner for the "Click"-coupling.[119] In addition, rather than couple propiolic acid directly to the amino group of mono-boc protected tether **20**, in keeping with the strategy of Jezowska, it was

decided to use a commercially available amino acid bifunctional synthon as a secondary tether. To this end a standard DCC/BtOH coupling of the propiolic acid and the benzylic amino group of the bifunctional tether proceeded to completion over two hours to afford **21** (**Figure 80**) in 35% yield, following a Celite filtration to remove the DCU by-product and followed by silica gel chromatography**.** The low yield of **21** could be attributed to di-/poly-merisations reactions occurring on reduced chemoselective grounds (two acids in reactants).

An alkyne singlet at 3.60 ppm and the benzylic methylene singlet at 4.46 ppm in the ^{1}H-NMR spectrum of **21** indicated a successful addition. The ^{13}C-NMR spectrum revealed five quaternary carbon signals at 169.7, 154.8, 144.5/131.2, and 78.0 ppm which, in order, represented the carboxylic and amide carbonyls, the ring's ipso and para positions, and the alkyne internal carbon.

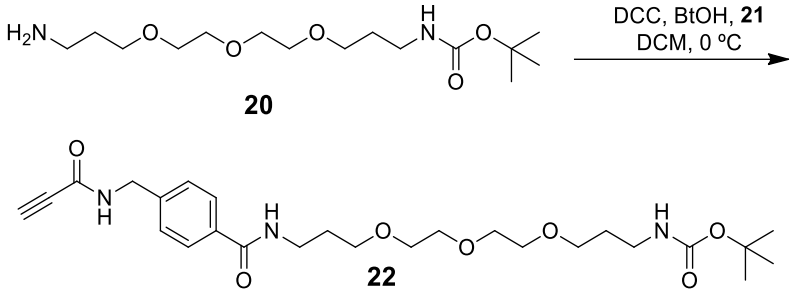

Figure 81: *Synthesis of* ***22***

20 and **21** were also conveniently coupled using DCC/BtOH, as depicted in **Figure 81**, to afford **22** in 84% yield after purification via silica gel column chromatography.

The diagnostic alkyne and *tert*-butyl singlets respectively at 3.64 ppm and 1.42 ppm, with an integration ratio of 1:9, in the ^{1}H-NMR spectrum signified a positive result. The analysis of the ^{13}C-NMR spectrum revealed all 22 distinct carbon signal and the HRMS data showed the $(M+H)^{+}$ molecular at 506.2866, while $C_{26}H_{40}N_3O_7$ required 506.2872, which together combined to give full confidence in the formation of **22**.

The subsequent low temperature (0 °C) Boc deprotection using TFA (10 eq) in DCM was carefully monitored via TLC. The consumption of **22** resulted in the appearance of a more polar spot that could be visualised with ninhydrin spray. At the three hour mark, the reaction mixture was concentrated under low-pressure to remove solvent and excess

TFA. Silica column chromatographic purification using MeOH:DCM (1:9) as eluent afforded the free base **23** in 88% yield by an unknown deprotonation mechanism.

The loss of the protecting group was supported by the absence of both the Boc *tert*-butyl singlet in the ^{1}H-NMR spectrum of **23** (**Figure 82**) as well as the *t*-butyl quaternary carbon signal in the ^{13}C-NMR spectrum. The alkyne terminal hydrogen (singlet) could not be discerned as it was masked by the six methylene signals adjacent to the ether oxygen atoms in the linker chain; nevertheless, the integration of the peak as 13H (6x 2 methylene + 1 alkyne protons) suggested its presence around 3.50 ppm. Additionally, the ^{13}C-NMR spectrum correctly showed all 19 carbon signals for **23**. Lastly, the molecular ion $(M+H)^{+}$ of 406.2342 in the HRMS spectrum, for which $C_{21}H_{32}N_3O_5$ required 406.2347, ratified our success.

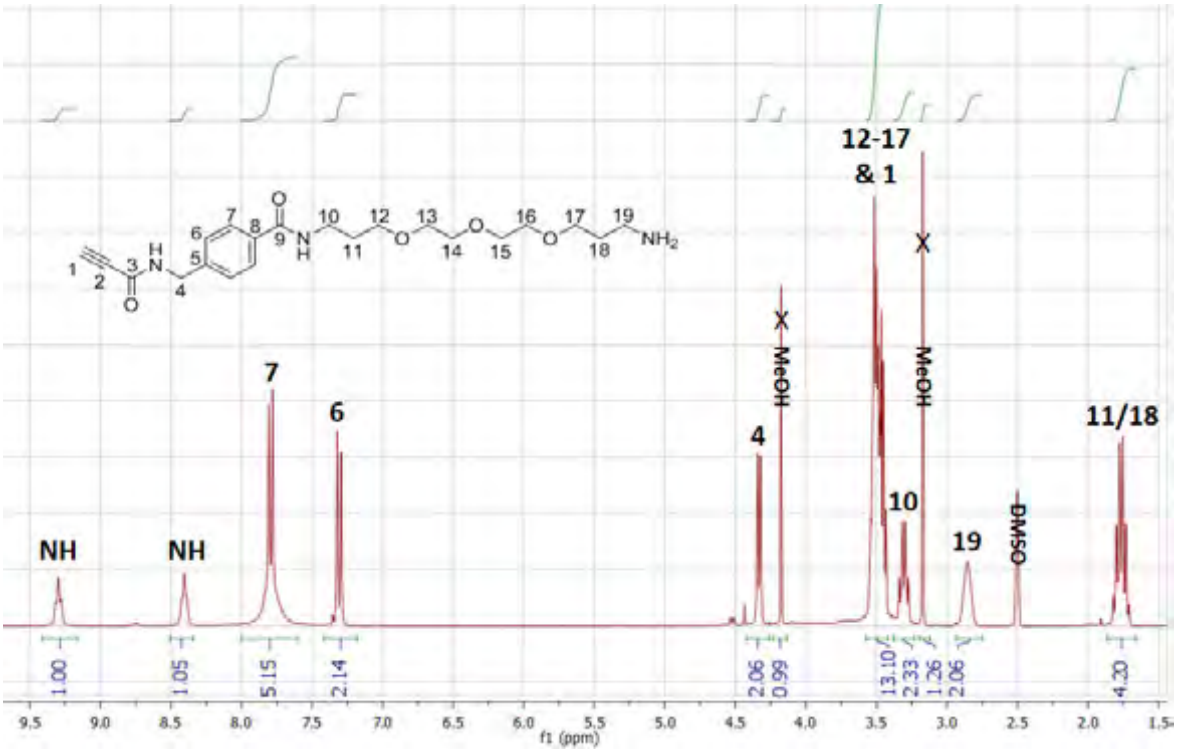

Figure 82: *^{1}H-NMR spectrum of **23***

The final part of the synthesis to obtain "Click"-coupling partner **25** is shown in **Figure 83**:

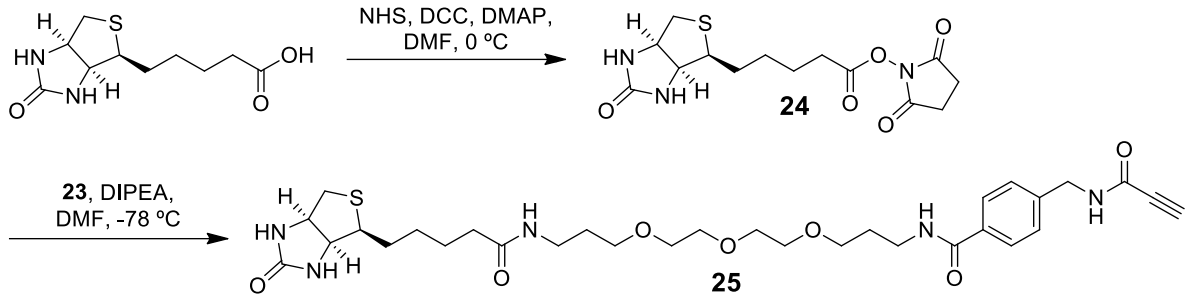

Figure 83: *Synthesis of alkyne-biotin linker,* ***25***

Initially, incorporation of the biotin moiety was envisioned as proceeding via a carbodiimde coupling between biotin and the amine partner but this was unsuccessful. A more extensive literature search then highlighted the use of biotin-N-hydroxysuccinimide ester as electrophilic partner in amide couplings and this proved to be very efficient.[120]

Hence, the required succinimide ester **24** was produced by reacting biotin with NHS (1.2 eq), DCC (1.2 eq) and DMAP (0.2 eq) in DMF at 0 °C for 24 hours. The resulting reaction mixture was filtered through Celite (removal of DCU), then gently heated under reduced pressure to remove the bulk of DMF and lastly triturated with diethyl ether to afford **24** as a solid in 65% yield.

The broad singlet integrating for four protons at 2.81 ppm representing the two NHS methylene proton signals in the ^{1}H-NMR spectrum and a melting point of 205-208 °C, where literature reported 206-207 °C,[120] was taken as sufficient evidence to continue on to the next step.

The final target **25** was reached when the amine **23** and the NHS-ester **24** were combined in DMF at -78 °C using DIPEA as a base. The full consumption of **23,** after two hours, gave a new UV-active less polar spot on TLC. After careful removal of DMF, the remaining residue was lyophilised and purified by silica gel column chromatography to afford **25** in 57% yield.

As before with **19**, this advanced intermediate was meticulously characterised by ^{1}H-NMR, ^{13}C-NMR, HSQC, IR and HRMS data. In addition to the previously described signals of **23** the spectrum featured biotin signals. The ^{1}H-NMR spectrum (**Figure 84**) showed biotin's characteristic c*is* ring junction protons (**H-26** and **H-27**) with a vicinal

coupling constant of 7.9 Hz at 4.50 and 4.31 ppm, respectively. **H-28** showed the strong diastereotopic splitting with a germinal J-value of 12.8 Hz, at 2.94 and 2.72 ppm for **H-28a** and **H-28b**. The highfield region of the spectrum contains the protons of the valeric acid chain (**H-21** to **H-24**), where the proximity to the chiral **H-25**, increased observed diastereotopic splitting. The ^{13}C-NMR spectrum showed 29 distinct carbon signals, of which the strongly deshielded ureido carbonyl (**C-29**) at 175.9 ppm and an additional amide carbonyl (**C-20**) at 169.7 ppm implied successful coupling to biotin. **Figure 85** shows the molecular ion $(M+H)^+$ at 632.3143 $(M+H)^+$ in the HRMS spectrum, where $C_{31}H_{46}N_5O_7S$ requires 632.3113, to give conclusive evidence for the formation of **23**.

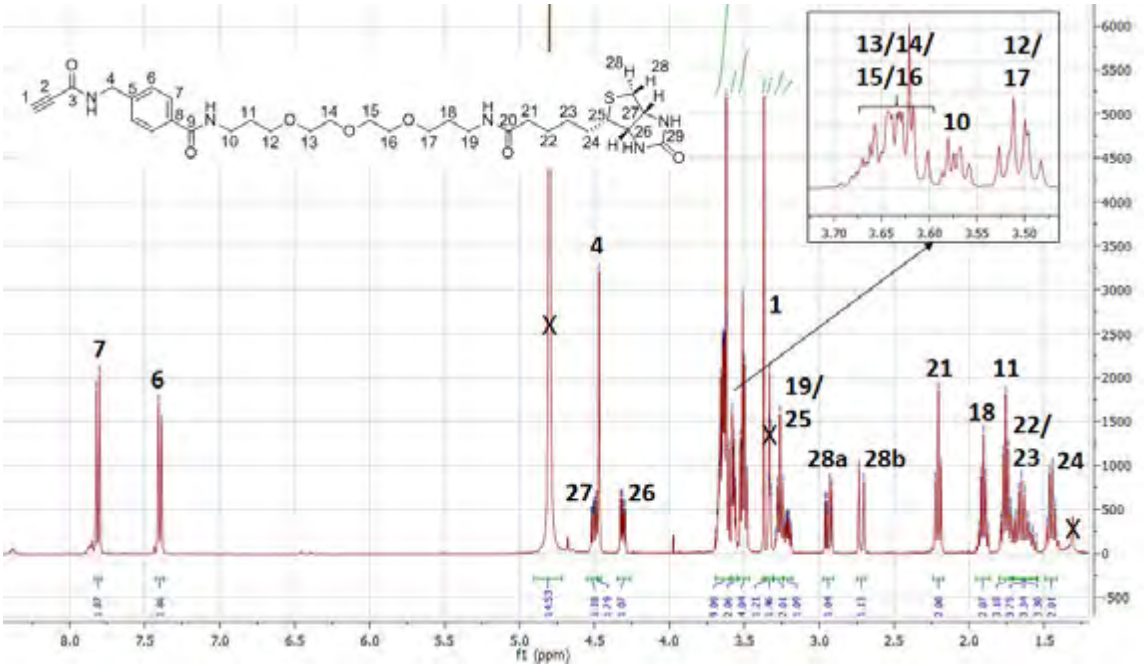

Figure 84: *^{1}H-NMR spectrum of **25***

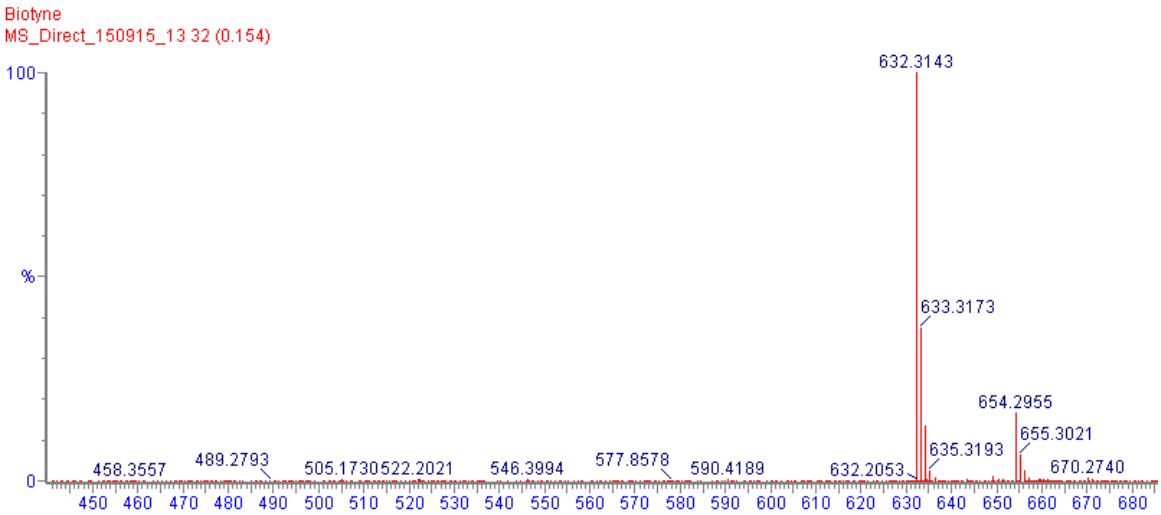

Figure 85: *HRMS spectrum of **25***

4.4 "Click"-coupling of fragments 19 and 25

The use of benign "Click"-technology in aqueous medium as the last step had sidestepped potential synthetic problems. Namely, chemoselectivity during sulfoxide oxidation (additional sulfide on biotin), difficulties in working with polar biotin and suspected sulfide/vinyl-disulfide reactivity between biotin and ajoene. Furthermore this methodology would enable to pre-treatment of cell lines with azide-ajoene **19** and then performing the "Click" on cell lysate with the biotin-alkyne **25** afterwards, as to counter the probe's potential *in vivo* size limitations. **Figure 86** shows the synthetic route to afford the probe **26**:

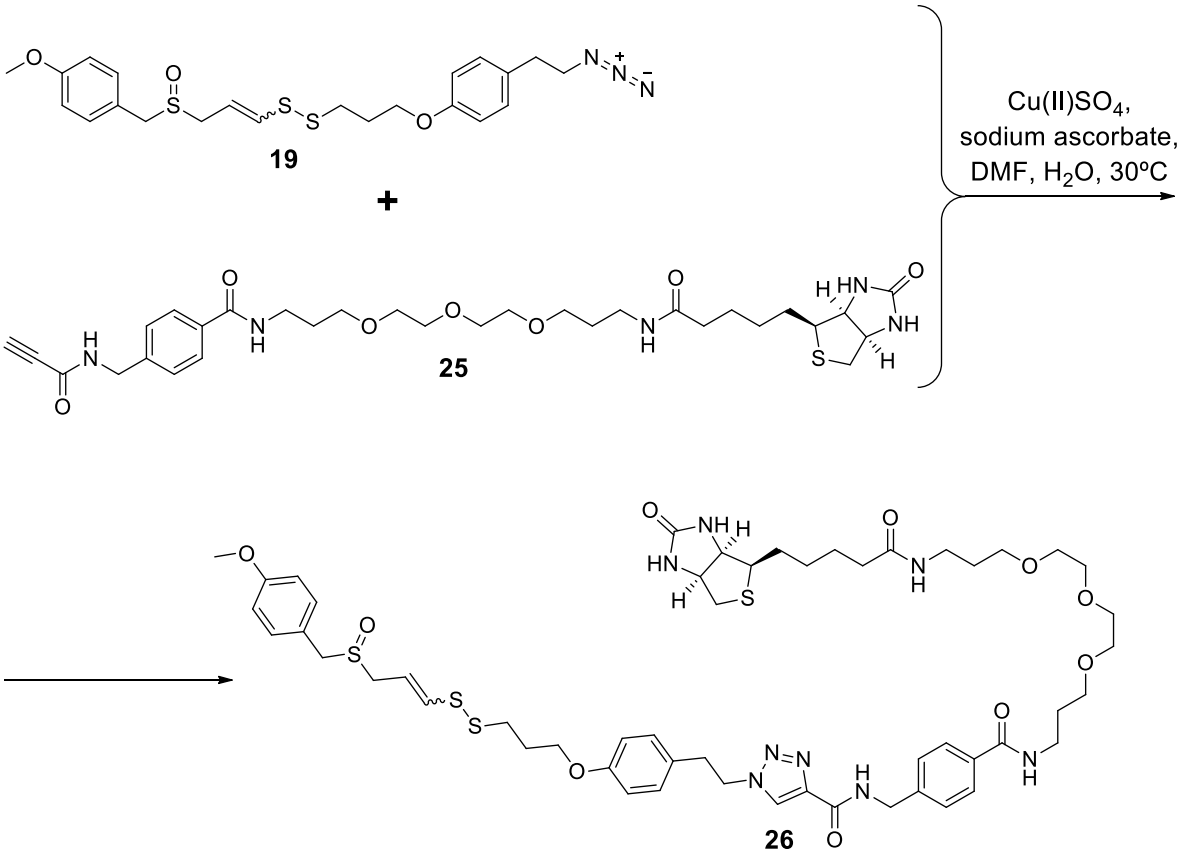

Figure 86: *Synthesis of biotin-ajoene,* ***26***

To a stirring aqueous solution of $CuSO_4$ and sodium ascorbate the azide **19** and alkyne **25**, both in DMF, were added and heated to 30 °C. The reaction was left to proceed overnight and resulted in the formation of a white precipitate. The solvents were removed via lyophilisation and the resulting residue was subject to silica gel column chromatography to afford the biotin-ajoene **26** as a 7:10 mixture of E/Z-isomer in 56% yield.

The probe was found to be insoluble in most conventional NMR solvents and had shown a high degree of instability in d_6-DMSO, the ^{1}H-NMR spectrum was thus run in 1:9 MeOD:$CDCl_3$ to mimic the solvent system that had been used in the column (1:9 MeOH:DCM). The resulting ^{1}H-NMR spectrum, shown in **Figure 87**, showed corresponding peaks attributed to both coupling partners, **19** and **25**. The correct integration ratio of all six aromatic doublets (2:2:2:2:2:2) gave the first indication of a successful reaction. The retention of the pharmacophore was seen as four vinylic signals characteristic of ajoene at 6.51, 6.29, 5.82 and 5.66 ppm which presented themselves in the usual *Z-E-E-Z* splitting pattern for **H-9*Z***, **H-9*E***, **H-8*E***, and **H-8*Z***, respectively. They showed *J*-values of 14.7 (*trans*) and 9.5 Hz (*cis*) for the *E*- and *Z*-isomer and their relative ratio of 7:10 (*E*:*Z*), compared to 2:3 in **19**, suggest that no isomerisation had occurred. The signals 4.37 and 4.17 ppm represent the two vicinal protons (**H-45** and **H-44**) at the ring junction of the biotin coupling partner. As with **25**, the magnetically non-equivalent proton pair of **H-26** was observed at 2.60 and within the multiplet at 2.84-2.76 ppm (overlap with **H-10**). Biotin's characteristic valeric acid chain is seen highfield at 1.29 and 2.09-2.00 for **H-41** and **H-40/-42**, respectively. The triazole (**H-19**) singlet showed up at 7.91 ppm and is the most diagnostic proton signal for the successful coupling. Using ^{13}C-NMR and HSQC data, all 47 carbon signals could be correctly assigned. Lastly, the HRMS data in **Figure 88** shows the molecular mass peak $(M+H)^+$ at 1109.4332 $(M+H)^+$, where $C_{53}H_{73}N_8O_{10}S_4$ requires 1109.4338, which corroborated the synthesis of our ajoene-biotin target **26**.

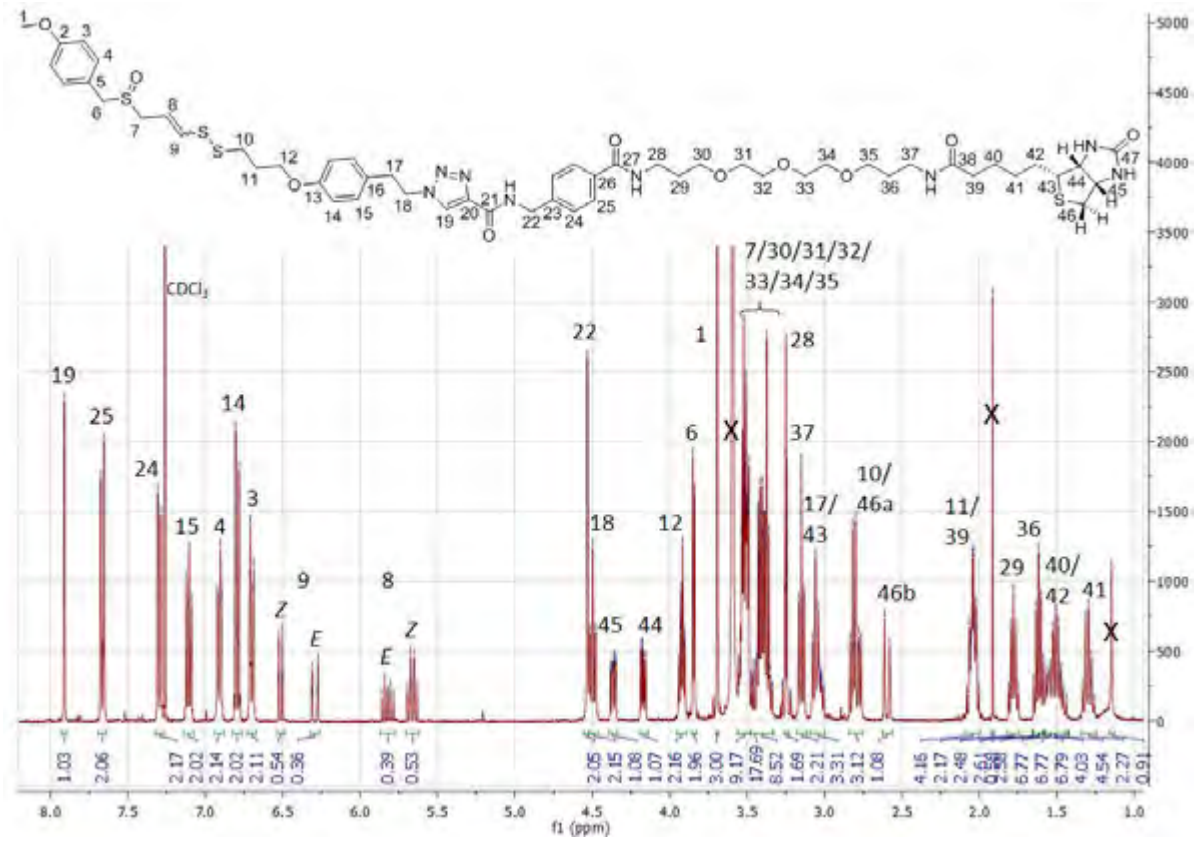

Figure 87: *^{1}H-NMR spectrum of* ***26***

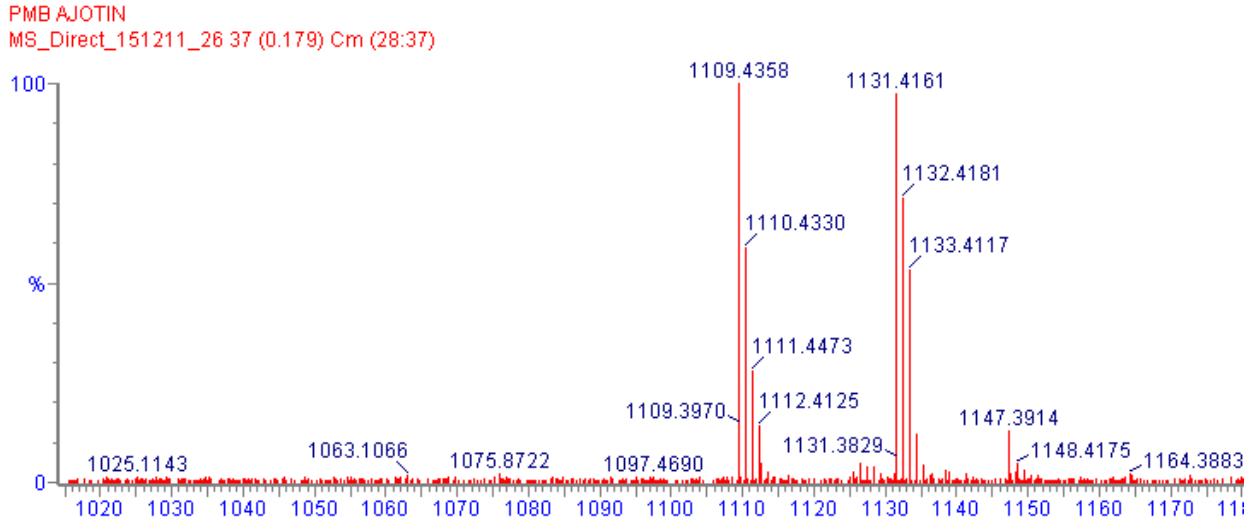

Figure 88: *HRMS spectrum of* ***26***

4.5 Biological evaluation of biotin-probe

4.5.1 Anti-proliferative activity

Ajoene has been shown to be an efficient cytotoxic agent to cancer cells both *in vitro* and *in vivo*. In this regard it has been shown to trigger events that lead to apoptosis and that inhibit cell proliferation. Although some of these pathways are known, only a handful of the specific ajoene drug targets have been identified. Previous studies in our lab have found that ajoene targets and *S*-thiolates multiple proteins in cancer cells. We aimed to identify these proteins using our newly synthesised probe.

It was important to first ascertain that the synthesised biotinylated ajoene still retains its activity in cancer cells. The probe's activity was therefore first validated in a MTT assay against WHCO1 cancer-cells. The azide ajoene **19** and alkyne biotin **25** were also tested as we anticipated their use for *in situ* "Click"-biotinylation experiments. The ajoene analogues could not be separated into *E*- and *Z*- isomers and were thus tested as *E*/*Z*-mixtures. The IC_{50} value obtained are shown in **Table 6**:

Table 6: *Activity of biotin-ajoene and its two "Click"-fragments against WHCO1 cell proliferation*

No.	Name	Structure	WHCO1 $IC_{50} \pm SD$ / μM
19	Azide-ajoene	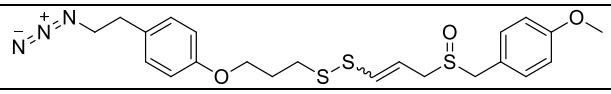	0.1 μM
25	Biotin-alkyne	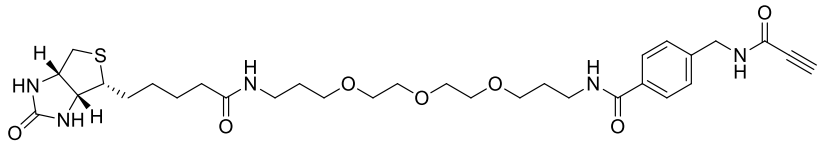	>200 μM
26	Biotin-ajoene	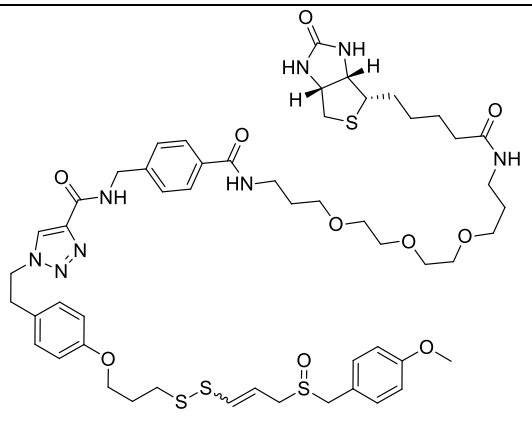	0.43 μM

Both the biotin-ajoene **26** and its azide-ajoene precursor **19** were found to be highly active. The biotin-alkyne **25** showed no activity above the maximum tested dose of 200 μM. This was expected, as it lacks the ajoene disulfide pharmacophore. Interestingly, **19** which contains an azide functional group is the most active ajoene analogue which we have synthesised to date.

When the fully assembled biotin probe **26** was solubilised in DMSO, it was found that degradation occurred. This was initially observed when the probe was solubilised in DMSO for NMR characterisation. An apparent degradation was observed by colour change, the forming of a gel and broadening of the ^{1}H-NMR signals in DMSO solvent. Subsequent methanol and chloroform were used as NMR solvents however these two solvents are not suitable for biological studies as they are toxic to cells. The aggregates which are formed in DMSO can be observed in the snapshot taken of the cancer cells following 48 hour incubation with **26** (**Figure 89**). Therefore the apparent cytotoxicity of **26** cannot be attributed to biotin-ajoene as this compound had degraded and formed a gel in the MTT assay.

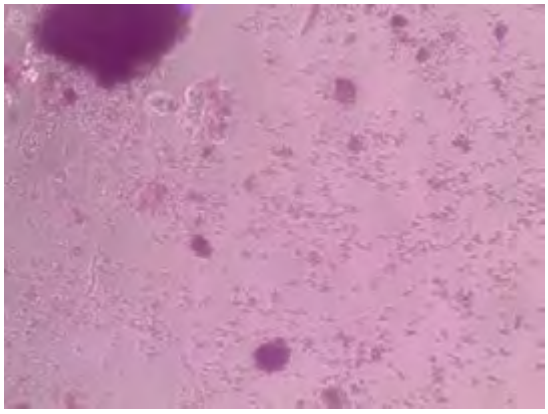

Figure 89: *Magnified image of treated WHCO1 cells showing aggregates of insoluble degraded biotin-ajoene following DMSO delivery*

We therefore developed a detergent-based solvent system to solubilize biotin-ajoene. We used a DMSO:H_2O:PEG400 solubilisation mixture in a 2:9:9 ratio which did not result in aggregation and the compound appeared stable when monitored by TLC.

5.4.2 Immunoblotting

After showing that our novel ajoene analogues **19** and **26** had retained their anti-proliferative activity, it was important to validate that the probe was able to undergo a disulfide exchange with reactive cysteine residues on proteins involving transfer of the biotin tag. In light of our findings that ajoene formed a disulfide bond with the Cys-93 residue on the β-subunits of human haemoglobin, we decided to perform a model reaction between biotin-ajoene and haemoglobin. Therefore, Hb in buffer (10 μM, PBS, pH 7.4) was incubated with 100 μM of either biotin-ajoene or azide-ajoene (in DMSO/H2O/PEG400). After one hour at 37 °C, an *in situ* "Click"-reaction was performed on the samples pretreated with azide-ajoene. It involved the addition of biotin-alkyne **25** and its Cu(I) catalyst (aq. $CuSO_4$/sodium ascorbate), followed by another hour of incubation at 37 °C. All Hb samples were then subjected to either reducing (DTT, 100 mM) or non-reducing conditions (without DTT) and loaded onto a polyacrylamide gel to perform electrophoresis. The resulting gel was washed to remove unbound ajoene, probed with an anti-biotin antibody and visualised using a secondary antibody conjugated to horseradish peroxidase. Chemiluminescence detection of the secondary antibody was visualised in a bioimager and the blot is shown in **Figure 90:**

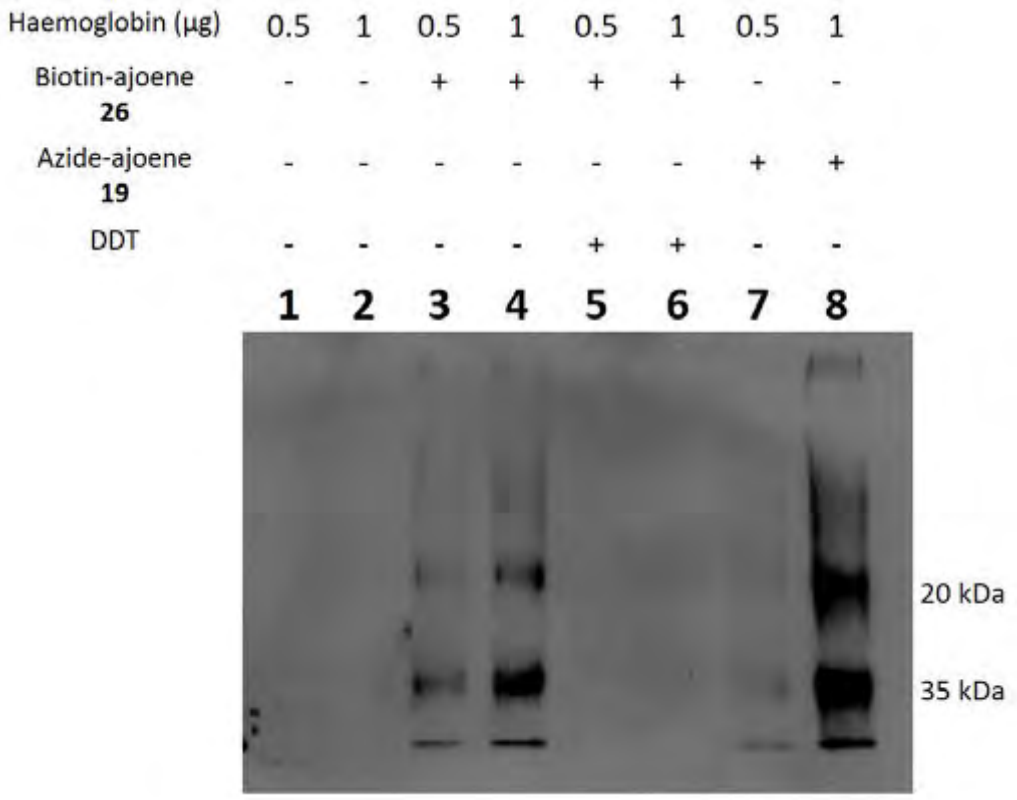

Figure 90: *Western blot showing biotinylated Hb*

The untreated Hb sample (Lanes **1** and **2** in **Figure 90**) did not show any chemiluminescence bands. This was expected as it did not contain any of the biotinylation reagent. Distinct chemiluminescence bands were observed for the Hb sample that had been treated with biotin-ajoene **26** (Lanes **3** and **4**) which demonstrates that the Hb protein was successfully labelled with biotin. It was significant to see that two fluorescent bands were observed on the gel. The molecular weight approximations (via the protein ladder) gave 35 kDa for the bottom and 20 kDa for the top band, as shown in **Figure 90**. These bands represent the β-subunit monomer (top) or the αβ-dimer (bottom) of the 64 kDa Hb tetramer. Lanes **5** and **6** which had been treated with the biotin probe **26** and then incubated with DTT failed to show a band which implies the biotin label had been cleaved off (ie reduced) supporting attachment via a disulfide linkage. The alternative *in situ* "Click"-strategy for biotinylation using **19** and **25** (Lanes **7** and **8**) proved to be successful with the appearance of chemiluminescence bands identical to those when using the intact probe **26**. This implies that both strategies transfer biotin to the same position and that the label has the same final structure (Protein-S-S-linker-biotin). We had already previously demonstrated by proteomics that Hb is one of the targets of ajoene. Therefore in this model study, we have now demonstrated that both biotin-ajoene

26 and azide-ajoene **19**, followed by *in vitro* "Click" with biotin-alkyne **25**, are able to successfully attach ajoene to the protein via a disulfide bond. With the successful synthesis and biological efficacy experiments of the biotin-ajoene probe, it can now be used to tag the binding partners of ajoene in cancer cells. After isolation of these tagged proteins via streptavidin beads, these proteins may be identified by proteomics.

4.6 Summary and outlook

In this chapter, we presented the convergent synthesis of biotin-ajoene **26** from two "Click"-able synthons (**19** and **25**). The azide-functionalised ajoene **19** was accessed via the UCT ajoene synthesis. In this synthesis, a novel sulfenylating agent **17** inserted the azide moiety at the non-vinyl sulfur of ajoene. The regioselectivity of the proposed thiolysis exchange at this position was crucial to ensure the successful transfer of the biotin label onto the protein target. Strategic amide coupling and substitution methodology afforded biotin-alkyne linker, where it was found that the NHS-ester **24** was most suited for the biotin coupling in the final step.

We were able to demonstrate that biotin-ajoene **26** is able to *S*-thiolate Hb *in vitro* by SDS-PAGE using an anti-biotin antibody. Attachment of the large biotin probe at the terminus of ajoene still rendered ajoene able to *S*-thiolate Hb via its sulfoxide vinyl-disulfide pharmacophore. The azide-ajoene **19** was the most cytotoxic ajoene analogue synthesised to date. With its antiproliferative activity in the nanomolar range and its use in the *in situ* "Click"-methodology, the azide-ajoene **19** has four main advantages over the fully assembled probe **26**. (1) It is easier to synthesize than biotin-ajoene making it more accessible; (2) the azide-ajoene analogue is a close structural relative to *bis*-PMB and ajoene, which means that it may have similar target specificity especially at residues that might be sterically restricted; (3) the "Click"-ligation can be easily performed on the treated cell lysate, and lastly, (4) biotin-ajoene does not meet three of the five parameters for reasonable drug absorption as popularised by Lipinski, where it has a molecular weight above 500 Da, has more than ten hydrogen bond acceptors and more than five hydrogen bond donors.[101,102] In future, the biotin-ajoene probe can be used on cancer cells to identify the protein targets of ajoene.

Chapter Five: Conclusion and Future Work

In this thesis we aimed to synthesise a *bis*-PMB ajoene analogue with improved blood stability with retained cancer cell cytotoxicity. A small library of eight analogues with improved aqueous solubility and variations in the sulfoxide/vinyl-disulfide pharmacophore were synthesised. The vinyl-disulfide series was synthesised via the UCT ajoene synthesis where the solubility modification was introduced via the phenol sulfenylating agent in the key *S*-thiolation step. A dialkylation strategy of 1,3-propanedithiol involving the sulfenylating agent successfully afforded the dihydroajoene series. The phenolic hydroxyl enabled direct access to the amide series via alkylation with iodoacetamide.

The compounds were tested against WHCO1 oesophageal cancer cell proliferation and their stability was evaluated *in vitro* in mouse blood. All the structural variations on the ajoene molecule produced strongly cytotoxic analogues with IC_{50}'s below 20 μM. Importantly, cytotoxicity and blood stability were established as being inversely related. It was found that the presence of the double bond (as the vinyl group) was important for strong cancer cell cytotoxicity (low blood stability). The analogues with amide functionalization were slightly less cytotoxic but also more stable in blood compared than those with a hydroxyl group. The role of the sulfoxide is not as clear but it appears to decrease activity of the vinyl-disulfides while increasing activity of the dihydroajoenes. This is presumably due to inhibition of disulfide activation in the vinyl-disulfides versus enhanced disulfide activation in the dihydroajoenes, the latter by a long range inductive electron-withdrawal via the sigma-framework.

It is proposed that thiolysis exchange with a cysteine thiolate or GSH constitutes the underlying mechanism of ajoene and that activation of the disulfide towards thiolysis exchange renders the compound more cytotoxic to cancer cells and less stable in blood. Owing to literature reports on the toxicity of garlic disulfides towards erythrocytes as well as the observed adverse effects of *bis*-PMB in animal studies from our group, we suspected that ajoene may interact with haemoglobin. We found from UV-Vis and MS studies, that ajoene can covalently modify human haemoglobin via thiolysis exchange at cysteine-93 in the β-subunit. Therefore the cytotoxicity of ajoene to erythrocytes may arise from reaction with GSH and Hb. Within the parameters of our aim, the

dihydroajoenes (**11**-**14**) present an improved lead structure for future *in vivo* experiments, where the removal of the double bonds resulted in acceptable blood half-lives of approximately 60 minutes (compared to about 5 minutes in *bis*-PMB), and the retention of strong *in vitro* cancer cell cytotoxicity (IC_{50}<25 μM for the weakest of the series).

We have previously shown that a synthetic fluorescent synthetic-derived dansyl-labelled ajoene regioselectively *S*-thiolates multiple protein targets within cancer cells via a thiol-disulfide exchange. In this thesis, we synthesised a novel biotin-labelled ajoene probe **26** via a "Click"-reaction in the final step between alkyne-biotin **25** and azidated ajoene **19**. The alkyne-biotin was afforded via a series of substitution and amide coupling reactions. In line with our design considerations, the sulfenylating agent **17** successfully placed of the azide functionality at the non-vinyl sulfur position, of the vinyl-disulfide pharmacophore, which directs the regioselective transfer of the biotin label onto protein targets.

The above-mentioned biotin-labelled ajoenes have been applied in biotin-streptavidin technology, aimed at the isolation and characterisation of ajoene's protein targets within cancer cells. In a model experiment, we showed that protein biotinylation via thiolysis could be achieved via two strategies, which were both successful and in agreement. In the first strategy the whole probe was used to directly label the cancer cell proteins, while in the second, the probe was assembled *in situ* via "Click"-chemistry after cancer cell pre-treatment with azide-ajoene. The successful transfer of the (biotin) label was demonstrated onto Hb protein by western blot using an anti-biotin antibody. This chemical biology tool will be used in my upcoming doctoral studies to investigate and identify ajoene's protein targets, and to explore their involvement in apoptotic and antiproliferative anticancer signalling pathways of ajoene.

Chapter Six: Experimental section

6.1 Synthetic Method

6.1.1 General

All solvents were freshly distilled. Dichloromethane was distilled over phosphorus pentoxide under nitrogen. Tetrahydrofuran was distilled under nitrogen and dried over sodium wire benzophenone. Acetonitrile was distilled from calcium hydride under nitrogen. Other reagents were purified according to standard procedures. All reagents were purchased from Sigma-Aldrich (South Africa) or Merck (Darmstadt, Germany) and were used without further purification. Room temperature refers to ambient temperature. Low temperature reactions were carried out using liquid nitrogen in acetone (-78 °C)/CH_3CN (-40 °C)/BnOH (-20 °C) or a slurry of water and ice (0 °C). Thin layer chromatography (TLC) was used to monitor reactions using aluminium backed Merck silica-gel 60 F_{254} plates. Compounds on TLC were visualised by a combination of ultra-violet light (V_{max} = 254nm), iodine vapour, by spraying with a 2.5% solution of anisaldehyde in a mixture of sulfuric acid and ethanol (1:10 v/v), ninhydrin (300 mg in 97 mL ethanol and 3 mL acetic acid) or $KMnO_4$ (1.5 g with 10g K_2CO_3 and 1.25 mL 10% NaOH in 200 mL H_2O) and then heating at 150°C. Column chromatography was performed using silica-gel 60 mesh (Merck 7734). All chromatography was carried out using petroleum ether (b.p. 40-60 °C), ethyl acetate, dichloromethane or methanol as eluents, or a combination of these. NMR spectra were recorded on either a Varian Mercury 300 MHz (75.5 MHz for ^{13}C-NMR) or a Bruker 400 MHz (101 MHz for ^{13}C-NMR) instrument and were carried out in chloroform-*d*, acetone-d_6, dmso-d_6, methanol-d_4 with the following references respectively in ppm: chloroform (δ 7.26 in ^{1}H-NMR and δ 77.16 in ^{13}C-NMR), acetone (δ = 2.05 in ^{1}H-NMR δ = 206.26 in ^{13}C-NMR), dimethylsulfoxide (δ = 2.50 in ^{1}H-NMR and δ = 39.52 in ^{13}C-NMR) or methanol (δ = 3.31 in ^{1}H-NMR δ = 49.00 in ^{13}C-NMR).[121] All Chemical shifts (δ) are reported in ppm and *J* values are quoted in Hz. Melting points were measured on a Reichert-Jung Thermovar hot-stage microscope and are uncorrected. Infrared spectra were recorded on a Perkin Elmer Spectrum 100 FT-IR Spectrometer. High-resolution mass spectrometry was performed at the Central Analytical Facilities, School of Chemistry, University of Stellenbosch on a Waters Synapt G2 machine in ESI mode.

6.1.2 *bis*-PMB analogues

(4-Methoxybenzyl)(prop-2-yn-1-yl)sulfane, **(1)**[66]

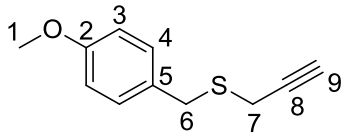

To a stirring solution of PMBCl (1.73 mL, 12.8 mmol, 1 eq) in acetonitrile (40 mL) under N_2 was added thiourea (1.17 g, 15.4 mmol, 1.2 eq) and the reaction heated to 85°C after which it was refluxed for 14 hours. The mixture was cooled in an ice bath and the resulting white precipitate was filtered, washed with ice-cooled acetonitrile (2 x 10 mL) and dried under reduced pressure to afford the isothiouronium salt as a white solid (2.80 g, 94%).

ν_{max}/ cm^{-1} (ATR): 2974, 2950 (N-H stretch x 2); Mp (CH_3CN): 161-162 °C.

The isothiouronium salt (2.80 g, 12.0 mmol, 1 eq) was added to a solution of KOH (1.35 g, 24.1 mmol, 2 eq), in anhydrous MeOH (24 mL) under N_2 at -20°C (benzyl alcohol/liquid nitrogen) and left stirring for two hours. Propargyl bromide (2 mL, 18.05 mmol, 1.5 eq) was then added and the reaction stirred at 0°C for 30 minutes upon which the reaction was quenched with saturated aqueous NH_4Cl (10 mL). The product was extracted with EtOAc (3 x 20 mL) and the combined fractions were washed with water (2 x 20 mL) and brine (1 x 15 mL). The solvent was removed under reduced pressure and the residue was purified via silica column chromatography (EtOAc:Hexane = 5:95) to afford propargyl sulfide **1** as a clear light-yellow oil (1.98 g, 85%).

R_f = 0.9 (EtOAc:Hexane, = 10:90); IR ν_{max}/ cm^{-1} (ATR): 3286 (alkyne C-H stretch); δ_H (300 MHz, $CDCl_3$) 7.26 (3H, d, *J* = 8.7 Hz, H-3), 6.86 (2H, d, *J* = 8.7 Hz, H-4), 3.83 (2H, s, H-6), 3.80 (3H, s, H-1), 3.07 (2H, d, *J* = 2.6 Hz, H-7), 2.28 (1H, t, *J* = 2.6 Hz, H-9); δ_C (101 MHz, $CDCl_3$) 158.9 (C-2), 130.2 (C-4), 129.5 (C-5), 114.1 (C-3), 80.1 (C-8), 71.3 (C-9), 55.4 (C-1), 34.8 (C-6), 18.4 (C-7).

S-(3-((4-Methoxybenzyl)thio)prop-1-en-1-yl) ethanethioate, **(2)**[66]

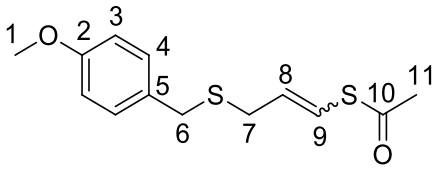

The propargyl sulfide **1** (1.4 g, 7.3 mmol, 1 eq) was suspended in toluene (35 mL) under N_2 and ACCN (0.18 g, 0.73 mmol, 0.1 eq) was added. The mixture was brought to reflux (85°C), at which point thiolacetic acid (0.62 mL, 8.7 mmol, 1.2 eq) was added drop-wise. The reaction was held at 85°C and was allowed to progress for three hours. The reaction was brought down to room temperature and quenched with saturated aqueous sodium bicarbonate (5 mL). The toluene was removed under reduced pressure and the product was extracted with EtOAc (3 x 20 mL). The combined fractions were washed with water (2 x 15mL) and brine (1 x 10 mL), then dried over $MgSO_4$ and concentrated. The silica column chromatography (EtOAc:Hexane = 10:90) afforded thioacetate **2** as a 1:2 mixture of *E/Z*-isomers and as an odiferous clear colourless oil (0.98 g, 45%).

E/Z mixture: R_f = 0.7 (EtOAc:Hexane, = 20:80); IR ν_{max}/ cm^{-1} (ATR): 1700 (C=O);

E-isomer: δ_H (300 MHz,$CDCl_3$): 7.22 (2H, d, *J* = 8.7 Hz, H-4), 6.85 (2H, d, *J* = 8.7 Hz, H-3), 6.50 (1H, dt, *J* = 15.6, 1.2 Hz, H-9), 5.82 (1 H, m, H-8), 3.80 (3H, s, H-1), 3.63 (2H, s, H-6), 3.12 (3H, dd, *J* = 7.4, 1.2 Hz H-7), 2.39 (3H, s, H-11); δ_C (75 MHz, $CDCl_3$): 193.1 (C-10), 158.9 (C-2), 130.3 (C-8), 130.2 (C-4), 129.9 (C-5), 119.5 (C-9), 114.1 (C-3), 55.4 (C-1), 34.5 (C-6), 33.3 (C-7), 30.5 (C-11).

Z-isomer: δ_H (300 MHz, $CDCl_3$): 7.22 (2H, d, *J* = 8.6 Hz, H-4), 6.85 (2H, d, *J* = 8.6 Hz, H-3), 6.67 (1H, dt, *J* = 9.6 Hz, 1.1, H-9), 5.86 (1 H, m, H-8), 3.80 (3H, s, H-1), 3.64 (2H, s, H-6), 3.13 (2H, dd, *J* = 7.6, 1.1 Hz, H-7) 2.40 (3H, s, H-11); δ_C (75 MHz, $CDCl_3$): 191.4 (C-10), 158.9 (C-2), 130.0 (C-4), 129.9 (C-5), 128.7 (C-8), 119.7 (C-9), 114.1 (C-3), 55.4 (C-1), 35.3 (C-6), 31.0 (C-7), 30.8 (C-11).

4-(2-Hydroxyethyl)-phenol, **(3)**[103]

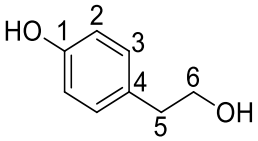

$LiAlH_4$ (2.00 g, 53.0 mmol, 2.2 eq) was added to THF (80 mL) at 0°C under N_2 and ethyl 2-(4-hydroxyphenyl)ethanoate (4.00 g, 24.1 mmol, 1 eq) in THF (20 mL) added drop-wise. After two hours the reaction was quenched with 1M HCl (80 mL). Upon filtration through Celite the filtrate was extracted using EtOAc (3 x 100 mL), washed with saturated aqueous sodium bicarbonate (50mL) and then brine (50mL). The combined organic fractions were dried over $MgSO_4$ and concentrated under reduced pressure. Purification via column chromatography (EtOAc: Hexane) yielded alcohol **3** as a white crystalline solid (3.26g, 98%), which was crystallised from EtOAc/Hexane.

R_f = 0.35 (EtOAc: Hexane = 50:50); Mp (EtOAc/Hexane): 91-93 °C, lit[103] Mp: 90 °C; IR ν_{max}/ cm^{-1} (ATR): 3384 (O-H), 3130 (aromatic O-H); δ_H (300 MHz, d_6 acetone): 8.10 (1H, brs, OH), 7.05 (2H, d, *J* = 8.7 Hz, H-3), 6.73 (2H, d, *J* = 8.7 Hz, H-2), 3.67 (2H, t, *J* = 7.2 Hz, H-6), 2.94 (1H, brs, OH') 2.70 (2H, t, *J* = 7.2 Hz, H-5); δ_C (101 MHz, d_6-acetone): 156.3 (C-1), 130.8 (C-4), 130.5 (C-3), 115.7 (C-2), 64.1 (C-6), 39.2 (C-5).

4-(2-Iodoethyl)-phenol, **(4)**[122]

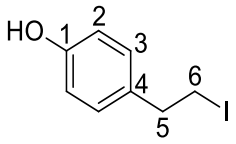

The alcohol **3** (3.26 g, 23.6mmol, 1 eq) dissolved in THF (45 mL) at 0° C under N_2 and imidazole (3.21 g, 47.2 mmol, 2 eq), triphenylphosphine (12.4 g, 47.2 mmol, 2 eq) and iodine (12.0 g, 47.2 mmol, 2 eq) were sequentially added to the reaction vessel. The mixture was allowed to warm to room temperature and after two hours the reaction was quenched with aqueous saturated sodium thiosulfate (30 mL). The organic products were extracted into EtOAc (3 x 40 mL), which was then washed with HCl (1 M, 20 mL), aqueous saturated sodium bicarbonate (30 mL) and brine (20 mL). The solvent was dried ($MgSO_4$) and removed under reduced pressure. The residue was purified by column chromatography (EtOAc:Hexane) to afford iodide **4** as a yellow crystalline solid (5.66 g, 97%).

R_f = 0.7 (EtOAc:Hexane = 30:70); Mp (EtOAc/Hexane): 109-113°C, lit[122] Mp: 111-112°C; IR ν_{max}/ cm^{-1} (ATR): 3198 (aromatic O-H); δ_H (400 MHz, $CDCl_3$): 7.06 (2H, d, *J*= 8.6 Hz, H-3), 6.78 (2H, d, *J* = 8.6 Hz, H-2), 4.80 (1H, brs, OH), 3.31 (2H, t, *J* = 7.8 Hz, H-6), 3.10 (2H, t,

J = 7.8 Hz, H-5); δ_C (101 MHz, $CDCl_3$) δ 154.5 (C1), 133.2 (C4), 129.7 (C-3), 115.6 (C-2), 39.6 (C-5), 6.4 (C-6).

S-4-Hydroxyphenethyl 4-methylbenzenesulfonothioate, **(5)**

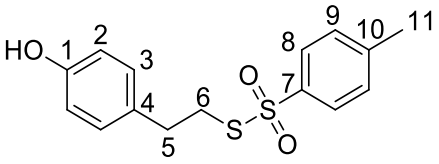

The Iodide **3** (1.20 g, 4.84 mmol, 1 eq) was dissolved in DMF (10 mL) under N_2 and potassium thiotosylate (2.19 g, 9.68 mmol, 2 eq) was added over 15 minutes. The reaction was allowed to proceed at room temperature overnight. The reaction mixture was diluted with EtOAc (15 mL) and water was added (10 mL). The product was extracted with EtOAc (3 x 15 mL). The combined organic fractions were washed copiously with water (4 x 15 mL) and brine (10 mL). The solvent was removed under reduced pressure and silica column chromatography (Hexane:EtOAc) afforded thiosulfonate **5** as a yellow clear oil (1.44 g, 97%).

R_f = 0.3 (EtOAc:Hexane, = 30:70); IR ν_{max}/ cm^{-1} (ATR): 3436 (phenolic O-H), 1136 (O=S=O), 521 (S-S); δ_H (300 Mhz,$CDCl_3$): 7.82 (2H, d, *J* = 8.3 Hz, H-8); 7.34 (2H, d, *J* = 8.3 Hz, H-9), 6.96 (2H, d, *J* = 8.7 Hz, H-3), 6.74 (2H, d, *J* = 8.7 Hz, H-2), 3.18 (2H, t, *J* = 7.5 Hz, H-5), 2.83 (2H, t, *J* = 7.7 Hz, H-6), 2.45 (3H, s, H-11); δ_C (101 MHz, $CDCl_3$): 154.7 (C-1), 145.0 (C-10), 142.2 (C-7), 130.9 (C-4), 130.0 (C-9), 129.9 (C-8), 127.2 (C-3), 115.7 (C-2), 37.6 (C-6), 34.4 (C-5), 21.8 (C-11).

4-(2-((3-((4-Methoxybenzyl)thio)prop-1-en-1-yl)disulfanyl)ethyl)phenol, **(6)**

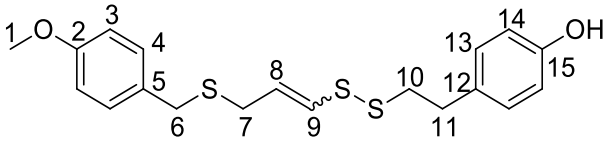

The vinyl thioacetate **2** (586 mg, 2.19 mmol, 1 eq) in anhydrous MeOH (1.95 mL, 1 M) was cooled to -40°C (Acetonitrile/liq. N_2) under N_2 and potassium hydroxide (129 mg, 2.30 mmol, 1.05 eq) in MeOH (2.05 mL, 1 M) was added. The reaction was stirred for 30 minutes upon which the reaction was cooled to -78°C and thiotosylate **5** (743 mg, 2.41 mmol, 1.1 eq) in MeOH (2.43 mL, 1 M) was added. The reaction was allowed to proceed for three hours and was quenched at room temperature with saturated aqueous

ammonium chloride (4 mL). The product was extracted with EtOAc (3 x 15 mL) and the combined organic fractions were washed with water (2 x 10 mL) followed by brine (1 x 10 mL). The solvent was removed under reduced pressure and the residue purified using silica column chromatography (EtOAc:Hexane = 15:85) to afford disulfide **6** as a clear colourless oil and as a 3:5 mixture of *E/Z* isomers (594 mg, 72%).

E/Z mixture: R_f = 0.35 (EtOAc:Hexane, = 20:80); IR ν_{max}/ cm^{-1} (ATR): 3382 (phenolic OH); HRMS (ES): *m/z* 379.0849 $[M+H]^+$, $C_{19}H_{23}O_2S_3$ requires 379.0860;[123]

E-isomer: δ_H (300 MHz, $CDCl_3$): 7.21 (2H, d, *J* = 8.7 Hz, H-4), 7.07 (2H, d, *J* = 8.5 Hz, H-13), 6.84 (2H, d, *J* = 8.7 Hz, H-14), 6.76 (2H, d, *J* = 8.5 Hz, H-3), 6.07 (1H, dt, *J* = 14.6, 1.0 Hz, H-9), 5.88 (1H, dt, *J* = 14.6, 7.3 Hz, H-8), 3.80 (3H, s, H-1), 3.62 (2H, s, H-6), 3.08 (2H, dd, *J* = 7.1, 0.7 Hz, H-7), 2.92 (4H, s, H-10/-11); δ_C (101 MHz, $CDCl_3$): 158.8 (C-2), 154.3 (C-15), 130.7 (C-12), 132.2 or 132.1 (C-5), 130.2 (C-4), 130.0 (C-14), 128.2 (C-9), 128.0 (C-8), 115.6 (C-3), 114.2 (C-13), 55.5 (C-1), 39.9 (C-10), 34.8 (C-6), 34.8 (C-11), 32.9 (C-7).

Z-isomer: δ_H (300 MHz, $CDCl_3$): 7.24 (2H, d, *J* = 8.7 Hz, H-4), 7.05 (2H, d, *J* = 8.5 Hz, H-13), 6.90 (2H, d, *J* = 8.5 Hz, H-14), 6.75 (2H, d, *J* = 8.7 Hz, H-3), 6.24 (1H, dt, *J* = 9.3, 1.0 Hz, H-9), 5.70 (1H, dt, *J* = 9.3, 7.3 Hz, H-8), 3.80 (3H, s, H-1), 3.69 (2H, s, H-6), 3.23 (2H, dd, *J* = 7.6, 0.8 Hz, H-7), 2.92 (4H, s, H10/-11); δ_C (101 MHz, $CDCl_3$): 158.8 (C-2), 154.3 (C-15), 132.4 (C-9), 132.2 or 132.1 (C-5), 130.7 (C-12) 130.2 (C-4), 130.0 (C-14), 128.3 (C-8), 115.6 (C-3), 114.2 (C-13), 55.5 (C-1), 40.6 (C-10), 35.6 (C-6), 34.8 (C-11), 29.5 (C-7).

4-(2-((3-((4-Methoxybenzyl)sulfinyl)prop-1-en-1-yl)disulfanyl)ethyl)phenol, **(7)**

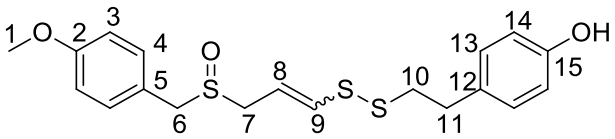

The sulfide **6** (250 mg, 0.66 mmol, 1 eq) was dissolved in DCM (10 mL) under N_2 and cooled to -78°C. *m*-CPBA (142 mg, 0.83 mmol, 1.25 eq) was added in portions and the reaction allowed to warm to room temperature over three hours before being quenched with saturated aqueous sodium bicarbonate (5 mL). The product was extracted with DCM (3 x 10 mL) and the combined fractions were washed with water (2 x 10 mL) followed by brine (5 mL). The solvent was removed under reduced pressure and the residue purified

via silica column chromatography (EtOAc:Hexane = 80:20) to afford ajoene analogue **7** as a pale-yellow oil and as a 2:1 mixture of *Z/E* isomers, (155 mg, 60%).

E/Z mixture: R_f = 0.45 (EtOAc:Hexane, = 70:30); IR ν_{max}/ cm^{-1} (ATR): 3171 (phenolic OH); HRMS (ES): *m/z* 393.0646 (M-H^+), $C_{19}H_{21}O_3S_3$ requires 393.0658;

E-isomer: δ_H (400 MHz, $CDCl_3$): 7.23 (2H, d, *J* = 8.6 Hz, H-4), 7.03 (2H, d, *J* = 8.6 Hz, H-13), 6.90 (2H, d, *J* = 8.6 Hz, H-3), 6.77 (2H, d, *J* = 8.6 Hz, H-14), 6.24 (1H, d, *J* = 14.8 Hz, H-9), 5.86 (1H, dt, *J* = 14.7, 7.6 Hz, H-8), 3.91 (2H, m, H-6), 3.81 (3H, s, H-1), 3.51-3.42 (1H, m, H-7a), 3.33 (1H, ddd, *J* = 13.2, 8.0, 0.9 Hz, H-7b), 2.87-2.67 (4H, m, H-10/-11); δ_C (101 MHz, $CDCl_3$): 160.0 (C-2), 155.0 (C-15), 135.1 (C-9), 131.4 (C-4), 131.3 (C-12), 129.9 (C-13), 121.4 (C-5), 116.4 (C-8), 115.8 (C-14), 114.7 (C-3), 56.4 (C-6), 55.5 (C-1), 52.9 (C-7), 40.4 (C-10), 34.8 (C-11).

Z-isomer: δ_H (400 MHz, $CDCl_3$): 7.23 (2H, d, *J* = 8.6 Hz, H-4), 7.02 (2H, d, *J* = 8.6 Hz, H-13), 6.90 (2H, d, *J* = 8.6 Hz, H-3), 6.76 (2H, d, *J* = 8.6 Hz, H-14), 6.57 (1H, d, *J* = 9.4 Hz, H-9), 5.76 (1H, dt, *J* = 9.5, 7.9 Hz, H-8), 3.96 (2H, m, H-6), 3.80 (3H, s, H-1), 3.55 (1H, ddd, *J* = 13.4, 7.7, 0.9 Hz, H-7a), 3.51-3.42 (1H, m, H-7b), 2.87-2.67 (4H, m, H-10/-11); δ_C (101 MHz, $CDCl_3$): 160.0 (C-2), 155.0 (C-15), 139.0 (C-9), 131.4 (C-4), 131.2 (C-12), 129.9 (C-13), 121.5 (C-5), 118.1 (C-8), 115.8 (C-14), 114.7 (C-3), 57.0 (C-6), 55.5 (C-1), 49.6 (C-7), 40.9 (C-10), 34.8 (C-11).

2-(4-(2-((3-((4-Methoxybenzyl)thio)prop-1-en-1-yl)disulfanyl)ethyl)phenoxy)acetamide **(8)**

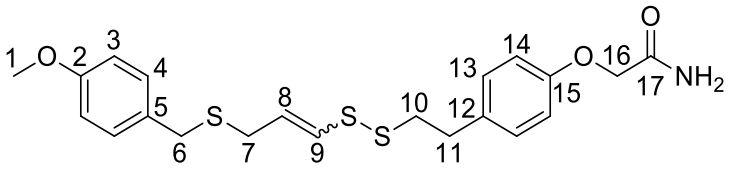

Phenol **6** (150 mg, 0.40 mmol, 1 eq) was suspended in acetonitrile (5 mL) under N_2 with potassium carbonate (111 mg, 0.80 mmol, 2 eq), 2-chloroacetamide (74 mg, 0.80 mmol, 2 eq) and *tert*-butylammonium iodide (15 mg, 0.04 mmol, 0.1 eq) and the mixture heated at 40°C. The reaction was allowed to proceed for 12 hours and was then quenched with saturated aqueous ammonium chloride (2 mL). The product was extracted into EtOAc (3 x 10 mL) and washed with water (2 x 5 mL) followed by brine (1 x 5 mL). The solvent was dried ($MgSO_4$), removed under reduced pressure and silica column chromatography

(MeOH:DCM = 2:98) afforded amide **8** as a clear light-yellow oil as a 3:4 mixture of *E/Z* isomers (70 mg, 40%).

E/Z mixture: R_f = 0.3 (MeOH:DCM = 5:95), IR ν_{max}/ cm^{-1} (APCI): 3438 (amide N-H), 1685 (amide C=O); HRMS (ES): *m/z* 436.1068 $(M+H)^+$, $C_{21}H_{26}NO_3S_3$ requires 436.1080;

E-isomer: δ_H (400 MHz, $CDCl_3$): 7.24 (2H, d, *J* = 8.7 Hz, H-4), 7.15 (2H, d, *J* = 8.5 Hz, H-13), 6.89-6.82 (4H, m, H-3/-14), 6.54 (1H, brs, NH), 6.08 (1H, dt, *J* = 14.7, 1.0 Hz, H-9), 5.89 (1H, brs, NH), 5.88 (1H, dt, *J* = 14.6, 7.3 Hz, H-8), 4.47 (2H, s, H-16), 3.79 (3H, s, H-1), 3.62 (2H, s, H-6), 3.08 (2H, dd, *J* = 7.2, 0.7 Hz, H-7), 2.94 (4H, s, H-10/-11); δ_C (101 MHz, $CDCl_3$): 171.2 (C-17), 158.9 (C-2), 156.0 (C-15), 133.7 (C-5), 130.2 (C-4), 130.1 (C-13), 130.0 (C-12), 128.5 (C-8), 128.0 (C-9), 114.9 (C-14), 114.1 (C-3), 67.5 (C-16), 55.4 (C-1), 39.6 (C-10), 34.8 (C-6), 34.7 (C-11), 32.9 (C-7).

Z-isomer: δ_H (400 MHz, $CDCl_3$): 7.20 (2H, d, *J* = 8.7 Hz, H-4), 7.13 (2H, d, *J* = 8.5 Hz, H-13), 6.89-6.82 (4H, m, H-3/-14), 6.54 (1H, brs, NH), 6.24 (1H, dt, *J* = 9.3, 1.0 Hz, H-9), 5.89 (1H, brs, NH), 5.71 (1H, dt, *J* = 9.3, 7.7 Hz, H-8), 4.47 (2H, s, H-16), 3.79 (3H, s, H-1), 3.68 (2H, s, H-6), 3.28 (2H, dd, *J* = 7.7, 0.8 Hz, H-7), 2.94 (4H, s, H-10/-11); δ_C (101 MHz, $CDCl_3$): 171.2 (C-17), 158.9 (C-2), 156.0 (C-15), 133.7 (C-5), 132.2 (C-9), 130.2 (C-4), 130.1 (C-13), 130.0 (C-12), 128.2 (C-8), 114.9 (C-14), 114.1 (C-3), 67.5 (C-16), 55.4 (C-1), 40.4 (C-10), 35.6 (C-6), 34.7 (C-11), 29.5 (C-7).

2-(4-(2-((3-((4-Methoxybenzyl)sulfinyl)prop-1-en-1-yl)disulfanyl)ethyl)phenoxy)acetamide, **(9)**

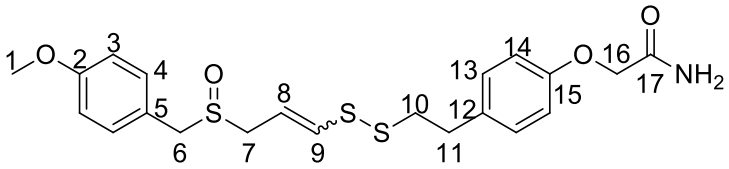

Sulfoxide **7** (107 mg, 0.27 mmol, 1 eq) was suspended in acetonitrile (2 mL) under N_2. Potassium carbonate (75 mg, 0.54 mmol, 2 eq) and 2-iodoacetamide (100 mg, 0.54 mmol, 2 eq) were added and the mixture was heated to 40°C. The reaction was left for 12 hours before being quenched with saturated aqueous ammonium chloride (5 mL). The product was extracted with EtOAc (3 x 5 mL) and washed with water (2 x 2 mL) followed by brine (2 mL). The combined organic fractions were dried over $MgSO_4$ and concentrated under reduced pressure. The residue was purified via silica column chromatography

(MeOH:DCM = 5:95), which afforded ajoene analogue **9** as a clear colourless oil (58 mg, 48%) and as a 3:2 mixture of *E/Z* isomers.

E/Z mixture: R_f = 0.65 (MeOH:DCM = 5:95), IR ν_{max}/ cm^{-1} (APCI): 3418 (amide N-H), 1716 (amide C=O); HRMS (ES): *m/z* 452.1026 $[M+H]^+$, $C_{21}H_{26}NO_4S_3$ requires 452.1024;[123]

E-isomer: δ_H (600 MHz, $CDCl_3$): 7.19 (2H, d, *J* = 8.7 Hz, H-4), 7.13 (2H, d, *J* = 8.6 Hz, H-13), 6.89 (2H, d, *J* = 8.7 Hz, H-3), 6.85 (2H, d, *J* = 8.6 Hz, H-14), 6.56 (1H, brs, NH), 6.34 (1H, dt, *J* = 14.8, 0.9 Hz, H-9), 5.92 (1H, dt, *J* = 14.8, 7.5 Hz, H-8), 5.86 (1H, brs, NH), 4.46 (2H, s, H-16), 3.91 (2H, s, H-6), 3.80 (3H, s, H-1), 3.48-3.42 (1H, m, H-7a), 3.30 (1H, ddd, *J* = 13.2, 8.1, 0.9 Hz, H-7b), 2.94 (4H, s, H-10/-11); δ_C (151 MHz, $CDCl_3$): 171.1 (C-17), 159.9 (C-2), 156.1 (C-15), 134.4 (C-9), 133.5 (C-5), 131.3 (C-4), 130.1 (C-13), 121.7 (C-12), 117.2 (C-8), 114.9 (C-14), 114.7 (C-3), 67.4 (C-16), 56.5 (C-6), 55.5 (C-1), 52.9 (C-7), 39.7 (C-10), 34.6 (C-11).

Z-isomer: δ_H (600 MHz, $CDCl_3$): 7.22 (2H, d, *J* = 8.7 Hz, H-4), 7.13 (2H, d, *J* = 8.6 Hz, H-13), 6.89 (2H, d, *J* = 8.7 Hz, H-3), 6.85 (2H, d, *J* = 8.6 Hz, H-14), 6.57 (1H, dt, *J* = 9.4, 0.9 Hz, H-9), 6.56 (1H, brs, NH), 5.86 (1H, brs, NH), 5.78 (1H, dt, *J* = 9.4, 7.9 Hz, H-8), 4.46 (2H, s, H-16), 3.92 (2H, s, H-6), 3.80 (3H, s, H-1), 3.54 (1H, ddd, *J* = 13.4, 7.7, 1.0 Hz, H-7a), 3.48-3.42 (1H, m, H-7b), 2.94 (4H, s, H-10/-11); δ_C (151 MHz, $CDCl_3$): 171.1 (C-17), 160.0 (C-2), 156.1 (C-15), 138.5 (C-9), 133.4 (C-5), 131.4 (C-4), 130.1 (C-13), 121.6 (C-12), 118.7 (C-8), 114.9 (C-14), 114.6 (C-3), 67.4 (C-16), 57.0 (C-6), 55.5 (C-1), 49.7 (C-7), 40.5 (C-10), 34.6 (C-11).

3-((4-Methoxybenzyl)thio)propane-1-thiol, **(10)**

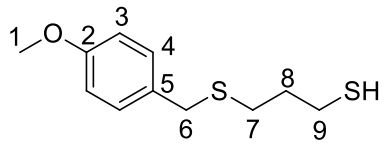

Propane-1,3-dithiol (0.93 mL, 9.2 mmol, 1.2 eq) was suspended in MeOH (30 mL) under N_2, and potassium hydroxide (0.73 g, 13 mmol, 1.4 eq) was added and the mixture left to stir at room temperature for 30 minutes. The reaction was then cooled to 0°C, PMBCl (1.2 g, 7.7 mmol, 1 eq) was added drop-wise and the reaction allowed to proceed for two hours. The reaction was quenched using aqueous HCl (20 mL, 1 M) and then neutralised to pH 7 using saturated aqueous sodium bicarbonate. The product was extracted using

EtOAc (3 x 30 mL). The combined fractions were washed with H_2O (2 x 30 mL) followed by brine (20 mL), dried over $MgSO_4$ and concentrated under reduced pressure. The resulting residue was purified via silica column chromatography (EtOAc:Hexane = 2:98) to afford thiol **10** as a clear, light-green oil (1.33 g, 88%).

R_f = 0.25 (EtOAc:Hexane = 2:98); δ_H (300 MHz, $CDCl_3$): 7.23 (2H, d, *J* = 8.8 Hz, H-4), 6.85 (2H, d, *J* = 8.8 Hz, H-3), 3.80 (3H, s, H-1), 3.66 (2H, s, H-6), 2.52 (2H, t, *J* = 7.1 Hz, H-9), 1.84 (2H, t, *J* = 7.1 Hz, H-7), 1.33 (1H, t, *J* = 8.0 Hz, SH), 1.31 (2H, p, H-8).

4-(2-((3-((4-Methoxybenzyl)thio)propyl)disulfanyl)ethyl)phenol, **(11)**

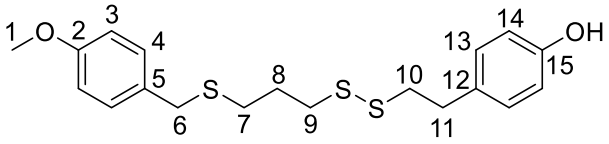

The thiol **10** (765 mg, 3.38 mmol, 1 eq) was taken up in MeOH (20 mL) under N_2 and cooled to -78°C. Triethylamine (0.68 mL, 4.9 mmol, 1.5 mmol) was added and after 20 minutes the thiotosylate **5** (1.44 g, 4.67 mmol, 1.4 eq) in MeOH (5 mL) was added. The mixture was allowed to warm to room temperature over one hour. The reaction was immediately quenched with saturated aqueous ammonium chloride (10 mL). The product was extracted with EtOAc (3 x 40 mL) and the combined fractions were washed with water (2 x 20 mL) followed by brine (10 mL). The organic solvent was dried with $MgSO_4$ and removed under reduced pressure. The resulting residue was purified via silica column chromatography (EtOAc:Hexane = 20:90) to afford disulfide **11** as a colourless waxy solid (992 mg, 77%).

R_f = 0.5 (EtOAc: Hexane = 20:80); Mp (EtOAc/Hexane): 84-86 °C; IR ν_{max}/ cm^{-1} (ATR): 3433 (phenolic OH), 550 (S-S); δ_H (400 Mhz, $CDCl_3$): 7.23 (2H ,d , *J* = 8.8 Hz, H-4), 7.06 (2H, d, *J* = 8.6 Hz, H-13), 6.85 (2H, d, *J* = 8.8 Hz, H-3), 6.76 (2H, d, *J* = 8.6 Hz, H-14), 3.80 (3H, s, H-1), 3.67 (2H, s, H-6), 2.89 (4H, brs, H10/-H11), 2.73 (2H, t, J = 7.1 Hz, H-9), 2.51 (2H, t, *J* = 7.1 Hz, H-7), 1.93 (2H, p, H-8); δ_C (101 MHz, $CDCl_3$): 158.8 (C-2), 154.3 (C-15), 132.3 (C-12), 130.5 (C-5), 130.0 (C-4), 129.9 (C-13), 115.5 (C-14), 114.1 (C-3), 55.4 (C-1), 40.7 (C-10), 37.6 (C-9), 35.8 (C-6), 34.9 (C-11), 29.9 (C-7), 28.6 (C-8); HRMS (ES): *m/z* 379.0860 $[M-H]^+$, $C_{19}H_{23}O_2S_3$ requires 379.0866.[124]

4-(2-((3-((4-Methoxybenzyl)sulfinyl)propyl)disulfanyl)ethyl)phenol, **(12)**

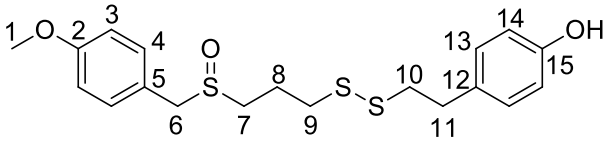

The sulfide **11** (200 mg, 0.53 mmol, 1 eq) was suspended in DCM (4 mL) under N_2 and cooled to -78°C. *m*-CPBA (178 mg, 0.8 mmol, 1.5 eq) was then added in portions and the reaction was allowed to warm up to room temperature over one hour. The reaction was quenched with saturated aqueous sodium bicarbonate (5 mL) and extracted with DCM (3 x 10 mL). The combined organic fractions were washed with water (2 x 10 mL) followed by brine (5 mL). The solvent was dried using $MgSO_4$ and the product was concentrated under reduced pressure. Purification via silica column chromatography (MeOH:DCM = 5:95) afforded sulfoxide **12** as a clear colourless oil (148 mg, 70%).

R_f = 0.25 (MeOH:DCM = 5:95); IR ν_{max}/ cm^{-1} (ATR): 3161 (S=O); δ_H (400 MHz, $CDCl_3$): 7.20 (2H, d, *J* = 8.6 Hz, H-4), 7.02 (2H, d, *J* = 8.4 Hz, H-13), 6.89 (2H, d, *J* = 8.6 Hz, H-3), 6.76 (2H, d, *J* = 8.4 Hz, H-14), 3.99 (1H, d, *J* = 13.0 Hz, H-6a), 3.95 (2H, d, *J* = 13.0 Hz, H-6b), 3.80 (3H, s, H-1), 2.92 – 2.82 (4 H, m, H-10/-11), 2.77-2.58 (4 H, m, H-7/-9), 2.19-2.07 (2H, m, H-8); δ_C (101 MHz, $CDCl_3$): 160.0 (C-2), 155.0 (C-15), 131.5 (C-5), 131.4 (C-4), 129.8 (C-13), 121.3 (C-12), 115.8 (C-3), 114.7 (C-14), 57.7 (C-6), 55.5 (C-1), 49.0 (C-7), 41.0 (C-11), 37.2 (C-9), 34.9 (C-10), 22.3 (C-8); HRMS (ES): *m/z* 397.0966 ($C_{19}H_{25}O_3S_3$ requires 397.0960.M+H)$^+$.

2-(4-(2-((3-((4-Methoxybenzyl)thio)propyl)disulfanyl)ethyl)phenoxy)acetamide, **(13)**

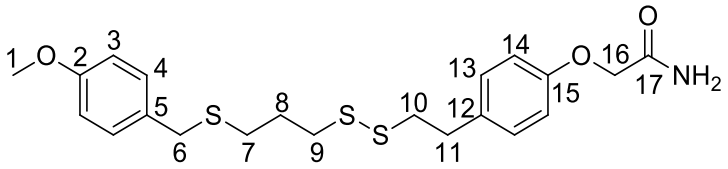

The sulfide **10** (222 mg, 0.58 mmol, 1 eq) was dissolved in acetonitrile (5 mL) under N_2. Cesium carbonate (286 mg, 0.88 mmol, 1.5 eq), *tert*-butylammonium iodide (22 mg, 0.58 mmol, 0.1 eq) and 2-chloroacetamide (81 mg, 0.87 mmol, 1.5 eq) were added and the reaction was left to stir at room temperature for 18 hours. The reaction was quenched with saturated aqueous ammonium chloride (5 mL) and the product extracted into DCM (3 x 15 mL). The combined organic fractions were washed with water (2 x 10 mL) followed by brine (5 mL). The dried ($MgSO_4$) solvent was removed under reduced

pressure. The resulting residue was purified via silica column chromatography (EtOAc:Hexane = 30:70) to afford sulfide **13** as a clear milky oil (195 mg, 77%).

R_f = 0.35 (EtOAc:Hexane = 20:80); IR ν_{max}/ cm^{-1} (ATR): 3380 (amide N-H) 3160 cm^{-1} (amide N-H) , 1659 cm^{-1} (amide C=O); δ_H (400 MHz, $CDCl_3$): 7.22 (2H, d, *J* = 8.8 Hz, H-4), 7.15 (2H, d, *J* = 8.8 Hz, H-13), 6.86 (2H, d, *J* = 8.5 Hz, H-3), 6.84 (2H, d, *J* = 8.5 Hz, H-14), 6.53 (1H, brs, NH), 5.71 (1H, brs, NH), 4.48 (2H, s, H-16), 3.79 (3H, s, H-1), 3.67 (2H, s, H-6), 2.97-2.85 (4H, m, H10/-11), 2.74 (2H, t, *J* = 7.0 Hz, H-9), 2.51 (2H, t, *J* = 7.1 Hz, H-7), 1.93 (2H, p, H-8); δ_C (101 MHz, $CDCl_3$): 171.1 (C-17), 158.8 (C-2), 156.0 (C-15), 134.0 (C-5), 130.4 (C-12), 130.1 (C-4), 130.0 (C-13), 114.9 (C-3), 114.1 (C-14), 67.5 (C-16), 55.4 (C-1), 40.4 (C-10), 37.7 (C-9), 35.8 (C-6), 34.8 (C-11), 29.9 (C-7), 28.6 (C-8); HRMS (ES): *m/z* 460.1046 $[M+ Na]^+$, $C_{21}H_{27}NNaO_3S_3$ requires 460.1051.[124]

2-(4-(2-((3-((4-Methoxybenzyl)sulfinyl)propyl)disulfanyl)ethyl)phenoxy)acetamide, **(14)**

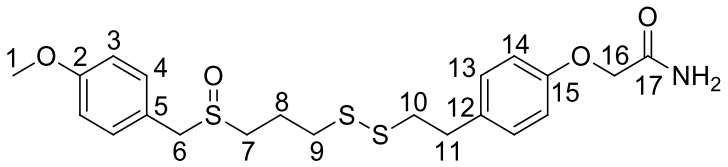

The sulfide **13** (104 mg, 0.24 mmol, 1 eq) was dissolved in DCM (3 mL) under N_2 and cooled to 78°C. *m*-CPBA (81 mg, 0.4 mmol, 1.5 eq) was added and the reaction allowed to warm to room temperature over two hours. The reaction was quenched with saturated aqueous sodium bicarbonate (4 mL) and the product extracted into DCM (3 x 10 mL). The combined organic fractions were washed with water (2 x 10 mL) and brine (5 mL). The solvent was dried with $MgSO_4$ and removed under reduced pressure. Silica column chromatography (MeOH:DCM = 5:95) afforded sulfoxide **14** as a clear light-yellow oil (78 mg, 72%).

R_f = 0.3 (MeOH:DCM = 5:95); IR ν_{max}/ cm^{-1} (ATR): 3413 (amide N-H), 3177 (S=O?) 1634 (amide C=O); δ_H (400 MHz, $CDCl_3$): 7.20 (2H, d, *J* = 8.7 Hz, H-4), 7.13 (2H, d, *J* = 8.7 Hz, H-13), 6.89 (2H, d, *J* = 8.7 Hz, H-3), 6.85 (2H, d, *J* = 8.7 Hz, H-14), 6.56 (1H, brs, NH), 6.06 (1H, brs, NH), 4.47 (2H, s, H-16), 3.96 (1H, t, *J* = 13.1 Hz, H-6a), 3.93 (1H, t, *J* = 13.1 Hz, H-6b), 3.79 (3H, s, H-1), 2.90 (4H, m, H-10/-11), 2.75 (2H, t, *J* = 6.9 Hz, H-9a), 2.74 (2H, t, *J* = 6.9 Hz, H-9b), 2.72-2.57 (2H, m, H-7) 2.22-2.08 (2H, m, H-8); δ_C (101 MHz, $CDCl_3$): 170.3 (C-

17), 158.9 (C-2), 155.0 (C-15), 132.7 (C-5), 130.3 (C-4), 129.1 (C-13), 120.6 (C-12), 113.9 (C14), 113.6 (C-3), 66.5 (C-16), 56.8 (C-6), 54.4 (C-1), 47.9 (C-7), 39.4 (C-11), 36.3 (C-9), 33.7 (C-10), 21.2 (C-8); HRMS (ES): *m/z* 454.1187 $(M+H)^+$, $C_{21}H_{28}NO_4S_3$ requires 454.1186.

6.1.3 Biotin-labelled ajoene

4-(2-Azidoethyl)-phenol, **(15)**[125]

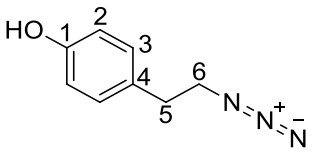

The Iodide **4** (560 mg, 2.26 mmol, 1eq) was suspended in DMF (3 mL) under N_2 and sodium azide (220 mg, 3.39 mmol, 1.5 eq) in DMF (1 mL) was added. The reaction was heated to 100°C and stirred for three hours. The reaction was cooled, diluted with 50 mL of diethyl ether, which was then washed copiously with H_2O (4 x 20 mL). The organic layer was dried over $MgSO_4$ and the solvent removed under reduced pressure. Column chromatography (EtOAc:Hexane) afforded azide **15** as a clear yellow oil (354 mg, 96%).

R_f = 0.3 (EtOAc:Hexane, = 10:90); IR ν_{max}/ cm^{-1} (ATR): 3342 (aromatic O-H), 2092 (N=N=N); δ_H (400 MHz, $CDCl_3$): 7.09 (2H, d, *J* = 8.5 Hz, H-3), 6.79 (2H, d, *J* = 8.5 Hz, H-2), 5.19 (1H, brs, OH), 3.46 (2H, t, *J* = 7.2 Hz, H-6), 2.83 (2H, t, *J* = 7.2 Hz, H-5); δ_C (75 MHz, $CDCl_3$): 154.5 (C-1), 130.3 (C-4), 130.1 (C-3), 115.7 (C-2), 52.8 (C-6), 34.6 (C-5).

1-(2-Azidoethyl)-4-(3-bromopropoxy)benzene, **(16)**

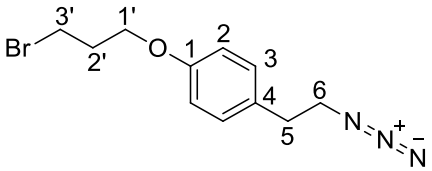

To a stirring solution of 1,3-dibromopropane (0.82 mL, 8.1 mmol, 3 eq) and Cs_2CO_3 (962 mg, 2.95 mmol, 1.1 eq) in acetonitrile (25 mL) was added the azide (**15**) (438 mg, 2.68 mmol, 1 eq) in acetonitrile (2 mL) slowly. The reaction was heated to 50°C and left stirring for six hours. It was then was quenched with saturated aqueous ammonium chloride (5 mL) and the product extracted with EtOAc (3 x 20 mL). The combined fractions were washed with brine (20 mL) and the solvent removed under reduced pressure. Column

chromatography (EtOAc:Hexane) afforded bromide **16** as a clear colourless oil (518 mg, 68 %).

R_f = 0.78 (EtOAc:Hexane, = 30:70); IR ν_{max}/ cm^{-1} (ATR): 2092 (N=N=N), 1240 (aryl alkyl C-O-C); δ_H (400 MHz, $CDCl_3$): 7.14 (2H, d, *J* = 8.6 Hz, H-3), 6.87 (2H, d, *J* = 8.6 Hz, H-2), 4.09 (2H, t, *J* = 5.8 Hz, H-1'), 3.60 (2H, t, *J* = 6.5 Hz, H-3'), 3.47 (2H, t, *J* = 7.2 Hz, H-6), 2.84 (2H, t, *J* = 7.2 Hz, H-5), 2.31 (2H, p, H-2'); δ_C (101 MHz, $CDCl_3$) 157.8 (C-1), 130.6 (C-4), 129.9 (C-3), 114.9 (C-2), 65.6 (C-1'), 52.8 (C-6), 34.7 (C-5), 32.9 (C-3'), 30.1 (C-2').

S-(3-(4-(2-Azidoethyl)phenoxy)propyl) 4-methylbenzenesulfonothioate, **(17)**

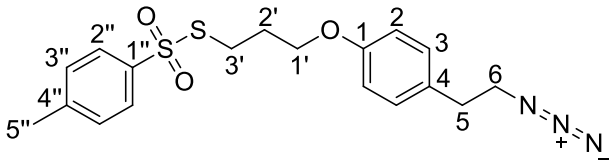

To a solution of potassium thiotosylate (639 mg, 2.83 mmol, 2 eq) in acetonitrile (10 mL) was added bromide **16** (400 mg, 1.41 mmol, 1 eq) in acetonitrile (5 mL) under N_2 and the reaction was heated to 60°C. The reaction was allowed to proceed over-night for 18 hours. The mixture was diluted with 25 mL EtOAc and washed with H_2O (3 x 20 mL). The organic layer was dried over $MgSO_4$ and the solvents removed under reduced pressure. Silica gel column chromatography (EtOAc:Hexane) afforded sulfonothioate ether **17** as a clear colourless oil (209 mg, 38%).

R_f = 0.3 (EtOAc:Hexane, = 20:80); IR ν_{max}/ cm^{-1} (ATR): 2090 (N=N=N); δ_H (300 MHz, $CDCl_3$): 7.82 (2H, d, *J* = 8.6 Hz, H-2''), 7.32 (2H, d, *J* = 8.4 Hz, H-3), 7.12 (2H, d, *J* = 8.6 Hz, H-3''), 6.78 (2H, d, *J* = 8.4 Hz, H-2), 3.95 (2H, t, *J* = 5.8 Hz, H-1'), 3.46 (2H, t, *J* = 7.1 Hz, H-6), 3.18 (2H, t, *J* = 7.2 Hz, H-3'), 2.83 (2H, *J* = 7.2 Hz, H-5), 2.44 (3H, s, H-5''), 2.12 (2H, p, H-2'); δ_C (101 MHz, $CDCl_3$): 157.6 (C-1), 144.9 (C-4''), 142.0 (C-1''), 130.6 (C-4), 130.0 (C-3''), 129.9 (C-3), 127.2 (C-2''), 114.8 (C-2), 65.7 (C-1'), 52.8 (C-6), 34.6 (C-5), 32.9 (C-3'), 28.9 (C-2'), 21.8 (C-5''); HRMS (ES): *m/z* 392.1103 $(M+H)^+$, $C_{18}H_{22}O_3N_3S_2$ requires 392.1108.

1-(3-(4-(2-Azidoethyl)phenoxy)propyl)-2-(3-((4-methoxybenzyl)thio)prop-1-en-1-yl)disulfane, **(18)**

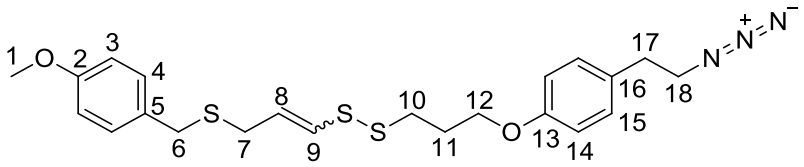

To stirred solution of thioacetate **2** (119 mg, 0.44 mmol, 1 eq) in MeOH (1 mL) at -40°C under N_2, was added potassium hydroxide (26 mg, 0.47 mmol, 1.05 eq) in MeOH (1.5 mL). The mixture was left for 20 minutes, upon which the temperature was lowered to -78°C and the azidothiotosylate **17** (191 mg, 0.49 mmol, 1.1 eq) in MeOH (0.49 mL, 1 M) was added drop-wise. The reaction was allowed to proceed to room temperature over two hours before being quenched with saturated aqueous ammonium chloride (1 mL). The product was extracted into EtOAc (3 x 10 mL) and the combined fractions were sequentially washed (2 x 5 mL water, 5 mL brine), dried over $MgSO_4$ and concentrated under reduced pressure. Silica gel column chromatography afforded disulfide **18** as a 2:3 mixture of *E/Z*-isomers and as a clear colourless oil (172 mg, 85%).

E/Z mixture: R_f = 0.6 (EtOAc:Hexane, = 20:80); IR ν_{max}/ cm^{-1} (ATR): 2086 (N=N=N); HRMS (ES): *m/z* 462.1344 $(M+H)^+$, $C_{22}H_{28}N_3O_2S_3$ requires 462.1349.

E-isomer: δ_H (300 MHz, $CDCl_3$): 7.22 (2H, d, *J* = 8.7 Hz, H-4), 7.12 (2H, d, *J* = 8.7 Hz, H-15), 6.85 (2H, d, *J* = 8.7, H-14), 6.84 (2H, d, *J* = 8.7 Hz, H-3), 6.09 (1H, dt, *J* = 14.7, 1.0 Hz, H-9), 5.89 (1H, dt, *J* = 14.6, 7.2 Hz, H-8), 4.07-4.02 (2H, m, H-12), 3.80 (3H, s, H-1), 3.63 (2H, s, H-6), 3.46 (2H, t, *J* = 7.2 Hz, H-18), 3.07 (2H, dd, *J* = 7.2, 1.0 Hz, H-7), 2.91 (2H, t, H-10), 2.83 (2H, t, *J* = 7.1 Hz, H-17), 2.22-2.12 (2H, m, H-11); δ_C (101 MHz, $CDCl_3$): 158.9 (C-2), 157.8 (C-13), 130.4 (C-5), 130.2 (C-15), 130.0 (C-16) 129.9 (C-4), 128.3 (C-8), 128.0 (C-9), 114.9 (C-14), 114.1 (C-3), 66.0 (C-12), 55.4 (C-1), 52.8 (C-18), 34.8 (C-6/-10), 34.6 (C-17), 32.9 (C-7), 29.0 (C-11).

Z-isomer: δ_H (300 MHz, $CDCl_3$): 7.22 (2H, d, *J* = 8.7 Hz, H-4)), 7.12 (2H, d, *J* = 8.7 Hz, H-15), 6.85 (2H, d, *J* = 8.7, H-14), 6.84 (2H, d, *J* = 8.7 Hz, H-3), 6.25 (1H, dt, *J* = 9.3, 1.0 Hz, H-9), 5.71 (1H, dt, *J* = 9.3, 7.6 Hz, H-8), 4.07-4.02 (2H, m, H-12), 3.80 (3H, s, H-1), 3.68 (2H, s, H-6), 3.46 (2H, t, *J* = 7.2 Hz, H-18), 3.21 (2H, dd, *J* = 7.6, 1.1 Hz, H-7), 2.91 (2H, t, H-10), 2.83 (2H, t, *J*= 7.2 Hz, H-17), 2.22-2.12 (2H, m, H-11); δ_C (101 MHz, $CDCl_3$): 158.9 (C-2), 157.8

(C-13), 132.1 (C-9), 130.4 (C-5), 130.2 (C-15), 130.0 (C-16), 129.9 (C-4), 128.6 (C-8), 114.9 (C-14), 114.1 (C-3), 66.0 (C-12), 55.4 (C-1), 52.8 (C-18), 35.6 (C-6/-10), 34.6 (C-17), 29.5 (C-7), 28.9 (C-11).

1-(3-(4-(2-Azidoethyl)phenoxy)propyl)-2-(3-((4-methoxybenzyl)sulfinyl)prop-1-en-1-yl)disulfane, **(19)**

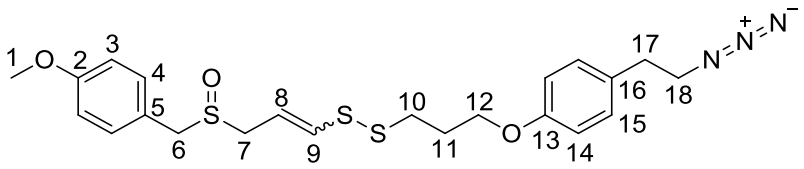

The sulfide **18** (50 mg, 0.11 mmol, 1 eq) was dissolved in DCM (0.5 mL) under N_2 and cooled to -78°C. *m*-CPBA (21 mg, 0.12 mmol, 1.1 eq) was added and the reaction was kept at -78°C, resulting in a more polar spot being observed on TLC (EtOAc:Hexane = 80:20). The reaction was allowed to warm to room temperature, and upon full consumption of the starting material by TLC the reaction was quenched with saturated aqueous sodium bicarbonate (2 mL). The product was extracted into DCM (3 x 3 mL) and the combined organic fractions were washed (2 x 2 mL water, 2 mL brine), dried over $MgSO_4$ and concentrated under reduced pressure. The purification via silica column chromatography afforded the azide-ajoene **19** as a 2:3 mixture of *E/Z*-isomers as a clear colourless oil (32 mg, 62%).

E/Z mixture: R_f = 0.4 (EtOAc:Hexane = 80:20); IR ν_{max}/ cm^{-1} (ATR): 2094 (N=N=N), 1031 (S=O); HRMS (ES): *m/z* 478.1303 $(M+H)^+$, $C_{22}H_{28}N_3O_3S_3$ requires 478.1293;

E-isomer: δ_H(400 MHz, $CDCl_3$): 7.21 (2H, d, *J* = 8.7 Hz, H-15), 7.12 (2H, d, *J* = 8.7 Hz, H-4), 6.90 (2H, d, *J* = 8.7 Hz, H-14), 6.83 (2H, d, *J* = 8.7 Hz, H-3), 6.36 (1H, dt, *J* = 14.8, 1.0 Hz, H-9), 5.96 (1H, dt, 14.8, 7.4 Hz, H-8), 4.04 (2H, t, *J* = 5.9 Hz, H-12), 3.91 (2H, s, H-6), 3.80 (3H, s, H-1), 3.48-3.41 (1H, m, H-7a), 3.46 (2H, t, *J* = 7.3 Hz, H-18), 3.29 (1H, ddd, *J* = 13.2, 8.0, 1.1 Hz, H-7b), 2.91 (2H, t, *J* = 7.0 Hz, H-10), 2.83 (2H, t, *J* = 7.2 Hz, H-17), 2.16 (2H, m, H-11); δ_C (101 MHz, $CDCl_3$): 160.0 (C-2), 157.8 (C-13), 134.4 (C-9), 131.3 (C-15), 130.5 (C-16), 129.9 (C-4), 121.7 (C-5), 117.5 (C-8), 114.9 (C-3), 114.7 (C-14), 66.0 (C-12), 56.6 (C-6), 55.5 (C-1), 52.9 (C-7), 52.8 (C-18), 34.9 (C-10), 34.6 (C-17), 29.0 (C-11).

Z-isomer: δ_H(400 MHz, $CDCl_3$): 7.21 (2H, d, *J* = 8.7Hz, H-15), 7.12 (2H, d, *J* = 8.7 Hz, H-4), 6.90 (2H, d, *J* = 8.7 Hz, H-14), 6.83 (2H, d, *J* = 8.7 Hz, H-3), 6.60 (1H, dt, *J* = 9.4, 1.0 Hz, H-

9), 5.80 (1H, dt, *J* = 9.4, 7.9 Hz, H-8), 4.05 (2H, t, *J* = 6.0 Hz, H-12), 3.92 (2H, s, H-6), 3.80 (3H, s, H-1), 3.53 (1H, ddd, *J* = 13.4, 7.6, 1.0 Hz, H-7a), 3.48-3.41 (1H, m, H-7b), 3.46 (2H, t, *J* = 7.3 Hz, H-18), 2.93 (2H, t, *J* = 7.1 Hz, H-10), 2.83 (2H, t, *J* = 7.2 Hz, H-17), 2.16 (2H, m, H-11); δ_C (101 MHz, $CDCl_3$): 160.0 (C-2), 157.8 (C-13), 138.3 (C-9), 131.4 (C-15), 130.5 (C-16), 129.9 (C-4), 121.8 (C-5), 118.9 (C-8), 114.9 (C-3), 114.7 (C-14), 65.9 (C-12), 57.1 (C-6), 55.5 (C-1), 52.8 (C-18), 49.7 (C-7), 35.7 (C-10), 34.6 (C-17), 28.9 (C-11).

tert-Butyl (3-(2-(2-(3-aminopropoxy)ethoxy)ethoxy)propyl)carbamate, **(20)**[126]

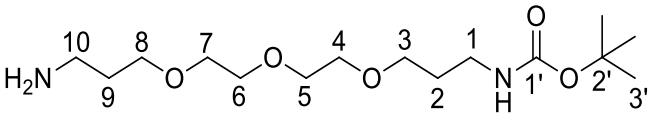

4,7,10-trioxatridecane-1,13-diamine (2.00 mL, 13.3 mmol, 1.5 eq) in DCM was reacted with di-*tert*-butyl dicarbonate (1.93 g, 8.86 mmol, 1 eq) at room temperature over two hours. The solvent was removed under reduced pressure and the resulting residue was purified via silica column chromatography (20% MeOH in DCM) to afford mono-Boc-protected diamine linker **20** as an amber oil (1.31 g, 46%).

R_f = 0.15 (MeOH:DCM = 20:80); IR ν_{max}/ cm^{-1} (ATR): 1694 (C=O); δ_H (400 MHz, $CDCl_3$): 5.21 (1H, brs, NH), 3.64-3.50 (12H, m, H-3/-4/-5/-6/-7/-8), 3.40 (2H, m, H-1), 3.19 (2H, t, *J* = 6.0 Hz, H-10), 2.76 (2H, s, NH_2), 1.80-1.71 (4H, m, H-2/-9), 1.41 (9H, s, H-3'); δ_C (101 MHz, $CDCl_3$): 156.2 (C-1'), 77.9 (C-2'), 70.7 (C-5/-6), 70.6 (C-7), 70.3 (C-4), 70.0 (C-8), 69.6 (C-3), 39.8 (C-10), 38.5 (C-1), 32.1 (C-9) 29.8 (C-2), 28.6 (C-3').

4-(Propiolamidomethyl)benzoic acid, **(21)**[119]

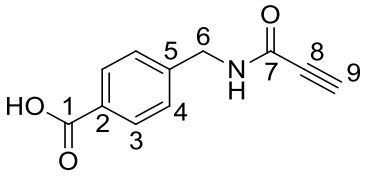

A solution of propiolic acid (0.49 mL, 7.9 mmol, 1.2 eq), 4-(aminomethyl)benzoic acid (1.00 g, 6.62 mmol, 1 eq) and hydroxybenzotriazole (202 mg, 1.32 mmol, 0.2 eq) in acetonitrile (40 mL) was cooled to 0°C under N_2, to which DCC (1.64 g, 7.94 mmol, 1.2 eq) was subsequently added. The reaction was kept at 0°C for one hour and then allowed to reach room temperature over one hour. The reaction mixture was filtered through Celite, and the solvent was removed under reduced pressure. The resulting oil was taken up in EtOAc (50 mL) and washed with H_2O (2 x 30 mL). Upon drying over $MgSO_4$ and removal

of the solvent, silica gel column chromatography (MeOH:DCM = 10:90) afforded amide **21** as a colourless crystalline solid (476 mg, 35%).

R_f = 0.5 (MeOH:DCM = 10:90); Mp (MeOH:DCM): 190-193 °C; IR ν_{max}/ cm^{-1} (ATR): 3268 (carboxylic O-H), 2110 (alkyne C-H), 1684 (C=O)**;** δ_H (300 MHz, MeOD): 7.99 (2H, d, *J* = 8.1 Hz, H-3), 7.38 (2H, d, *J* = 8.1 Hz, H-4), 4.46 (2H, s, H-6), 3.60 (1H, s, H-9); δ_C (101 MHz, MeOD): 169.7 (C-1), 154.8 (C-7), 144.5 (C-2), 131.2 (C-5), 131.0 (C-3), 128.5 (C-4), 78.0 (C-8), 76.2 (C-9), 43.9 (C-6).

tert-Butyl (1-oxo-1-(4-(propiolamidomethyl)phenyl)-6,9,12-trioxa-2-azapentadecan-15-yl)carbamate, **(22)**

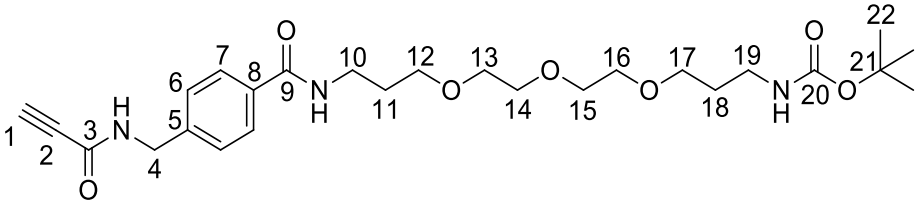

The acid **21** (250 mg, 1.46 mmol, 1 eq) and HOBt (246 mg, 1.61 mmol, 1.1 eq) were suspended in DCM (15 mL) at 0°C under N_2. DCC (392 mg, 1.84 mmol, 1.3 eq) and the amine **20** (592 mg, 1.85 mmol, 1.3 eq) in DCM (2 mL) were sequentially added, and the reaction was left to warm to room temperature. After four hours, the reaction was filtered through Celite and the solvent evaporated under reduced pressure. Silica gel column chromatography (MeOH:DCM = 10:90) afforded alkyne **22** as a clear-yellow oil. (620 mg, 84%).

R_f = 0.75 (MeOH:DCM = 10:90); IR ν_{max}/ cm^{-1} (ATR): 3340 (amide N-H), 2116 (alkyne C-H), 1696 (C=O)**;** δ_H (300 MHz, $CDCl_3$): 7.77 (2H, d, *J* = 8.2 Hz, H-7), 7.32 (2H, d, *J* = 8.2 Hz, H-6), 7.29 (1H, brs, NH), 6.87 (1H, brs, NH), 4.85 (1H, brs, NH), 4.51 (2H, d, *J* = 6.0 Hz, H-4), 3.68 – 3.56 (10H, m, H-13/-14/-15/-16/-17), 3.49 – 3.42 (4H, m, H-12/-19), 3.13 (2H, q, H-10), 2.82 (1H, s, H-1), 1.93-1.85 (2H, p, H-18), 1.69-1.63 (2H, p, H-11), 1.42 (9H, s, H-22); δ_C (101 MHz, $CDCl_3$): 167.0 (C-9), 156.3 (C-20), 152.4 (C-3), 140.7 (C_{quat}), 134.3 (C_{quat}), 127.9 (C-7), 127.6 (C-6), 79.3 (C-21) 77.4 (C-2), 73.9 (C-1), 71.0 (C-17), 70.6 (C-14/-15), 70.5 (C-13), 70.2 (C-16), 69.5 (C-12),43.5 (C-4), 39.3 (C-19), 38.6 (C-10), 29.8 (C-18), 28.9 (C-11), 28.6 (C-22); HRMS (ES): *m/z* 506.2866 $(M+H)^+$, $C_{26}H_{40}N_3O_7$ requires 506.2872.

N-(3-(2-(2-(3-aminopropoxy)ethoxy)ethoxy)propyl)-4-propiolamidomethyl)benzamide, **(23)**

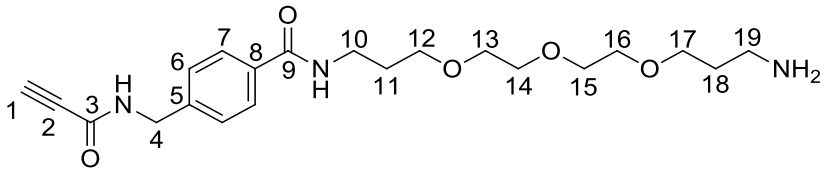

Carbamate **22** (437 mg, 0.86 mmol, 1 eq) was dissolved in DCM (6.4 mL) at 0°C under N_2, trifluoroacetic acid (0.66 mL, 8.6 mmol, 10 eq) was added and the mixture was allowed to warm to room temperature over three hours. The solvent and remaining acid reactant were then removed under reduced pressure. The resulting residue was purified via silica gel column chromatography (MeOH:DCM = 10:90) to afford the amine **23** as a clear-yellow oil (307 mg, 88%).

R_f = 0.65 (MeOH:DCM = 20:80); IR ν_{max}/ cm^{-1} (ATR): 3244 (N-H), 2106 (alkyne C-H), 1680 (C=O)**;** δ_H (300 MHz, d_6-DMSO): 9.30 (1H, brs, NH), 8.41 (1H, brs, NH), 7.79 (2H, d, *J* = 8.2 Hz, H-7), 7.31 (2H, d, *J* = 8.2 Hz, H-6), 4.33 (2H, d, *J* = 6.1 Hz, H-4), 3.54-3.43 (12H, m, H-12/-13/-14/-15/-16/-17), 3.17 (s, 1H, H-1), 3.30 (2H, q, *J* = 6.3 Hz, H-10), 2.86 (2H, m, H19), 1.82-1.71 (4H, m, H-11/-18); δ_C (101 MHz, d_6-DMSO): 165.9 (C-9), 151.7 (C-3), 141.5 (C_{quat}), 133.4 (C_{quat}), 127.2 (C-7), 127.0 (C-6), 78.1 (C-2), 76.1 (C-1), 69.7 (C-14), 69.6 (C-15), 69.5 (C-13), 69.4 (C-16), 68.3 (C-17), 67.3 (C-12), 42.0 (C-4), 36.8 (C-19), 36.6 (C-10), 29.3 (C-18), 27.1 (C-11); HRMS (ES): *m/z* 406.2342 $(M+H)^+$, $C_{21}H_{32}N_3O_5$ requires 406.2347.

2,5-Dioxopyrrolidin-1-yl 5-((3a*R*,4*R*,6a*S*)-2-oxohexahydro-1*H*-thieno[3,4-*d*]imidazol-4-yl)pentanoate, **(24)**[120]

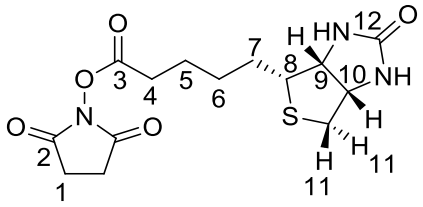

To a solution of biotin (500 mg, 2.05 mmol, 1eq), DMAP (37.0 mg, 0.31 mmol, 0.15 eq) and DCC (550 mg, 2.66 mmol, 1.3 eq) in DMF (10 mL) at 0 °C under N_2 was added N-hydroxysuccinimide (280 mg, 2.46 mmol, 1.2 eq). The reaction was allowed to warm to room temperature and stirred for 24 hours. The mixture was filtered through Celite and the bulk of the DMF removed by gentle heating in a steaming water bath under reduced

pressure on the rotoevaporator. Trituration with diethyl ether afforded a copious precipitate, which was filtered and washed with ice-cold diethyl ether (3 x 10 mL) to afford succinimide ester **24** (451 mg, 65%).

Mp (DMF:Diethyl Ether): 205-208 °C, lit[120] Mp: 206-207 °C; IR ν_{max}/ cm^{-1} (ATR): 3226 (N-H), 1747, 1728, 1700 (3 x C=O)**;** δ_H (300 MHz, DMSO): 6.39 (1H, s, NH), 6.34 (1H, s ,NH), 4.31 (1H, dd, *J* = 7.6, 5.2 Hz, H-9), 4.15 (1H, m, H-10), 3.11 (1H, m, H-8), 2.83 (1H, dd, *J* = 12.4, 5.1 Hz, H-11a), 2.81 (4H, brs, H-1), 2.66 (2H, t, *J* = 7.3 Hz, H-4), 2.58 (1H, d, *J* = 12.4 Hz, H-11b), 1.72-1.36 (6H, m, H-5/-6/-7).

N-(15-Oxo-19-((3a*R*,4*R*,6a*S*)-2-oxohexahydro-1*H*-thieno[3,4-d]imidazol-4-yl)-4,7,10-trioxa-14-azanonadecyl)-4-(propiolamidomethyl)benzamide, **(25)**[98]

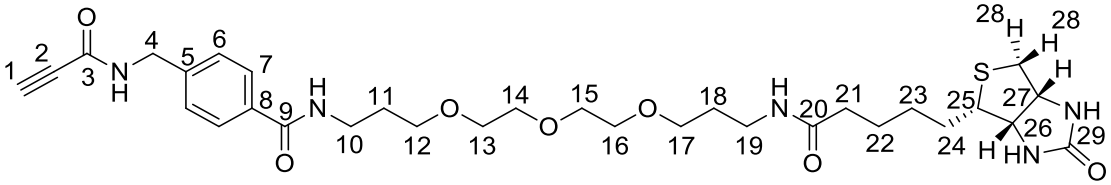

The amine **23** (449 mg, 0.86 mmol, 1.2 eq) and Ester **24** (246 mg, 0.72 mmol, 1 eq) were dissolved in DMF (2 mL) under N_2 and cooled to -78°C. DIPEA (0.25 mL, 1.4 mmol, 2eq) was added and the mixture was left to stir for two hours, while warming to room temperature. The bulk of the solvent was then removed under reduced pressure and the residue was lyophilised. Silica gel column chromatography (MeOH:DCM = 5:95) afforded biotin-alkyne **25** as a clear colourless wax (236 mg, 57%).

R_f = 0.60 (MeOH:DCM = 10:90); IR ν_{max}/ cm^{-1} (ATR): 3266 (amide N-H), 2106 (alkyne C-H), 1694 (C=O)**;** δ_H (400 MHz, MeOD): 7.81 (2H, d, *J* = 8.4 Hz, H-7), 7.40 (2H, d, *J* = 8.4 Hz, H-6), 4.50 (2H, ddd, *J* = 7.9, 4.9, 0.6 Hz, H-27), 4.47 (2H, s, H-4), 4.31 (1 H, dd, *J* = 7.9, 4.5 Hz, H-26), 3.68-3.62 (8H, m, H-13/-14/-15/-16), 3.57 (2H, t, *J* = 6.2 Hz, H-10), 3.51 (2H, t, H-17), 3.50 (2H, t, H-12), 3.37 (1H, s, H-1) 3.29-3.19 (3H, m, H-19/-25), 2.94 (1H, dd, *J* = 12.8, 5.0 Hz, H-28a), 2.72 (1H, d, *J* = 12.8 Hz, H-28b), 2.21 (2H, t, *J* = 7.4 Hz, H-21), 1.90 (2H, p, H-18), 1.76 (2H, p, H-11), 1.70-1.55 (4H, m, H-22/-23), 1.48-1.42 (2H, m, H-24); δ_C (101 MHz, MeOD): 175.9 (C-29), 169.7 (C-20), 166.0 (C-3), 154.7 (C-9), 143.0 (C_{quat}), 134.9 (C_{quat}), 128.7 (C-7), 128.6 (C-6), 78.1 (C-2), 76.2 (C-1),71.5 (C-14 or 15), 71.5 (C-14 or 15), 71.3 (C-13), 71.2 (C-16), 70.4 (C-12), 70.0 (C-17), 63.4 (C-27), 61.6 (C-26), 57.0

(C-25), 43.9 (C-4), 41.0 (C-28), 38.8 (C-19), 37.8 (C-10), 36.9 (C-21), 30.4 (C-11 or 18), 30.4 (C-11 or 18), 29.8 (C-24), 29.5 (C-23), 26.9 (C-22); HRMS (ES): *m/z* 632.3143 $(M+H)^+$, $C_{31}H_{46}N_5O_7S$ requires 632.3113.

1-(4-(3-((3-((4-Methoxybenzyl)sulfinyl)prop-1-en-1-yl)disulfanyl)propoxy)phenethyl)-*N*-(4-((15-oxo-19-((3a*R*,4*R*,6a*S*)-2-oxohexahydro-1*H*-thieno[3,4-d]imidazol-4-yl)-4,7,10-trioxa-14-azanonadecyl)carbamoyl)benzyl)-1H-1,2,3-triazole-4-carboxamide, **(26)**

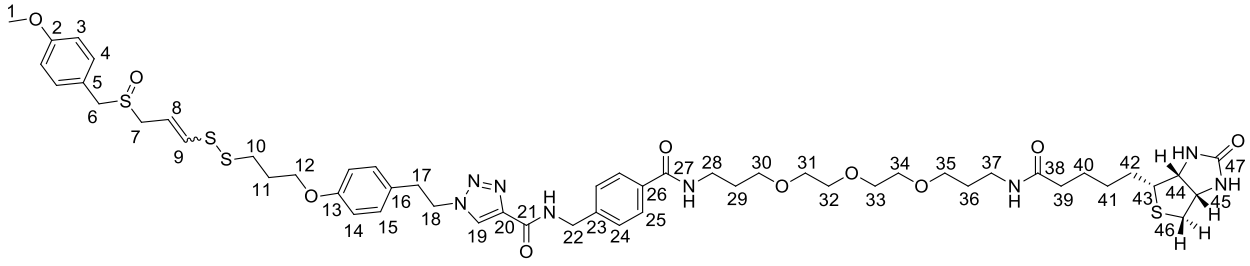

The reaction vessel was loaded with $CuSO_4.5H_2O$ (2.5 mg, 0.01 mmol, 0.1 eq) and sodium ascorbate (5.9 mg, 0.03 mmol, 0.3 eq) in H_2O (1 mL) under N_2. To the rapidly stirring solution the azide-ajoene **19** (52 mg, 0.11 mmol, 1 eq) in DMF (1 mL) and biotin-alkyne **25** (69 mg, 0.11 mmol, 1 eq) in DMF (1 mL) were added. The reaction was heated to 30°C and left to stir over-night for 18 hours. The solvents were removed via lyophilisation and the off-white solid residue was subjected to silica gel column chromatography (MeOH:DCM = 10:90) to afford biotin-ajoene **26** as 7:10 mixture of *E/Z*-isomers and as a white crystalline solid (68 mg, 56%).

E/Z mixture: R_f = 0.7 (MeOH:DCM = 0.2:0.8); IR ν_{max}/ cm^{-1} (ATR): 3310 (amide N-H), 1696/1649 (C=O); HRMS (ES): *m/z* 1109.4332 $(M+H)^+$, $C_{53}H_{73}N_8O_{10}S_4$ requires 1109.4338;

E-isomer: δ_H (400 MHz, MeOD:$CDCl_3$ = 1:9): 7.91 (1H, s, H-19), 7.66 (2H, d, *J* = 8.4 Hz, H-25), 7.30 (2H, d, *J* = 8.4 Hz, H-24), 7.11 (2H, d, *J* = 8.7 Hz, H-15), 6.91 (2H, d, *J* = 8.7 Hz, H-4), 6.79 (2H, d, *J* = 8.7 Hz, H-14), 6.70 (2H, d, *J* = 8.7 Hz, H-3), 6.29 (1H, dt, *J* = 14.7, 1.0 Hz, H-9), 5.82 (1H, dt, *J* = 14.8, 7.8 Hz, H-8), 4.53 (2H, s, H-22), 4.50 (2H, t, *J* = 7.3 Hz, H-18), 4.37 (1H, ddd, *J* = 7.8, 5.0, 0.9 Hz, H-45), 4.17 (1H, dd, *J* = 7.8, 4.6 Hz, H-44), 3.93 (2H, m, H-12), 3.85 (2H, d, *J* = 4.1 Hz, H-6), 3.69 (3H, s, H-1), 3.56 – 3.35 (14H, m, H-7/-30/-31/-32/-33/-34/-35), 3.27-3.22 (2H, m, H-28), 3.15 (2H, t, *J* = 6.6 Hz, H-37), 3.08-3.01 (3H, m,

H-17/-43), 2.84-2.76 (2H, m, H-10/-46a), 2.60 (1H, d, *J* = 12.8 Hz, H-46b), 2.09 – 2.00 (4H, m, H-11/-39), 1.78 (2H, p, H-29), 1.62 (2H, p, H-36), 1.57 – 1.43 (4H, m, H-40/42), 1.29 (2H, p, H-41); δ_C (101 MHz, MeOD:$CDCl_3$ = 1:9): 173.8 (C_{quat}), 167.7 (C_{quat}), 164.0 (C_{quat}), 160.5 (C_{quat}), 159.9 (C_{quat}), 159.6 (C_{quat}), 157.9 (C_{quat}), 142.5 (C_{quat}), 141.5 (C_{quat}), 134.7 (C-9), 133.6 (C_{quat}), 131.2 (C-15), 129.6 (C-4), 128.7 (C_{quat}), 127.6 (C-25), 127.4 (C-24), 126.1 (C-19), 116.7 (C-8), 114.9 (C-3), 114.5 (C-14), 70.4 (C-32), 70.3 (C-33), 70.1 (C-28), 69.9 (C-31), 69.9 (C-34), 69.4 (C-37), 65.8 (C-12), 61.9 (C-45), 60.1 (C-44), 56.1 (C-6), 55.5 (C-43), 55.2 (C-1), 52.7 (C-7), 52.1 (C-18), 42.6 (C-22), 40.3 (C-46), 38.1 (C-30), 37.2 (C-35), 35.8 (C-39), 35.5 (C-17), 34.6 (C-10), 28.9 (C-36), 28.9 (C-29), 28.7 (C-11), 28.4(C-41), 28.1 (C-42), 25.4 (C-40).

Z-isomer: δ_H (400 MHz, MeOD:$CDCl_3$ = 1:9): 7.91 (1H, s, H-19), 7.66 (2H, d, *J* = 8.4 Hz, H-25), 7.30 (2H, d, *J* = 8.4 Hz, H-24), 7.11 (2H, d, *J* = 8.7 Hz, H-15), 6.91 (2H, d, *J* = 8.7 Hz, H-4), 6.79 (2H, d, *J* = 8.7 Hz, H-14), 6.70 (2H, d, *J* = 8.7 Hz, H-3), 6.51 (1H, dt, *J* = 9.5, 0.9 Hz, H-9), 5.66 (1H, dt, *J* = 14.8, 7.8 Hz, H-8), 4.53 (2H, s, H-22), 4.50 (2H, t, *J* = 7.3 Hz, H-18), 4.37 (1H, ddd, *J* = 7.8, 5.0, 0.9 Hz, H-45), 4.17 (1H, dd, *J* = 7.8, 4.6 Hz, H-44), 3.92 (2H, m, H-12), 3.85 (2H, d, *J* = 4.1 Hz, H-6), 3.69 (3H, s, H-1), 3.56 – 3.35 (14H, m, H-7/-30/-31/-32/-33/-34/-35), 3.27-3.22 (2H, m, H-28), 3.15 (2H, t, *J* = 6.6 Hz, H-37), 3.08-3.01 (3H, m, H-17/-43), 2.84-2.76 (2H, m, H-10/-46a), 2.60 (1H, d, *J* = 12.8 Hz, H-46b), 2.09 – 2.00 (4H, m, H-11/-39), 1.78 (2H, p, H-29), 1.62 (2H, p, H-36), 1.57 – 1.43 (4H, m, H-40/42), 1.29 (2H, p, H-41); δ_C (101 MHz, MeOD:$CDCl_3$ = 1:9): 173.8 (C_{quat}), 167.7 (C_{quat}), 164.0 (C_{quat}), 160.5 (C_{quat}), 159.9 (C_{quat}), 159.6 (C_{quat}), 157.9 (C_{quat}), 142.5 (C_{quat}), 141.5(C_{quat}), 138.6 (C-9), 133.6 (C_{quat}), 131.3 (C-15), 129.6 (C-4), 128.7 (C_{quat}), 127.6 (C-25), 127.4 (C-24), 126.1 (C-19), 118.2 (C-8), 114.9 (C-3), 114.5 (C-14), 70.4 (C-32), 70.3 (C-33), 70.1 (C-28), 69.9 (C-31), 69.9 (C-34), 69.4 (C-37), 65.7 (C-12), 61.9 (C-45), 60.1 (C-44), 56.6 (C-6), 55.5 (C-43), 55.2 (C-1), 52.1 (C-18), 49.4 (C-7), 42.6 (C-22), 40.3 (C-46), 38.1 (C-30), 37.2 (C-35), 35.8 (C-39), 35.5 (C-17), 35.5 (C-10), 28.9 (C-36), 28.9 (C-29), 28.6 (C-11), 28.4(C-41), 28.1 (C-42), 25.4 (C-40).

6.2 Biological method

6.2.1 General

The oesophageal cancer cell-line WHCO1 was derived from biopsy of primary oesophageal squamous cell carcinoma of South African origin.[127] Cells were all incubated at 37 °C under 5% CO_2 and cultured with antibiotics in DMEM (Dulbecco's Modified Eagle Medium) containing 10% heat-inactivated FBS (Fetal Bovine Serum, Gibco, Life Technologies, South Africa). The cells were cultured in 100 mm petri dishes and allowed to reach 80-95% confluence prior to being split. The splitting procedure that was done under a sterile hood and involved removal of the growth media and a quick wash to remove excess media with phosphate buffer (PBS) (3-4 mL) at pH 7.4, followed directly by incubating the cells in 0.05% trypsin-EDTA (2 mL) for three minutes at 37 °C. The trypsin was used to detach the cells from the surface of the dish, and it was then deactivated with the growth media (3 mL). The cells were then pelleted by centrifugation for four minutes at 40000 rpm using a Hettich EBA 20 centrifuge. The pellet was then resuspended into growth media (1 mL) and using 10% of the cells to propagate further.

6.2.2 Cell proliferation analysis

The anti-proliferative effects of the analogues on tumour cells was measured by the 3-(4,5-Dimethylthiazol-2-yl)-2,5-diphenyltetrazolium bromide (MTT, Sigma Aldrich, South Africa) cellular viability assay Each experiment was performed in quadruplet in a 96-well-plate (Costar, Corning Inc., USA). The cells were plated in 90 µL of growth media at a cell density of 2500 WHCO1 cells per well. After plating, the cells were allowed to settle in an incubator overnight.

On day two, a stock dilution series ranging from 200 – 0 mM of drug was prepared in DMSO. Each solution was further diluted 100 fold into media, after which 10 µL was added to the cells to give a final drug concentration of 200 – 0 µM of the original solutions and 0.1% DMSO. The cells were then incubated with the drugs at 37°C, 5% CO_2 for 24 hours.

On day three, 10 µL of the MTT reagent (5 mg/mL) was added to each well and the cells were incubated for a further four hours; followed by the addition of 100 µL 10% SLS in 0.01 M HCl (Merck, Darmstadt Germany) to solubilise the formazan crystals.

On day five, the plates were read at 595 nm on a Multiscan FC plate reader (Thermo Fischer Scientific, Life Technologies, South Africa) and the background absorbance of the media, drugs and MTT (without cells) was also recorded at 595 nm. The background absorbance (with media only) was then subtracted from each reading and the data was analysed using Graphpad Prism 6, using a non-linear regression analysis fitted to sigmoidal dose-response curve with A595nm-baseline versus Log C to obtain the IC_{50} at 95% confidence interval.

6.2.3 Blood stability

Blood was collected from 10 mice in K_2EDTA coated tubes. A concentration of 0.4 mg/mL compound was added to the whole blood and incubated at 37 °C. At the indicated time points, aliquots of 10 µL were removed and extracted on ice into 100 µL CH_3CN by vortex, sonication and then centrifugation. The CH_3CN phase was then removed and diluted into mobile phase (1:1) and analysed by LC-MS/MS on an API 2000 MS/MS (AB Sciex) using Luna PFP 5 µm, 50 x 2.0 mm (Phenomenex) column. Mobile phase: CH_3CN and 10 mM ammonium acetate using a gradient from 60% CH_3CN to 100% CH_3CN in six minutes, then 100% CH_3CN for one minute followed by a three minute equilibration time at 60% CH_3CN with a flow rate of 300 µL/minute with a total run time of ten minutes. Peak areas were quantitated relative to a calibration curve.

6.2.4 UV-Vis spectroscopy

Stock solutions of 200 mM *Z*-ajoene were prepared in DMSO. Fresh blood was collected from one Balb/C mouse and placed on ice in a heparin coated tube. A 10 µL aliquot of the blood was diluted into 2 mL of PBS buffer, pH 7.4 in a 2 mL quartz cuvette. The background spectrum was recorded from 700-230 nm in a Shimadzu UV1800 UV–visible spectrophotometer against a blank containing PBS alone. To both test sample and the blank was added increasing concentrations (0 – 200 µM) of *Z*-ajoene to reach a maximum concentration of 0.1% DMSO.

6.2.5 Proteomics

A stock solutions of 500 µM human Hb (Sigma) was were prepared in 0.02 M HEPES buffer (pH 7.4). After 25-fold dilution to 20 µM, to one Hb aliquot *Z*-ajoene in DMSO (10 mM) was added to give a final concentration of 100 µM. The other (untreated) sample

was prepared by adding the same volume of only vehicle (DMSO). The samples were incubated for two hours and stored overnight at 3 °C before being delivered to the CPGR.

Approximately 6μg of Hb protein was aliquoted into a 1.5 mL centrifuge tube to a final volume of 20 μL. Trypsin (Promega) was resuspended in Millipore Water and added to each sample to give a final trypsin:protein ratio of 1:20. The volume was then corrected to 50 μL with 50 mM triethylammonium bicarbonate (Sigma). Samples were digested for 18 hours at 37 °C. Peptide samples were dried by vacuum centrifugation and resuspended in 0.1% formic acid (Sigma), 2.5% acetonitrile (Anatech) to a final concentration of 500 ng/μL. Samples were then stored at -80°C and analysed using LCMS.

Nano-RPLC chromatography was performed on a Dionex Ultimate 3000 nano-HPLC system. LC–MS/MS analysis was conducted with a Q-Exactive quadrupole-Orbitrap mass spectrometer (Thermo Fisher Scientific, USA) coupled with a Dionex Ultimate 3000 nano-HPLC system. The mobile phases consisted of solvent A (0.1% formic acid in water) and solvent B (100% CH_3CN, and 0.1% formic acid). The HPLC fractionated peptides were dissolved in sample loading buffer (2.5% CH_3CN, 0.1% formic acid, water) and loaded on a C18 trap column (100 μm×20 mm×5 μm). Chromatographic separation was performed with a C18 column (75 μm×250 mm×3.6 μm). The mass spectrometer was operated in positive ion mode with a capillary temperature of 250 °C. The applied electrospray voltage was 1.95 kV.

6.2.6 Immunoblotting

The gels were prepared using standard protocols: The separating gel was made using acrylamide concentration of 10%, with the pH of 8.8 in Tris buffer. The Stacking gel was made using 3% acrylamide in Tris buffer, pH of 6.8. The 10 μM Hb stock solution was made in PBS. A 10 mM stock solution of ajoene in DMSO:PEG400:PBS (10:50:40) was made. The individual samples were prepared, as follows:

Untreated	**Whole probe**	**Whole probe + DTT**	***in situ* "Click"**
10 µM Hb +1% vehicle	10 µM Hb +100µM biotin-ajoene +1% vehicle	10 µM Hb +100 µM biotin-ajoene +1% vehicle	10 µM Hb +100 µM azide-ajoene +1% vehicle
Incubate: 30 minutes at 37 °C			
		+100 mM DTT	+100 µM biotin-alkyne +1 mM aq. sodium ascorbate +1 mM aq. $CuSO_4$
Incubate: 60 minutes at 37 °C			

Protein in 3 µL sample buffer (0.25M Tris (pH 6.8), 4% SDS, 20% glycerol, Bromophenol Blue) was loaded onto the stacking gel to obtain a final protein mass of 0.5 µg or 1.0 µg in each lane, respectively. The gel tank (Bio-Rad Mini-Protean 3 Cell Assembly) was filled with running buffer (3% Tris, 14% Glycine, 1% SDS) and the gels were run at 100 V while the protein moved through the stacking gel. Once the dye front reached the running gel, the voltage was increased to 200 V for the remainder of the experiment. The protein was then transferred to a nitrocellulose membrane, followed by blocking overnight at 4 °C with 5% non-fat milk in PBS containing Tween-20; followed by an overnight incubation with the anti-biotin primary antibody (1:10000) (Santa Cruz, Whitehead Scientific) at 4 °C. The specific biotinylated protein was detected using a horseradish peroxidase-conjugated secondary anti-body (1:5000) and the LumiGLO chemiluminescent reagent (KPL, Bicom Biotech, South Africa). A protein ladder (Thermo Fischer Scientific, Life Technologies) was used to estimate the molecular weight of proteins.

Chapter Seven: References

1 S. B. Moyers, *Garlic in health, history, and world cuisine*, Suncoast Press, 1996.

2 A. H Bower, *Curr. Immunol. Rev.*, 2014, **10**, 113–121.

3 A. Cardelle-Cobas and A. Soria, *A comprehensive survey of garlic functionality*, 2010.

4 J. C. Harris, S. L. Cottrell, S. Plummer and D. Lloyd, *Appl. Microbiol. Biotechnol.*, 2001, **57**, 282–286.

5 M. R. Gamboa-Le??n, I. Aranda-Gonz??lez, M. Mut-Mart??n, M. R. Garc??a-Miss and E. Dumonteil, *Scand. J. Immunol.*, 2007, **66**, 508–514.

6 N. Caporaso, S. M. Smith and R. H. Eng, *Antimicrob. Agents Chemother.*, 1983, **23**, 700–702.

7 Y. Zhou, W. Zhuang, W. Hu, G. Liu, T. Wu and X. Wu, *Gastroenterology*, 2011, **141**, 80–89.

8 G. Schäfer and C. H. Kaschula, *Anticancer. Agents Med. Chem.*, 2014, **14**, 233–40.

9 L. H. Kasper and A. T. Reder, *Ann. Clin. Transl. Neurol.*, 2014, **1**, 622–631.

10 E. Kyo, N. Uda, a Suzuki, M. Kakimoto, M. Ushijima, S. Kasuga and Y. Itakura, *Phytomedicine*, 1998, **5**, 259–67.

11 E. Kyo, N. Uda, S. Kasuga and Y. Itakura, *J. Nutr.*, 2001, **131**, 1075S--1079S.

12 J. Borlinghaus, F. Albrecht, M. C. H. Gruhlke, I. D. Nwachukwu and A. J. Slusarenko, *Molecules*, 2014, **19**, 12591–12618.

13 A. Stoll and E. Seebeck, *Helv. Chim. Acta*, 1948, **31**, 189–210.

14 and R. A.-C. Eric Block, Saleem Ahmad, James L. Catalfamo, Mahendra K. Jain, *Am. Chem. Soc.*, 1986, **108**, 7045–7055.

15 S. Durairaj, S. Srinivasan and P. Lakshmanaperumalsamy, *Electr. J. Biol.*, 2009, **5**, 5–10.

16 S. Ankri and D. Mirelman, *Microbes Infect.*, 1999, **1**, 125–129.

17 F. S. S. Jalali, H. Tajik, H. Javadi, B. H. Mohammadi, S. S. A. Athari and others, *J Anim Vet Adv*, 2009, **8**, 655–659.

18 E. Block and S. Ahmad, *J. Am. Chem. SOC*, 1984, **106**, 8295–8296.

19 H. Amagase, *J. Nutr.*, 2006, **136**, 716S--725S.

20 H. Amagase, B. L. Petesch, H. Matsuura, S. Kasuga and Y. Itakura, *J. Nutr.*, 2001, **131**, 955S–962.

21 C. H. Kaschula, R. Hunter and M. Iqbal Parker, *BioFactors*, 2010, **36**, 78–85.

22 E. Block, *Sci. Am.*, 1985, **252**, 114–119.

23 D. Mnayer, A. S. Fabiano-Tixier, E. Petitcolas, T. Hamieh, N. Nehme, C. Ferrant, X. Fernandez and F. Chemat, *Molecules*, 2014, **19**, 20034–20053.

24 M. Yoo, S. Lee, S. Kim, J. B. Hwang, J. Choe and D. Shin, *Food Sci. Biotechnol.*, 2014, **23**, 337–344.

25 M. T. Naznin, Y. Kitaya, T. Shibuya, R. Endo, H. Hirai and M. G. Lefsrud, *Biol. Sci. Sp.*, 2015, **29**, 1–7.

26 M. H. Brodnitz, V. J. Pascale and L. Van Derslice, *J. Agric. Food Chem.*, 1971, **19**, 273–275.

27 L. D. Lawson and Z. J. Wang, *J. Agric. Food Chem.*, 2005, **53**, 1974–1983.

28 M. T. Naznin, M. Akagawa, K. Okukawa, T. Maeda and N. Morita, *Food Chem.*, 2008, **106**, 1113–1119.

29 M. Iciek, I. Kwiecień and L. Włodek, *Environ. Mol. Mutagen.*, 2009, **50**, 247–265.

30 U. Münchberg, A. Anwar, S. Mecklenburg and C. Jacob, *Org. Biomol. Chem.*, 2007, **5**, 1505–1518.

31 E. A. O'Gara, D. J. Hill and D. J. Maslin, *Appl. Environ. Microbiol.*, 2000, **66**, 2269–2273.

32 S. M. Tsao and M. C. Yin, *J. Med. Microbiol.*, 2001, **50**, 646–649.

33 T. Ariga and T. Seki, *Biofactors*, 2006, **26**, 93–103.

34 R. Munday, J. S. Munday and C. M. Munday, *Free Radic. Biol. Med.*, 2003, **34**, 1200–1211.

35 T. Chatterji, K. Keerthi and K. S. Gates, *Bioorg. Med. Chem. Lett.*, 2005, **15**, 3921–4.

36 T. Ariga, A. Takeda, S. Teramoto and T. Seki, in *Food Factors for Cancer Prevention*, Springer, 1997, pp. 231–234.

37 T. Seki, T. Hosono, T. Hosono-Fukao, K. Inada, R. Tanaka, J. Ogihara and T. Ariga, *Asia Pac. J. Clin. Nutr.*, 2008, **17**, 249–252.

38 R. Apitz-Cástro, S. Cabrera, M. R. Cruz, E. Ledezma and M. K. Jain, *Thromb. Res.*, 1983, **32**, 155–169.

39 M. Yoo, S. Lee, S. Kim and D. Shin, *Food Sci. Nutr.*, 2014, **2**, 605–11.

40 H. A. Perez, M. De la Rosa and R. Apitz, *Antimicrob. Agents Chemother.*, 1994, **38**, 337–9.

41 J.-Y. Yang, M. A. Della-Fera, C. Nelson-Dooley and C. A. Baile, *Obesity (Silver Spring).*, 2006, **14**, 388–97.

42 S. Rayalam, M. A. Della-Fera and C. A. Baile, *J. Nutr. Biochem.*, 2008, **19**, 717–26.

43 R. Naganawa, N. Iwata, K. Ishikawa, H. Fukuda, T. Fujino and A. Suzuki, *Appl. Envir. Microbiol.*, 1996, **62**, 4238–4242.

44 S. Yoshida, S. Kasuga, N. Hayashi, T. Ushiroguchi, H. Matsuura and S. Nakagawa, *Appl. Envir. Microbiol.*, 1987, **53**, 615–617.

45 G. San-Blas, F. San-Blas, F. Gil, L. Marino and R. Apitz-Castro, *Antimicrob. Agents Chemother.*, 1989, **33**, 1641–1644.

46 S. R. Davis, *J. Antimicrob. Chemother.*, 2003, **51**, 593–597.

47 A. A. Powolny and S. V. Singh, *Cancer Lett.*, 2008, **269**, 305–314.

48 H. T. Hassan, *Leuk. Res.*, 2004, **28**, 667–71.

49 A. Arora, C. Tripathi and Y. Shukla, *Curr. Cancer Ther. Rev.*, 2005, **1**, 199–205.

50 J. Ferlay, I. Soerjomataram, R. Dikshit, S. Eser, C. Mathers, M. Rebelo, D. M. Parkin, D. Forman and F. Bray, *Int. J. Cancer*, 2015, **136**, E359–E386.

51 D. Hanahan and R. A. Weinberg, *Cell*, 2000, **100**, 57–70.

52 D. Hanahan and R. A. Weinberg, *Cell*, 2011, **144**, 646–674.

53 F. Nouroz, M. Mehboob, S. Noreen, F. Zaidi and T. Mobin, 2015, **23**, 1145–1151.

54 S. Oommen, R. J. Anto, G. Srinivas and D. Karunagaran, *Eur. J. Pharmacol.*, 2004, **485**, 97–103.

55 X.-J. Wu, Y. Hu, E. Lamy and V. Mersch-Sundermann, *Environ. Mol. Mutagen.*, 2009, **50**, 266–75.

56 N. S. Nagaraj, K. R. Anilakumar and O. V Singh, *J. Nutr. Biochem.*, 2010, **21**, 405–12.

57 V. M. Dirsch, D. S. M. Antlsperger, H. Hentze and A. M. Vollmar, *Leuk. Off. J. Leuk. Soc. Am. Leuk. Res. Fund, U.K*, 2002, **16**, 74–83.

58 A. Herman-Antosiewicz, A. A. Powolny and S. V. Singh, *Acta Pharmacol. Sin.*, 2007, **28**, 1355–1364.

59 M. Li, J.-R. Ciu, Y. Ye, J.-M. Min, L.-H. Zhang, K. Wang, M. Gares, J. Cros, M. Wright and J. Leung-Tack, *Carcinogenesis*, 2002, **23**, 573–579.

60 C. H. Kaschula, R. Hunter, H. T. Hassan, N. Stellenboom, J. Cotton, X. Q. Zhai and M. I. Parker, *Anticancer. Agents Med. Chem.*, 2011, **11**, 260–6.

61 V. M. Dirsch, A. L. Gerbes and A. M. Vollmar, *Mol. Pharmacol.*, 1998, **53**, 402–407.

62 X.-J. Wu, F. Kassie and V. Mersch-Sundermann, *Mutat. Res.*, 2005, **579**, 115–24.

63 A. Das, N. L. Banik and S. K. Ray, *Cancer*, 2007, **110**, 1083–1095.

64 R. Nepravishta, R. Sabelli, E. Iorio, L. Micheli, M. Paci and S. Melino, *FEBS J.*, 2012, **279**, 154–67.

65 C. J. Cavallito, J. S. Buck and C. M. Suter, *J. Am. Chem. Soc.*, 1944, **66**, 1952–1954.

66 C. H. Kaschula, R. Hunter, N. Stellenboom, M. R. Caira, S. Winks, T. Ogunleye, P. Richards, J. Cotton, K. Zilbeyaz, Y. Wang, V. Siyo, E. Ngarande and M. I. Parker, *Eur. J. Med. Chem.*, 2012, **50**, 236–254.

67 A. Rabinkov, T. Miron, D. Mirelman, M. Wilchek, S. Glozman, E. Yavin and L. Weiner, *Biochim. Biophys. Acta - Mol. Cell Res.*, 2000, **1499**, 144–153.

68 E. D. WILLS, *Biochem. J.*, 1956, **63**, 514–20.

69 P. Klatt and S. Lamas, *Eur. J. Biochem.*, 2000, **267**, 4928–4944.

70 D. M. Townsend, K. D. Tew and H. Tapiero, *Biomed. Pharmacother.*, 2003, **57**, 145–155.

71 J. T. Pinto, B. F. Krasnikov and A. J. L. Cooper, *J. Nutr.*, 2006, **136**, 835–841.

72 M. Fratelli, H. Demol, M. Puype, S. Casagrande, I. Eberini, M. Salmona, V. Bonetto, M. Mengozzi, F. Duffieux, E. Miclet, A. Bachi, J. Vandekerckhove, E. Gianazza and P. Ghezzi, *Proc Natl Acad Sci U S A*, 2002, **99**, 3505–3510.

73 D. Xiao, J. T. Pinto, J.-W. Soh, A. Deguchi, G. G. Gundersen, A. F. Palazzo, J.-T. Yoon, H. Shirin and I. B. Weinstein, *Cancer Res.*, 2003, **63**, 6825–6837.

74 H. Gallwitz, S. Bonse, A. Martinez-Cruz, I. Schlichting, K. Schumacher and R. L. Krauth-Siegel, *J. Med. Chem.*, 1999, **42**, 364–72.

75 R. Sabelli, E. Iorio, A. De Martino, F. Podo, A. Ricci, G. Viticchiè, G. Rotilio, M. Paci and S. Melino, *FEBS J.*, 2008, **275**, 3884–99.

76 Y. Gargouri, H. Moreau, M. K. Jain, G. H. de Haas and R. Verger, *Biochim. Biophys. Acta - Lipids Lipid Metab.*, 1989, **1006**, 137–139.

77 E. Ledezma, R. Apitz-Castro and J. Cardier, *Cancer Lett.*, 2004, **206**, 35–41.

78 T. Hosono, T. Fukao, J. Ogihara, Y. Ito, H. Shiba, T. Seki and T. Ariga, *J. Biol. Chem.*, 2005, **280**, 41487–41493.

79 C. Teyssier and M.-H. Siess, *Drug Metab. Dispos.*, 2000, **28**, 648–654.

80 H. Gallwitz, S. Bonse, A. Martinez-Cruz, I. Schlichting, K. Schumacher and R. L. Krauth-Siegel, *J. Med. Chem.*, 1999, **42**, 364–372.

81 *Advances in Enzymology and Related Areas of Molecular Biology, Volume 63*, John Wiley & Sons, 2009.

82 D. Barford, *Curr. Opin. Struct. Biol.*, 2004, **14**, 679–86.

83 S. M. Marino and V. N. Gladyshev, *J. Biol. Chem.*, 2012, **287**, 4419–25.

84 I. Dalle-Donne, A. Milzani, N. Gagliano, R. Colombo, D. Giustarini and R. Rossi,

Antioxid. Redox Signal., 2008, **10**, 445–473.

85 R. Hunter, C. H. Kaschula, I. M. Parker, M. R. Caira, P. Richards, S. Travis, F. Taute and T. Qwebani, *Bioorganic Med. Chem. Lett.*, 2008, **18**, 5277–5279.

86 J. A. Kampmeier and G. Chen, *J. Am. Chem. Soc.*, 1965, **87**, 2608–2613.

87 C. G. Overberger, H. Biletch, A. B. Finestone, J. Lilker and J. Herbert, *J. Am. Chem. Soc.*, 1953, **75**, 2078–2082.

88 R. S. Sukhai, R. de Jong, J. Meijer and L. Brandsma, *Recl. des Trav. Chim. des Pays-Bas*, 2010, **99**, 191–194.

89 L. D. Lawson, D. K. Ransom and B. G. Hughes, *Thromb. Res.*, 1992, **65**, 141–156.

90 J. Taucher, A. Hansel, A. Jordan and W. Lindinger, *J. Agric. Food Chem.*, 1996, **44**, 3778–3782.

91 F. Freeman and Y. Kodera, *J. Agric. Food Chem.*, 1995, 2332–2338.

92 C. Egen-Schwind, R. Eckard and F. H. Kemper, *Planta Med.*, 1992, **58**, 301—305.

93 L. D. (Murdock H. S. U. (USA)) Lawson and Z. J. Wang, in *41st Annual Congress on Medicinal Plant Research, Duesseldorf (Germany), 31 Aug - 4 Sep 1993*, 1993.

94 P. Taylor, R. Noriega, C. Farah, M.-J. Abad, M. Arsenak and R. Apitz, *Cancer Lett.*, 2006, **239**, 298–304.

95 C. H. Kaschula, R. Hunter, J. Cotton, R. Tuveri, E. Ngarande, K. Dzobo, G. Schäfer, V. Siyo, D. Lang, D. A. Kusza, B. Davies, A. A. Katz and M. I. Parker, *Mol. Carcinog.*, 2015, n/a-n/a.

96 M. Wilchek and E. A. Bayer, *Anal. Biochem.*, 1988, **171**, 1–32.

97 G. Elia, *Proteomics*, 2008, **8**, 4012–4024.

98 M. Jezowska, J. Romanowska, B. Bestas, U. Tedebark and M. Honcharenko, *Molecules*, 2012, **17**, 14174–14185.

99 H. C. Kolb, M. G. Finn and K. B. Sharpless, *Angew. Chem. Int. Ed. Engl.*, 2001, **40**, 2004–2021.

100 L. Jin, D. R. Tolentino, M. Melaimi and G. Bertrand, *Sci. Adv.*, 2015, **1**, e1500304–

e1500304.

101 C. A. Lipinski, F. Lombardo, B. W. Dominy and P. J. Feeney, *Adv. Drug Deliv. Rev.*, 1997, **23**, 3–25.

102 C. A. Lipinski, *Drug Discov. Today Technol.*, 2004, **1**, 337–341.

103 S. Venkateswarlu and G. K. Panchagnula, 2006, **45**, 1063–1066.

104 T. Mosmann, *J. Immunol. Methods*, 1983, **65**, 55–63.

105 M. Smith, R. Hunter, N. Stellenboom, D. A. Kusza, M. I. Parker, A. N. H. Hammouda, G. Jackson and C. H. Kaschula, *Biochim. Biophys. Acta - Gen. Subj.*, 2016, **1860**, 1439–1449.

106 R. Munday and E. Manns, 1994, 959–962.

107 C. C. Winterbourn, *Semin. Hematol.*, 1990, **27**, 41–50.

108 M. Dayer and A. Moosavi-Movahedi, *Protein Pept. Lett.*, 2010, **17**, 473–479.

109 K. D. Vandegriff, A. Malavalli, C. Minn, E. Jiang, J. Lohman, M. A. Young, M. Samaja and R. M. Winslow, *Biochem. J.*, 2006, **399**, 463–71.

110 L. Regazzoni, A. Panusa, K. J. Yeum, M. Carini and G. Aldini, *J. Chromatogr. B Anal. Technol. Biomed. Life Sci.*, 2009, **877**, 3456–3461.

111 M. C. Garel, Y. Beuzard, J. Thillet, C. Domenget, J. Martin, F. Galacteros and J. Rosa, *Eur. J. Biochem.*, 1982, **123**, 513–519.

112 M. C. Garel, C. Domenget, J. Caburi-Martin, C. Prehu, F. Galacteros and Y. Beuzard, *J. Biol. Chem.*, 1986, **261**, 14704–9.

113 C. T. Craescu, C. Poyart, C. Schaeffer, M. C. Garel, J. Kister and Y. Beuzard, *J. Biol. Chem.*, 1986, **261**, 14710–6.

114 S. Wodak, J. De Coen, S. Edelstein, H. Demarne and Y. Beuzard, *J. Biol. Chem.*, 1986, **261**, 14717–14724.

115 C. H. Kaschula, R. Hunter, J. Cotton, R. Tuveri, E. Ngarande, K. Dzobo, G. Schäfer, V. Siyo, D. Lang, D. A. Kusza, B. Davies, A. A. Katz and M. I. Parker, *Mol. Carcinog.*, 2015.

116 J. P. Brennan, *Mol. Cell. Proteomics*, 2005, **5**, 215–225.

117 L. Mi, Z. Xiao, T. D. Veenstra and F. L. Chung, *J. Proteomics*, 2011, **74**, 1036–1044.

118 C. Pike, University of Cape Town, 2013.

119 M. Wenska, M. Alvira, P. Steunenberg, Å. Stenberg, M. Murtola and R. Strömberg, *Nucleic Acids Res.*, 2011, **39**, 9047–9059.

120 A. Kayushin, A. Demekhina, M. Korosteleva, A. Miroshnikov and A. Azhayev, *Nucleosides. Nucleotides Nucleic Acids*, 2012, **30**, 490–502.

121 H. E. Gottlieb, V. Kotlyar and A. Nudelman, *J. Org. Chem.*, 1997, **62**, 7512–7515.

122 C.-S. Cheng, C. Ferber, R. I. Bashford and G. F. Grillot, *J. Am. Chem. Soc.*, 1951, **73**, 4081–4084.

123 M. Mabunda, University of Cape Town, 2013.

124 J. Biwi, University of Cape Town, 2014.

125 Y. Y. Yang, J. M. Ascano and H. C. Hang, *J Am Chem Soc*, 2010, **132**, 3640–3641.

126 M. Braun, U. Hartnagel, E. Ravanelli, B. Schade, C. Böttcher, O. Vostrowsky and A. Hirsch, *European J. Org. Chem.*, 2004, **2004**, 1983–2001.

127 R. B. Veale and A. L. Thornley, *S. Afr. J. Sci.*, 1989, **85**, 375–379.